# Politecnico di Torino

Corso di Laurea Magistrale in

INGEGNERIA PER L'AMBIENTE E IL TERRITORIO

Climate Change

A.a. 2023/2024
Sessione di Laurea Ottobre 2024

# Green gutter as a Natural Based Solution for mitigation and adaptation strategy in urban environments

Experimental study

Referents:

Fulvio Boano (DIATI)
Lineker Max Goulart Coelho (DTU-Denmark)

Candidates:

Ludovica Maria Bellani

# Abstract

In recent decades, one of the most discussed topics revolves around the issue of climate change and how humans can act to address this problem in the urban environment, given the profound impact of this on human daily life. The overarching goal is the reduction of the causes and the sources of climate change, in order to promote the well-being of the environment, doing the best for it. However, this altruistic pursuit often contends with human predispositions toward self-interest, which are its first concern. A loftier pursuit entails not only mitigating the repercussions and proactively adapting to the yet evolving circumstances, but also doing it in the most natural and environmentally friendly way. Within this paradigm, urban environments emerge as ideal fields where to develop this prospect, particularly through the application of Nature Based Solutions. Urban areas represent focal points where the impacts of climate change will be intensively felt, as they are the heart of the problem, being both victims and sources of it. Numerous sources of pollution and their consequential impacts stem from human activity. Cities must enact integrated policies to achieve greater sustainability, resource efficiency, energy conservation, pollutant reduction, and effective water management.

The main goal of this study is to evaluate the efficacy of a gutter as a prospective green wall, in managing water rainfall. The aim is to develop and propose a system capable of mitigating the risk of inundation and flooding, since it would be able to handle extreme rainfall events.

The key targets assessed include the system's capacity to reduce peak flow, delay the arrival time of peak flow, and retain water. Additionally, the duration required for the system to completely empty and fully recover its operational functionality will be examined to estimate when it would be ready to manage the subsequent rainfall events.

The experimental tests were carried out at the DTU, dept of Engineering Technology, Ballerup, Denmark. The experimental apparatus consists in a prospective green gutter filled with Rockflow by Rockwool's company, a special type of mineral wool designed to be used in water delay systems, capable of dealing with heavy rain phenomena. The green gutter will represent a mitigation and adaptation strategy that, when integrated into an urban catchment, would serve and help as an additional measure to address climate change. Key finding is the ability to manage the shorter rainfall, so the most intense precipitation events. This could be a significant contribution to enhanced resilience against flooding and inundation, supporting sustainable urban development and climate change adaptation efforts. By effectively delaying peak flow and managing runoff, this system can contribute to establishing a comprehensive framework for water management within a larger project. This may involve incorporating multiple gutters within a catchment area, strategically distributed at key points.

# Table of contents

# 1. Introduction

The green gutter system discussed in this study is a Nature-Based Solution (NBS) designed to address urban water management challenges exacerbated by climate change.

Its primary objective is to mitigate and adapt to extreme rainfall events by managing rainwater more effectively. By doing so, it helps alleviate the pressure on conventional drainage systems, thereby reducing the risk of flooding and inundation in urban areas.

This system supports sustainable urban development by delaying runoff and promoting resilience against flooding in areas vulnerable to heavy rainfall events.

The main intention of the present research is to evaluate this potential new Nature Based Solution from the hydraulic point of view, addressing its efficacy in water management, underlining the main properties to deal with rainwater and support drainage system.

Hence, the key targets for the evaluation include the system's capacity to reduce peak flow, delay the arrival time of the peak flow, and retain water. Additionally, the time required for the system to completely empty and fully recover its operational functionality will be examined to estimate when it would be ready to manage the subsequent rainfall events.

The aim is to develop and propose a system capable of mitigating the risk of inundation and flooding, since it would be able of handling extreme rainfall events, slowing their runoff. As a part of this effort, the study will assess the system's ability, as a Nature Based Solution, to alleviate strain on urban drainage systems.

The experimental setup, currently a metal box filled with permeable material, is intended to be enhanced with a vegetative layer. As a prospective green wall, this addition will provide further benefits to both the building and the urban environment. The covering of the metal box has already been planned by the DTU department, which is preparing to initiate an analysis to identify the most suitable vegetation for this purpose.

The green gutter, design to manage water during rainfall, will represent a mitigation and adaptation strategy that, when integrated into an urban catchment, would serve and help as an additional measure to address climate change.

## 1.1 NBS for urban areas

In recent decades, one of the most discussed topics revolves around the issue of climate change and how humans can act to address this problem in the urban environment, given the profound impact of this on human daily life.

The overarching goal is the reduction of the causes and the sources of climate change, in order to promote the well-being of the environment, and do the best for it. However, this altruistic pursuit

often contends with human predispositions toward self-interest, which are its first concern. A loftier pursuit entails not only mitigating the repercussions and proactively adapting to the yet evolving circumstances, but also doing it in the most naturally and environmentally way.

Within this paradigm, urban environments emerge as ideal fields where develop this prospect, particularly through the application of Nature Based Solutions (NBS). These approaches embody human ingenuity with natural processes, offering a holistic framework for implementing mitigation and adaptation solutions within cities. They constitute the key, as a pivotal means, to ameliorate the present and its current conditions, while endeavouring to shape a better and more sustainable future. Probably, it is only through the reconciliation of urban and environmental spheres that a harmonious equilibrium may be attainable, heralding a transformative shift in our collective trajectory.

Urban areas represent focal points where the impacts of climate change will be intensively felt, as they are the hearth of the problem, being both victim and source of it.
Numerous sources of pollution and their consequential impacts stem from human activity. In the urban environment, effects and causes are mixed. A key concern is the growing lack of natural elements in these areas, a trend largely attributable to dense urbanization. This process exacerbates various environmental challenges, particularly by reducing cities' resilience to hazards and increasing their overall vulnerability (Besir & Cuce, 2018).

Today, most of the world's population lives in cities, and there is a growing tendency to urban life year after year. According to a recent report of United Nations, the population living in cities is expected to increase up to 67%, by 2050 (Nations, 2012). Also, cities occupy only 3% of the Earth's land but account for 60–80% of global energy consumption, 75% of global carbon emissions and more than 60% of resource use (Nations, 2020).

Cities encompass the majority of people, goods and infrastructures, and since population continue to increase, they are growing denser and larger. This constitutes the main cause of their vulnerability to meteorological hazards (Masson V., 2020).
The risks of climate change in cities are complex and multifaceted, as complex and multifaced is their environment. Given the concentration of people and the interconnectedness of infrastructures, a better strategic planning are required, without which they are completely vulnerable (Sebestyén V., 2023).

One of the United Nations' 17 Sustainable Development Goals, specifically Goal 11 'Sustainable cities and communities', pertains exactly to this topic. This objective underscores the imperative for cities to reassess their infrastructural frameworks and devise solutions geared towards mitigating and adapting to climate change. The goal aims to enhance urban resilience to hazards,

thereby reducing the direct economic losses attributable to disasters, which are usually mostly water-related disasters, alleviating pressure on existing infrastructures (11-Sustainable Cities And Communities, 2015).

With acute awareness, cities must enact integrated policies to achieve greater sustainability, resource efficiency, energy conservation, pollutant reduction, and effective water management (Omri A., 2024). These measures are essential for enhancing urban environmental and social conditions, even more since welfare level beckons more and more citizens to move towards big cities (Chatti W., 2022). The escalating urbanization coupled with diminishing green spaces exacerbates many critical issues, further emphasizing the aforementioned challenges (Ahmad M., 2021) (Besir & Cuce, 2018). These circumstances underscore the imperative for such initiatives.

In this scenario, Nature-Based Solutions exhibit significant potential (Nature-based solutions research policy, s.d.).

## 1.2 Flooding, short-intensity rainfall event and NBS

The primary theme treated in this thesis is related to water management issues, assessing the impact of climate change on urban drainage system, and how NBS can partly solve it.
The urgency to address climate change and enhance urban life quality underscores the importance of this study in the current context.

The European Commission defines nature-based solutions as "solutions that are inspired and supported by nature, which are cost-effective, simultaneously provide environmental, social, and economic benefits and help build resilience. Such solutions bring more, and more diverse, nature and natural features and processes into cities, landscapes, and seascapes, through locally adapted, resource-efficient and systemic interventions" (The EU and nature-based solutions, s.d.).

Nature-based solutions offer multiple benefits, including environmental such as the thermal comfort and carbon sequestration (Getter K.L., 2009), air pollution filtering (Tomson M., 2021), water retention (Almaaitah T., 2022) and biodiversity enhancement (Hoeben A.D., 2021), social cohesion and contribution to well-being (Roggero M., 2020) and economic advantages.

A closer look at the built environment shows that opportunities lie in transforming buildings with nature-based solutions for fostering climate resilience: to evolve into green infrastructures, like green roofs and green walls (Kandel S., 2024).

One of the most significant hazards impacting urban areas is flooding, which occurs following extreme rainfall events. Urban flooding represents the most common yet severe environmental threat to cities and towns worldwide (Affairs, 2012).

The phenomenon of increased flood risk in urban areas is largely driven by the impervious nature of urban environments (Ulysse Pasquier, 2022). As cities expand, green areas are always more replaced by impermeable materials such as concrete, asphalt, and buildings. These surfaces hinder water from infiltrating the ground, significantly enhance surface runoff during rainfall events (Locatelli, et al., 2017). The obtained result is an elevated risk of urban flooding, as stormwater cannot be absorbed by the soil and instead accumulates on the surface, often overwhelming drainage systems and leading to flash floods (Sohn, Kim, Li, Brown, & Jaber, 2020).

Future changes in extreme rainfall events are likely to exacerbate this threat (Conrad Wasko, 2015). Climate change is expected to change the intensity and frequency of heavy rainfall by increasing humidity (H. J. Fowler G. L., 2021). Changes in large-scale atmospheric circulation and convective storm dynamics, combined with rising temperatures, lead to increased intensity of storms. Warmer air can retain more moisture, which means that when rainfall occurs, a greater volume of water is available in the atmosphere, leading to more intense downpours. (H. J. Fowler H. A., 2021).

Furthermore, evidence indicates that subhourly extreme rainfall exhibits a positive trend (Hooman Ayat, 2022). Short-duration intense rainfalls are the one more responsible to cause flash flooding with associated impacts. However, there is a limited number of studies addressing changes in subdaily rainfall patterns. Because sub-daily rainfall extremes often occur over small areas, they can be missed by rain gauge networks, overlooked by satellite measurements, and are poorly predicted by regional climate models. This is primarily due to the high costs of very high-resolution (kilometre-scale) climate models required to accurately capture hourly rainfall extremes. (Elizabeth J. Kendon, 2018).

# 2. Literature Review

## 2.1 Greenery systems

Firstly, greenery systems were considered from only an architectural style aspect point of view (Manso M., 2015).

The widening environmental awareness is now driving the exploitation of the effective utilization of these systems to enhance building performance, and not only in new ones, but also to retrofit the oldest (Vijayaraghavan K., 2016) (Dunnett & Kingsbury, 2008). This enhancement extends beyond creating desirable indoor and outdoor environments to ensuring environmental efficiency through reduction and optimization of building energy consumption (Besir & Cuce, 2018), mitigation of urban heat island effect (Santamouris M., 2007) with substantial reduction in temperature (Santamouris M., 2014), carbon emissions sequestration (Shafique, Xue, & Luo, 2020), improvement of air pollution (Tomson, et al., 2021), stormwater management (Paithankar D. N., 2020) and provision of high-quality water increase of sound insulation, ecological preservation and breed biodiversity and dense vegetation,

In addition to the notable positive environmental impacts, greenery systems yield supplementary benefits for the public. Socially, the presence of green spaces has been extensively studied for its psychological and therapeutic benefits, fostering a deeper connection with nature, and creating a serene atmosphere, that human humour and sensibilities appreciated (Twohig-Bennett C., 2018). Economically, the visual appeal of green spaces in estates and cities contributes to the appreciation of property values, raising the price of them (Ichihara K, 2011).

Green systems primarily consist of green roofs and green walls, which encompass all vegetative cover surfaces of buildings leading to the growth of various types of vegetation. Green roofs and green walls delineate two distinct surfaces: the former situated atop buildings with a horizontal layer, while the latter manifests as a vertical layer enveloping lateral surface. Thus, the primary disparity lies in their potential installation sites, often representing a discrete selection between them, albeit with the prospect of a complementary solution.

## 2.1.1 Green roofs

Green roof, also known as eco-roofs, roof gardens and living roofs can be defined as the roofs coated with green vegetation and growing medium (Shafique, Kim, & Rafiq, 2018). It is composed by a set of layers, that protect, support and improve the system performance. From bottom to top, the lower layers are water proofing membrane, the insulation and the structural layer, than a root barrier and a protection layer, the drainage element (moisture retention) in the middle, the growing medium (substrate) and the vegetation at the upper (Besir & Cuce, 2018).
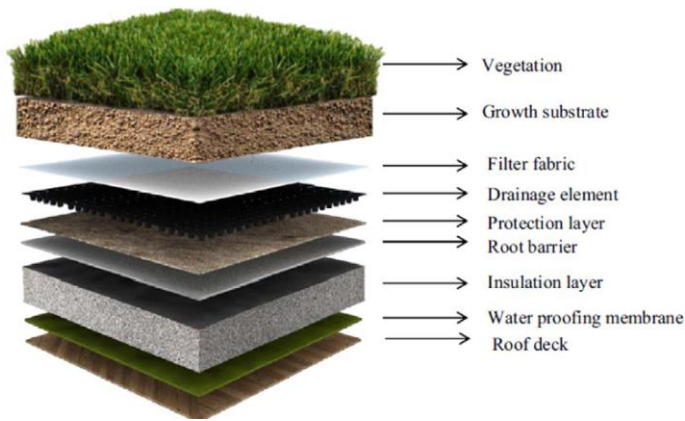
*Figure 1. Layer structure of green roof (Vijayaraghavan, 2016)*

The climatic conditions of the weather zone of interest could interfere with the decision to add some other elements or not, like the irrigation system, in arid and hot regions (Castleton, Stovin, Beck, & Davison, 2010).

Green roofs can be split in three main categories based on design characteristics, as the weight, the thickness of the substrate layer, and plant community, and economical aspect, as maintenance, cost, and irrigation system: intensive, semi-intensive and extensive roof.



*Figure 2. Classification of green roofs: extensive, semi-intensive and intensive (Besir & Cuce, 2018)*

The first one, the intensive roof, are the heavier as they have the higher substrate layer thickness, more than 150 mm, for this reason, obviously, they have also the most expensive cost and high level of maintenance services. The common types of vegetation are lawn or perennials, shrubs and trees. But as positive aspect they could be use as park like garden.

The polar opposite type is the extensive roof, which has a substrate layer smaller than 150mm, therefore lighter and cheaper, commonly they are greenery with moss, sedum, and grasses. Shallower growth substrates offer less plenty of vegetation, so, in contrary, they represent just more an ecological protection layer.

In the middle, the semi-intensive roof is more or less a green roof liveable, has periodically maintenance and irrigation, and the thickness layer, vegetation and cost are a weighing of the other two.

*Table 1. Summary classification of main aspect of the three types of green roofs (Besir & Cuce, 2018)*

|  | *Extensive* | *Semi intensive* | *Intensive* |
|---|---|---|---|
| Hight of substrate | < 150 mm | 120-250 mm | >150 mm |
| Type of vegetation | moss, sedum and grasses | grass-herbs and shrubs | lawn or perennials, shrubs, and trees |
| Use | ecological protection layer | liveable green roof | garden like |
| Cost | low | middle | high |
| Irrigation and maintenance | low | periodically | regularly |

Roofs account for nearly 20–25% of overall urban surface areas (Besir & Cuce, 2018), the great potential of green roof is to be able to cover this empty surface with vegetation with great environmental positive effects.

There are aspects as cost and irrigation requirements that make someone question, but technology improvement, some tricks and further in-depth and specific studies could upgrade these aspects, as by using local vegetation and growing medium (Bevilacqua, Mazzeo, Bruno, & Arcuri, 2016).

## 2.1.2 Green walls

Green wall is simply defined as a greenery system envelop on vertical layer. Green wall is also named as vertical greenery system, vertical garden, vertical green, vertical landscaping, and bio walls (Manso & Castro-Gomes, 2015).

There two main different systems: green façade and living wall, based on how the vegetation grows over the building (Besir & Cuce, 2018).

| **Green façade** | **Living wall** |
|---|---|
| In green facade, plants are rooted on the ground in soil and climb on facade and covers elevation. | Living walls are pre-vegetated sheets that are attached to a structural wall or frame. |
|  |  |

*Figure 3. Classification of green wall (Safikhani, Abdullah, Ossen, & Baharvand, 2014)*

Green façades are characterised by the application of climbing plants, directly against the wall, with at maximum an indirect support system along the wall (Addo-Bankas, Zhao, Vymazal, Yuan, & Fu, 2021). Plants can grow downward or upward naturally covering the walls (Timur & &

Karaca, 2013). This required a specific plant selection, counting also that they have to remain green all the year to not affect the performance and aesthetics (Perini, Ottelé, Haas, & Raiteri, 2011).

Green facades are the cheapest types of green wall systems. However, one major drawback is that plants take a long time to cover the wall completely, often more than a decade (Radić, Dodig, & Auer, 2019).

The sub-categorization splits green faced into direct and indirect facades (Safikhani, Abdullah, Ossen, & Baharvand, 2014). The key distinction is that in the first case climbing plants grow to directly cover the wall, with growing media stays on the ground. Instead, in the second case it is necessary a support structure, along which plants grow. The support structure can be as continuous type, or modular one, called respectively double-skin green façade and modular trellis (Besir & Cuce, 2018). The continuous structure consists in a single vertical structure that has an air cavity between the wall and itself. Whereas modular trellis has perimeter flowerpots for vegetation roof.
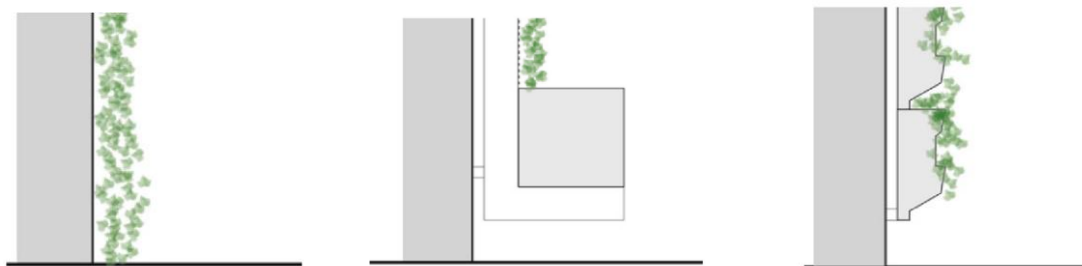


*Figure 4. Direct facade, Double-skin green facade, Modular trellis (Perini, Ottelé, Haas, & Raiteri, 2011)*

Living walls consist of pre-vegetated plants, grown on separate structural system which can be freestanding or attached to the wall (Loh, 2008), presenting as a cladding structure for coating the building façade uniformly, as plenty of plants. Due to this system of pre-cultivation, living walls offer a great variety of plants and an easy way to replace the damaged plant with the fresh one (Charoenkit & Yiemwattana, 2016).

The major distinction between green facades and living walls is that living walls are self-sufficient green walls (Addo-Bankas, Zhao, Vymazal, Yuan, & Fu, 2021).

Plant nutrients and water supply is not sourced from the ground but rather from the vertical support system (Manso & Castro-Gomes, 2015), so frequent irrigation and nutrient supply are required, and some essential material as supporting elements growing substrate and irrigation system have to be added. Therefore, maintenance costs are notably high respect green façade, that also not need this additional material. But, at the end of all, well-functioning living wall systems have a uniform growth and green appearance vegetation, obtaining better performance, being more self-sufficient (Besir & Cuce, 2018).

Also living walls are subcategorised into continuous or modular types, based on the growing media and the application method (Addo-Bankas, Zhao, Vymazal, Yuan, & Fu, 2021) (Besir & Cuce, 2018). The first case is based on a single support structure. It applies a permeable screen, the growing media is not required, as there is a geotextile membrane that works as soil substrate, and plants grow through irrigation using hydroponic techniques (Charoenkit & Yiemwattana, 2016). The second one result from the installation of several modular elements, together forming the whole greenery. It is characterised by containers carrying substrate material as soil and mineral granules, inserted into a supporting structure, one above the other, or directly fixed on the vertical surface (Manso & Castro-Gomes, 2015). result from cascading elements, affixed to the wall in a linear way (Scharf, Pitha, & Oberarzbache, 2012).
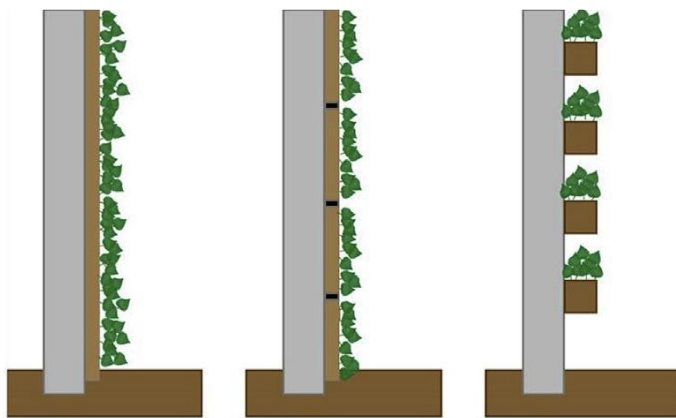


*Figure 5. Continuous or modular types living walls (Medl, Stangl, & Florineth, 2017)*

Compared to green roofs, green walls are more environmentally advantageous since they offer more area for vegetative cover, especially in modern style high rising buildings, where it could be 20 times more. (Pérez, Coma, Martorell, & Cabeza, 2014) (Kingsbury & Kingsbury, 2004).

## 2.2 Benefits

The efforts, which have been done over the past decade, are mainly conducive to mitigate the impact of human on the environment and climate through sustainable practices and the adoption of green technology and development (Jato-Espino et al., 2019).

The urban developments which act in this terms it is called low impact developments (LIDs) and it developed in recent years toward several environmentally sustainable constructions, designs and practices strategies (Zhao et al., 2018). Green infrastructure including green walls and green roofs are among the most environmentally friendly technologies for cleaning water and air in urban settlements (Addo-Bankas, Zhao, Vymazal, Yuan, & Fu, 2021). They are the most desired form of architecture in recent times with the aim of harnessing the sustainable benefits and

compensating some environmental benefits lost through urban development (Besir & Cuce, 2018).

The application of green walls has recently broadened from solely offering aesthetic values to focusing on solving urban environmental challenges (Addo-Bankas, Zhao, Vymazal, Yuan, & Fu, 2021).

Green systems at the building scale offer multiple advantages, including energy savings, reduction in sound transmission, greywater treatment, enhanced durability of building envelopes, and added property value. When implemented at a larger urban scale, green roofs and green walls can extend these benefits, amplifying their impact across the city. These systems contribute significantly to climate change mitigation and adaptation by addressing key urban environmental challenges, such as mitigating the urban heat island effect, improving water management, attenuating urban noise, and enhancing air quality. (Manso & Castro-Gomes, 2015)

In addition to these environmental benefits, green systems provide crucial ecosystem services by fostering biodiversity and addressing food security issues through their potential use in urban agriculture. Beyond their practical applications, they offer aesthetic and social benefits, enhancing the recreational value of public spaces and promoting citizens' health and well-being. (Manso & Castro-Gomes, 2015)

*Energy features*

The implementation of NBS on buildings has an impact on the thermal behaviour of buildings (Suzanne Kandel, 2024). Energy performance of a building in terms of building envelope can be described as minimising the energy requirement for heating and cooling owing to the structural properties of the envelope (Besir & Cuce, 2018). The thermal benefits of greenery systems on buildings are achieved through several mechanisms (Besir & Cuce, 2018).

These systems function primarily as thermal buffers, adding an insulating layer that reduces heat exchange between the building and the surrounding atmosphere. This means that less heat enters the building during hot periods, and less heat escapes during cold period (Nadia Saifi, 2023).

In addition, plants provide an evaporative cooling effect. Through the process of evapotranspiration, plants absorb heat and release moisture into the atmosphere, thereby cooling the surrounding air and decreasing the building's cooling load. This natural cooling effect also helps mitigate the urban heat island effect, particularly in dense urban areas, by reducing the overall ambient temperature (Alexandra Price, 2015).

Moreover, greenery systems reduce the amount of solar radiation absorbed by the building's surface, helping to lower indoor temperatures and further cut down on cooling energy consumption (Maria Manso, 2021).

Overall, based on general research and case studies reported in multiple articles on green walls and green roofs, it is possible to assess that green wall can reduce cooling costs by 15-25%, and save heating energy up to 20% (Mohammed, 2022). While green roofs have a cooling energy reduction effect by up to 75% and heating savings of 25% (Besir & Cuce, 2018).

*Air quality*

Depending on their form and dimension, plant species can sequester air pollutants and consume carbon dioxide to develop their vital functions. In that way greenery system would be highly beneficial for improving air quality through particular matter filtration, absorption of gaseous pollutants and production of oxygen (Serena Vitaliano, 2024).

Plants in green walls and green roofs capture particulate matter (PM) from the air, including dust, soot, and other pollutants. Leaves, stems, and other plant parts trap these particles, reducing their concentration in the surrounding environment, up to 40-60%, contributing air near buildings (Mamatha Tomson, 2021).

Plants absorb gaseous pollutants, such as nitrogen oxides (NOx), sulphur dioxide (SO2), carbon dioxide (CO2), and volatile organic compounds (VOCs), through their stomata during the photosynthesis process while release oxygen, improving the overall air quality making the environment healthier for people living in densely populated cities. It is studied that, in a sunny day, a green roof my lower CO2 concentration in the nearby region as much as 2% (Jian-feng Li, 2010). However, the order of magnitude of carbon sequestration is significantly smaller than for the decrease in energy consumption, for cooling and heating system (Suzanne Kandel, 2024)

By lowering ambient temperature, these systems reduce the formation of smog and decrease the formation of ground-level ozone, which typically forms at higher temperatures and are harmful to human health (Gourdji, 2018).

*Sound features*

Greenery systems can offer significant benefits in reducing urban noise and sound transmission. The combination of sound absorption, diffusion, and physical barriers provided by plants and substrate layers makes green walls and green roofs essential for noise control in urban environments. Their capacity to mitigate high- and low-frequency sounds helps create quieter, more liveable spaces.

Plants, soil, and the structural layers of green walls and roofs help absorb sound. Plant foliage, branches, and trunks scatter sound waves, dissipating sound energy and leading to diffusion. This process reduces reverberation by breaking up large, flat surfaces that would otherwise reflect sound. (A.M. Lacasta, 2016). Additionally, vertical green systems, such as green walls, can act as physical barriers, decreasing noise infiltration into buildings and surrounding areas by scattering

and blocking sound waves (A. M. Lacasta, 2018). The actual studied absorption range varied for 2/3 dB for green walls and from 5 to 20 dB for green roofs, depending on the frequencies (Gabriel Pérez, 2016).

*Water features*

Greening system, with the presence of vegetation, contribute to water runoff quality, decreasing the amount of dust, pollutants and nutrients that would be sent to the sewer system and the receiving stream (S.S.G. Hashemi, 2015).

Green systems filter water through soil and plant roots, which act as natural biofilters. Microorganisms in the soil break down pollutants, while plant roots absorb excess nutrients and contaminants. This biological filtration can significantly reduce the concentration of harmful substances such as nitrates and phosphates, improving the overall water quality (Imane Hachoumi, 2021).

New solutions and technologies for water recovery and water treatment can significantly contribute to buildings reduction of potable water consumption. Green roofs and green walls have the potential to be natural greywater treatment technologies. Their process of using plant root and porous natural media for contaminants removal is similar to other centralized solutions, as constructed wetlands and sand filtration. Their substrate and plants function as a biofilter, treating greywater through oxidation, filtration, sedimentation, adsorption, microbial assimilation and activity (Veljko Prodanovic, 2017).

Therefore, the water collected from the green systems can represent a source of water as greywater with different scopes. Providing simultaneous treatment, greywater could be a cost-effective and sustainable alternative instead of using freshwater to fulfil certain water requirements in buildings, like irrigation or toilet flushing (Snigdhendubala Pradhan, 2019).

Linked to this activity, it's the topic of water scarcity, both as resources and primary commodity. Climate change acts a crucial role in this topic since with extreme events, humans have to face with long period of scarcity and then strong events of precipitations, flooding and uncontrollable volume of water. Therefore, in addition to ensure water quality, also water management is a crucial topic (Ding, 2024).

Commonly, rainwater is drained directly to the sewage, but intense rainfall events may overload the sewage system, causing inundations (Yao Li, 2024).
Stormwater runoff is an increasing problem in urban areas due to more and more areas built and the application of ground impermeable materials, which don't help to absorb part of the water (Maria Manso, 2021).

Green walls and green roofs can help to manage in part this problem. More studies were conducted on green roofs, while green walls are still less explored for this feature.

Green roofs are known to retain rainwater and delay peak flow, thereby reduce the risk of flooding. The benefit of stormwater management depends on the system characteristics, as the roof age, slope, substrate thickness, composition, pore volume and degree of saturation, plant selection and type of drainage layer. Also, weather factors as rainfall volume and pattern determine the retention capacity of green roofs (Ayako Nagase, 2012).

Overall, extensive green roofs contribute, in average 57%, to decrease stormwater runoff, even if large variability is identified across studies. Concerning to intensive green roofs, 79% average stormwater runoff retention, which represents a 22% higher water retention capacity compared to extensive green roofs. This increase may be due to substrate depth (Maria Manso, 2021).

Several studies have also proven that green roofs have the capacity to not only retain but also have the potential to delay the peak of stormwater runoff. The capacity of vegetation to retain water, can reduce the peak flow retaining water, and avoid the immediate release of water, helping to drain the flow, and release it slowly. Peak runoff attenuation is influenced by substrate hydraulic conductivity and moisture, and by drainage system characteristics. The antecedent rainfall timing and intensity, as well as the evapotranspiration process, also interfere in the runoff behaviour (M. Uhl, 2008). Considering all studies, a 71% total average peak runoff attenuation was identified (Maria Manso, 2021).

*Envelope's longevity and property value*

Acting as a membrane, greening systems could protect the roof, bettering the longevity of it. They act as a waterproof membrane, avoid direct exposure to solar ultraviolet radiation and help to limit the diurnal temperature fluctuation of buildings external surface, having higher albedo than conventional cladding systems (Cascone, 2019). Even if green roofs could be more expensive, they often have an in-service life longer than traditional reflective materials with which are made of roofs, so the main benefits are obtained in cost-benefits analyses (Maria Manso, 2021).

According to studies, the average in-service life of current green roof systems is expected to be of 40 years. For green walls, there is still a lack of information regarding their life expectancy, as most living wall systems are recent technologies, but some estimated a duration of 50 years around (Katia Perini, 2013)

Although, many maintenance procedures and costs are to be considered: like request of irrigation, plant's pruning, and the replacement of the substrate materials and plants after a period of time, like pipes of the systems too (Paolo Rosasco, 2018).

All things considered, it is important to account that green roofs and green walls add property value to buildings. Several authors, using several methodologies, spent their attention to estimate how the presence of green spaces, like green roofs and green walls, can influence property value. Based on some results, it was determined an average increase of 8,24% (Maria Manso, 2021).

*Social and ecological function*

These systems foster biodiversity by offering habitats creation and improving ecosystem multifunctionality, which is particularly important in urban environments where natural ecosystems are often fragmented or lost (Amit Kumar, 2023).

Due to the vegetation, an improvement in fauna species is observed with the installation of NBS on buildings: the more vegetation, the more hospitable the environment is for fauna (V. Benedito Dur`a, 2023). The type of plant impacts species richness. For example, native plants attract pollinators like bees and butterflies, while green roofs and walls provide vertical habitats for birds and insects (J. Jacobs, 2023).

Such areas will delineate "biodiversity corridors" that connect fragmented ecosystems, allowing wildlife to move through urban landscapes, thus promoting genetic diversity and resilience (Flavie Mayrand, 2018).

Additionally, green roofs and green walls can be used by citizens for urban agriculture, address food security issues, reinforcing a more sustainable local production of food and reducing the community ecological footprint. The success of these solutions depends on their accessibility, maintenance needs and climate conditions (Brenda B. Lin, 2017).

Beyond these practical benefits, green infrastructure enhances the aesthetic and recreational value of public spaces, improving the overall quality of life in cities. By offering areas for social interaction, exercise, and relaxation, these spaces promote physical and mental health and well-being.

Human well-being is improved with the presence of NBS on buildings, since the presence of urban green spaces promote mental and physical health, providing psychological relaxation and stress alleviation, resulting in strong positive feelings, such as a feeling of spaciousness, freedom, or safety (Hedblom M, 2019).

Health and well-being benefits may be gained without the physical use of green space, as a positive psychological effect may derive from simply viewing a green space, even if not accessible. Natural scenery helps people to cope with stress-related psychosocial symptoms and supports a faster recovery from stress by providing pleasant visual quality (Egorov A, 2016).

The benefits of green infrastructure in urban areas are not limited to subjective positive feelings but are also evidenced by measurable improvements in physical health. Urban residents are subject to the adverse effects of excessive heat stress, which can lead to reduced sleep quality and general discomfort. Vegetation mitigates these effects by lowering ambient temperatures, contributing to reduce urban heat island (T. Kjellstrom, 2013). Additionally, the capacity of plants to absorb and reduce noise disturbances further enhances well-being by diminishing the negative impacts of urban noise pollution (Anita Gidlof-Gunnarsson, 2007).

When these aspects are considered collectively, it becomes evident that green infrastructure significantly contributes to enhancing human health and well-being in urban environments.

# 3. Experimental setup

The experimental tests were carried out at the DTU, dept. of Engineering Technology, located in Ballerup, Denmark. The experimental apparatus consists of a prospective green gutter filled with Rockflow by Rockwool's company a special type of mineral wool designed to be used in water delay systems, capable of dealing with heavy rain phenomena.

The so-called green gutter comprises a metal box filled with mineral wool. Water enters at the top of the mineral wool and flows downward through the system. Moisture sensors embedded at various levels within the porous material facilitate monitoring of the filling and emptying process based on water content.

The structure measures 4 meters in height, width 0,6 m, and depth 0,1 m. Along its elevation, 8 moisture sensors (DFRobot) divided into 2 lines of 4 are embedded within the filling material to assess saturation levels and water content. This facilitates the estimation of drainage processes and the system's water retention capacity. Real-time monitoring data was accessible through a web-based open platform (ThingSpeak®). Behind the gutter, a Digital Temperature Humidity Sensor (Fafeicy FS400-SHT3X) is positioned to monitor humidity and temperature fluctuations. The inflow and outflow are monitored using flow meters. The system presents a pump and valves used to control the flow rate according to the desired values. The inflow is pumped by a Scala-2 pump, giving the input value in litres per hour (l/h). Conversely, the outflow is measured by a flow meter 'Aquatrans AT600', which provides data in litres per second (l/s). This information paves the way for the determination of delay intervals and the duration of drainage processes.
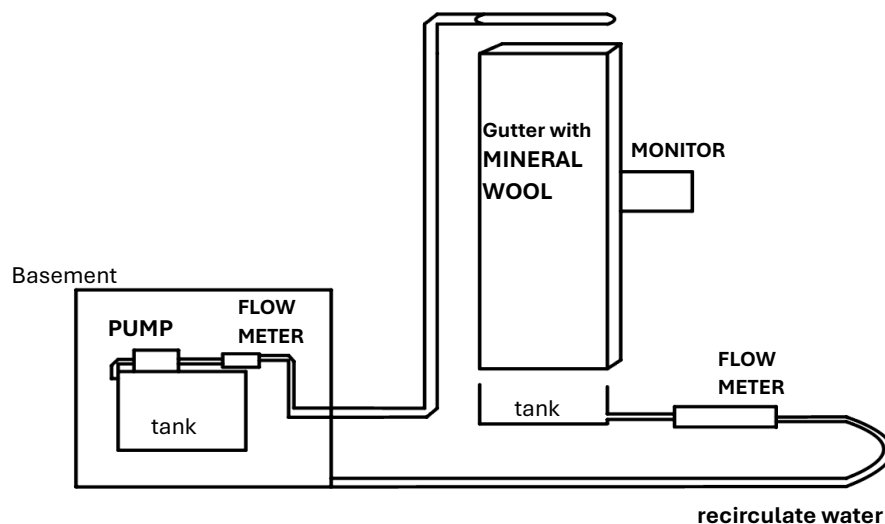


*Figure 6. Schematic diagram of the experimental apparatus*

*Figure 7. Photo representing the system: the gutter, the 8-moisture sensor numerated and on the left the screen connected to the flow meter.*

## 3.1 Rockflow by Rockwool's company

The material utilized within the gutter system is Rockflow, supplied by Rockwool. This special type of mineral wool is designed to be used in water management systems, particularly those aimed at delaying water flow to handle stormwater runoff during heavy rainfall events. Rockflow's capacity to absorb large volumes of water allows for effective rainwater management at the source, reducing the burden on urban drainage systems and creating additional green spaces in cities.

Rockwool International A/S is a Danish multinational manufacturer of mineral wool (stone wool) products. The company is renowned for its high-quality insulation products that are used in a variety of applications including building industrial insulation, and horticultural solutions.
Founded in 1937, Rockwool's headquarters is located in Hedehusene, Denmark.
Rockwool has always placed a significant emphasis on sustainability, aiming to reduce its carbon footprint and support a circular economy, designing the products to improve energy efficiency while lowering $CO_2$ emissions.
The company invests heavily in research and development to innovate and improve their product offerings. Rockwool collaborates with universities, research institutions, and other industry leaders to drive innovation. Focus areas include energy efficiency, fire safety, acoustic performance, and sustainable materials. The latter are experimented especially in new fields of research for the purpose of work out environmental issues. (Rockwool - Our heritage, s.d.).

Rockwool's decision to design Rockflow was driven by the need to address the critical urban water management challenges through an innovative, sustainable, and practical solution. It helps

cities mitigate flooding, manage runoff, and improve water quality increasing climate resilience and urban living conditions (Rethink urban water, s.d.).

Rockwool's stone wool, used in Rockflow, is an amorphous silicate produced from natural volcanic rock, primarily basalt, which is melted and spun into a highly porous and lightweight material. This material's low density facilitates easy handling and installation while providing excellent water management properties. The stone wool fibers are bound together to form a durable structure that maintains integrity under various environmental conditions and exhibits good compression resistance. The high porosity of Rockflow, with its open-cell structure, is essential for effective water absorption and retention. Additionally, the material is non-toxic and does not release harmful substances, and its waste is not considered as dangerous, as other building material. It is recyclable infinitely, moreover its solutions are designed to be long-lasting and maintain their effectiveness over time, reducing the need for frequent replacements and maintenance, supporting sustainable and circular economy principles. (Rockwool, Rockflow attenuation and infiltration systems- Durable and easy to maintain).



*Figure 8. Rockwool material*

The hydraulic characteristics that discern from that are the high-water absorption capacity with excellent infiltration rate, a well water retention capacity and controlled release, that are all linked with its high permeability. These features make the material capable of absorbing up to 95% of its volume in water, and the rapid water infiltration effectively reduces surface runoff during heavy rainfall. The porous structure of Rockflow holds substantial amounts of water and releases it slowly over time, preventing flooding and efficiently managing stormwater. This controlled release also helps recharge groundwater levels and maintain soil moisture, supporting sustainable water management. Furthermore, Rockflow's high permeability ensures that water flows easily through the material, minimizing surface pooling and enabling efficient drainage (Rockwool, Rockflow attenuation and infiltration systems- High absorption capacity).

Rockwool's production of stone wool dates back 80 years. In 2001, the International Agency for Research on Cancer (IARC) classified Rockwool products as non-carcinogenic, addressing previous concerns about their asbestos-like structure. This classification confirms Rockwool's commitment to the purpose of "releasing the natural power of stone to enrich modern living."

Rockflow offers a combination of excellent hydraulic and physical characteristics, synthesised in the Table 2 below.

| Rockflow | Value |
| --- | --- |
| material | 97% raw material basalt and recycled stone wool. |
| density | 5% |
| porosity | 95% |
| k-value (permeability/hydraulic conductivity) | 50 to 200 meters per 24 hours |
| lifespan | 50 years |

*Table 2. Physical characteristics of the mineral wool used in the experimental setup*

## 3.2 Pump

The pump SCALA2 is a fully integrated pressure booster pump, provided by Grundfos. The solution consists of pump, motor, tank, sensor, speed-regulated drive and non-return valve in the same compact unit.

The built-in sensor constantly measures the discharge pressure. If the pressure drops below the desired level, SCALA2 immediately increases the output to compensate for the pressure loss. It is called intelligent pump regulation, because SCALA2 automatically adapts to the pattern needed. The result is stable pressure (SCALA2).
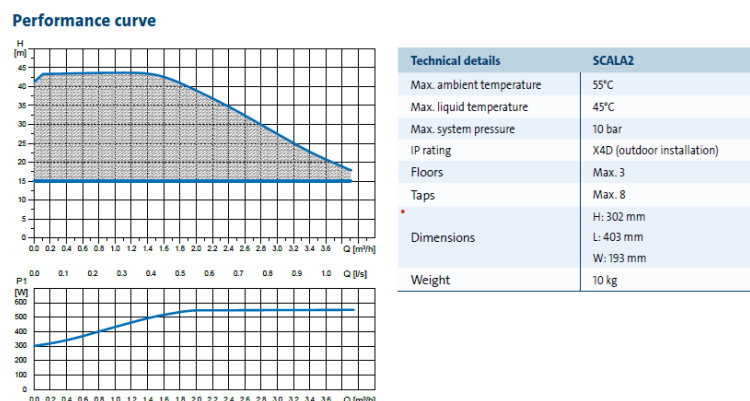


*Figure 9. Pump Scala-2 performance curve and details*

The results are directly converted and showed as litres per hour by Kamstrup Varmemåler multical®403, widely used in Denmark. It is a heat meter, with fully programmable data logger with minute logger (Kamstrup Heat meter multical®403 1.5m3/h, 110 mm with battery, return).

## 3.3 Flow Meter

GE's new AquaTrans™ AT600 clamp-on ultrasonic flowmeter is a single-path liquid meter designed to be accurate, durable, and cost-effective (Aquatrans AT600 clamp-on flowmeter).



*Figure 10. GE's new AquaTrans™ AT600 clamp-on ultrasonic flowmeter*

An ultrasonic flow meter measures the velocity of a fluid using ultrasound to calculate volume flow. The clamp-on type is a non-intrusive variety, specifically an open-channel flow meter. In this configuration, the ultrasonic element measures the height of the water in the open channel, and the flow can be determined from this measurement by knowing the geometry of the channel. The ultrasonic sensor typically includes a temperature sensor, as the speed of sound in air is affected by temperature (Ultrasonic flow meter).

Clamp probes are used with some meters to measure electrical power and energy. The clamp measures the current, while other circuitry measures the voltage; the true power is the product of the instantaneous voltage and current integrated over a cycl*e* (Current clamp).

Ultrasonic flow meters are influenced by the acoustic properties of the fluid and can be impacted by factors such as temperature, density, viscosity, and suspended particulates, depending on the specific flow meter. While their purchase price varies significantly, they are often inexpensive to use and maintain due to the absence of moving parts, in contrast to mechanical flow meters (Ultrasonic flow meter).

In this study, the acoustic aspects are not considered in the evaluation of the measurements; only the flow rate, expressed in litres per second (l/s), is taken into account.

## 3.4 Moisture sensors

'Gravity: Analog Waterproof Capacitive Soil Moisture Sensor' designed by DFRobot is a new type of waterproof soil moisture sensor.

*Figure 11. Gravity: Analog Waterproof Capacitive Soil Moisture Sensor' designed by DFRobot*

The sensor will detect soil moisture based on the principle of capacitive sensing and works with analogy output. It is waterproof and anti-corrosion.

Compared with the resistive sensor, the capacitive soil moisture sensor solves the problem that the resistive sensor is easily corroded and can be inserted into the soil for a long time without being corroded. The sensor has increased waterproof performance, and the sensor can still be used normally after being immersed in water; the length of the capacitive electrode plate is increased, and the soil moisture information can be measured more accurately. The sensor has a wide input voltage and can work in a wide voltage range of 3.3V-5.5V.

A capacitive moisture sensor operates by measuring changes in capacitance caused by variations in the dielectric material. Soil and sensor form a capacitor where the capacitance varies according to the water content present in the soil. The capacitance is converted into voltage level basically from 3.3V to 5.5V maximum. The capacitance of the sensor is measured by means of a circuit that produces a voltage proportional to the capacitor inserted in the soil. The greater is the soil moisture, the higher the capacitance of the sensor. One can then measure this voltage by use of an Analog to Digital Converter (ADC), which produces a number that can be interpreted as soil moisture (Capacitive Soil Moisture Sensor).

Because the final output value of the sensor will be affected by the depth of the soil and the tightness of the soil, only the relative humidity of the soil can be detected.

Through the Hardware 'DFRduino UNO', it has to be calibrated, recording the sensors value as "Value 1" when the probe is exposed to air. This is the boundary value of dry soil "Humidity: 0%RH". After that, taking a cup of water and inserting the sensor in, it reaches the "Value 0", and it is the boundary value of moist soil "Humidity: 100%RH". (Gravity: Analog Waterproof Capacitive Soil Moisture Sensor)

Assuming linearity, it is possible to convert these values to a "percent" of water. Just remember that, even if it is assumed in the field, in reality "dry" is not 0% humidity and "water" may not be 100% humidity, at least at the lowest values. Still, it is a useful measurement.

# 4. Design of experiments

## 4.1 Preliminary tests

The initial phase of experimentation pertains to preliminary tests conducted to ascertain the functionality and response of the system to its initial input. To facilitate this, initial data were acquired and methodologies for data processing were established.

Following, the gutter underwent testing with two distinct flow rates as input parameters. The first flow rate was tested under the minimum power setting of the pump, it is set at approximately 200 litres per hour, for a duration of 1 hour. This represents a rain event with intensity 12mm/h. These trials were conducted iteratively, with intervals of 48 hours between runs, ensuring adequate time for the system to return to its driest state.

Through these preliminary experiments, an assessment of the performance of the flow meter and moisture sensors was conducted, focusing on their data collection capabilities, and informing subsequent adjustments to their dimensions or configurations as necessary.

Further, higher flow conditions were imposed to assess the system's response under those. Therefore, two supplementary tests were executed, each spanning one hour, with the pump operating at maximum capacity. This yielded a flow rate of 400 litres per hour, double that of the preceding trials, corresponding to 25 mm/h.

Through this process, the time interval required for the system to return to its driest condition, as indicated by the moisture sensors, was determined to be approximately 4 hours from the conclusion of the preceding test.

Building upon these findings, it was decided to conduct tests lasting only 4 hours each to further understand the system's behaviour. It was observed that during the second test, the system operated in a manner consistent with the initial trial, indicating a complete resumption of its operational functions.

The second primary phase aimed to find out the maximum capacity of the system, with the objective of discerning its principal purpose. This endeavour sought to discern whether the system's primary purpose lay in water retention for subsequent use or in the attenuation of peak flow averting flood and inundation occurrence, thereby serving as a pertinent strategy for both mitigating and adapting to rainfall events.

A series of experiments were conducted to assess the system's performance under varying flow conditions. Initially, a test was carried out with a very low flow rate to determine when the first outflow would occur. However, this approach proved unreliable as it was observed that water was not effectively retained within the gutter, resulting in a delayed outflow despite the low flow rate.

Therefore, the system was subjected to its highest flow rate to discover its maximum capacity without experiencing overflow at the top of the gutters. Following trials at a flow rate of 800 litres per hour, equal to 49 mm/h, double the previous rate of the preliminary experiments, it was determined that the maximum capacity was at 1200 litres per hour, which corresponds to an intensity of 74 mm/h. This indicates that gutter will experience overflow when rainfall is larger than 74 mm, since the buffering capacity is exceeded, and the gutter cannot retain more water.

Based on these findings, attention has been directed toward addressing the challenge of high-intensity rainfall events and the capacity to attenuate and delay their peak flows. The primary focus lies in exploring the potential and effectiveness of gutter systems in mitigating the adverse impacts of such intense precipitation events. Short-duration intense rainfalls are key triggers for urban hazards, and gutters may serve as a viable adaptation strategy in the context of climate change-induced scenarios.

## 4.2 Set of experiments – constant flow rate

In the wake of preliminary tests, the framework for the actual set of experiments was established. The primary objective is to comprehend how the system works as the parameters vary. The two most influential parameters are the flow rate and the duration of event, which has to be assessed.

Adhering to engineering and statistical methodologies, it was decided to analyse these parameters through Intensity-Duration-Frequency (IDF) curves, considering two different return periods for subsequent comparison. The IDF curves were derived from literature, specifically from the book 'Aflobsteknik' (Leif Winther, 2011).This reference provides the corresponding rainfall intensity for each return period, varying the duration.

To obtain the volume per hour of rain, it is considered the roof of DTU laboratory, approximately 16 m$^2$, and multiplied it for the intensity of rain. To evaluate the total rainfall in millimetres, the intensity is multiplied by the duration, with appropriate adjustments made to the units of measurement. The same approach is applied for determining the volume of water in cubic meters, with intensity expressed in litres per hour.

The orange cells denote the intensity of cloudburst events. In Copenhagen, a cloudburst is defined as a rainfall event where precipitation reaches or exceeds 15 mm within a 30-minute period. This equates to an intensity of 30mm/h. For each return period, the first occurrence of an event exceeding this intensity threshold is identified and highlighted.

The green cells, instead, are the flow meter already tested in the preliminary tests.

| surface m² | 16.32 | | | | | | | | | |
|---|---|---|---|---|---|---|---|---|---|---|
| **Return period T** | Rainfall duration | min | 5 | 10 | 15 | 20 | 25 | 30 | 60 | 120 |
| 20 | intensity | µm/s | 35 | 28 | 24 | 20.5 | 17.2 | 14.9 | 8.6 | 6.4 |
| | volume/h | l/h | 2056 | 1645 | 1410 | 1204 | 1011 | 875 | 505 | 376 |
| | total rainfall | mm of rain | 11 | 17 | 22 | 25 | 26 | 27 | 31 | 46 |
| | volume | m³ | 0.17 | 0.27 | 0.35 | 0.40 | 0.42 | 0.44 | 0.51 | 0.75 |
| 10 | intensity | µm/s | 31 | 23 | 19 | 17 | 14.2 | 12.3 | 7.2 | 4.3 |
| | volume/h | l/h | 1821 | 1351 | 1116 | 999 | 834 | 723 | 423 | 253 |
| | total rainfall | mm of rain | 9 | 14 | 17 | 20 | 21 | 22 | 26 | 31 |
| | volume | m³ | 0.15 | 0.23 | 0.28 | 0.33 | 0.35 | 0.36 | 0.42 | 0.51 |
| 5 | intensity | µm/s | 26 | 19 | 16 | 12.8 | 10.8 | 9.4 | 5.6 | 3.3 |
| | volume/h | l/h | 1528 | 1116 | 940 | 752 | 635 | 552 | 329 | 194 |
| | total rainfall | mm of rain | 8 | 11 | 14 | 15 | 16 | 17 | 20 | 24 |
| | volume | m³ | 0.13 | 0.19 | 0.24 | 0.25 | 0.26 | 0.28 | 0.33 | 0.39 |
| 2 | intensity | µm/s | 20 | 14 | 11.4 | 9.2 | 7.8 | 6.8 | 4.3 | 2.6 |
| | volume/h | l/h | 1175 | 823 | 670 | 541 | 458 | 400 | 253 | 153 |
| | total rainfall | mm of rain | 6 | 8 | 10 | 11 | 12 | 12 | 15 | 19 |
| | volume | m³ | 0.10 | 0.14 | 0.17 | 0.18 | 0.19 | 0.20 | 0.25 | 0.31 |
| 1 | intensity | µm/s | 15 | 11 | 8.8 | 7.2 | 6.1 | 5.4 | 3.3 | 2.1 |
| | volume/h | l/h | 881 | 646 | 517 | 423 | 358 | 317 | 194 | 123 |
| | total rainfall | mm of rain | 5 | 7 | 8 | 9 | 9 | 10 | 12 | 15 |
| | volume | m³ | 0.07 | 0.11 | 0.13 | 0.14 | 0.15 | 0.16 | 0.19 | 0.25 |
| 0.5 | intensity | µm/s | 11 | 8.3 | 6.4 | 5.3 | 4.6 | 4.1 | 2.6 | 1.7 |
| | volume/h | l/h | 646 | 488 | 376 | 311 | 270 | 241 | 153 | 100 |
| | total rainfall | mm of rain | 3 | 5 | 6 | 6 | 7 | 7 | 9 | 12 |
| | volume | m3 | 0.05 | 0.08 | 0.09 | 0.10 | 0.11 | 0.12 | 0.15 | 0.20 |

Based on the obtained table, an assessment was conducted to determine which values would be compatible with the system.

Given that the maximum flow rate is 1200 l/h and the delay interval observed during the preliminary tests was nearly always 10 minutes, the highest return period was set at 5 years. This was chosen because the 10-minute test for this return period produced a flow rate close to the

system's maximum capacity. A return period of half a year, shorter than the one before, was selected to evaluate less intense but more frequent events.

Regarding duration, it was chosen to advance 10 minutes by 10 minutes, and to double the 30 minutes by 1 hour.

Therefore, the experiments were carried out with the pre-determined constant flow rate and for the corresponding durations, adjusting the values to account for the manual operation of the pump.

*Table 4. Set of constant flow tests*

| duration | min | 10 | 20 | 30 | 60 |
|---|---|---|---|---|---|
| T-5 | mm/h | 68 | 46 | 30 | 20 |
| | l/h | 1117 | 750 | 500 | 330 |
| | l/s | 0.31 | 0.21 | 0.14 | 0.09 |
| | | | | | |
| T-0.5 | mm/h | 30 | 19 | 15 | 9 |
| | l/h | 500 | 330 | 240 | 150 |
| | l/s | 0.14 | 0.09 | 0.07 | 0.04 |

## 4.3 Successive rainfall events

Thus far, the system has been tested on single and isolated events. The purpose of this new phase is to analyse the ability of the gutter to handle close events, simulating the occurrence of a new rainfall after a short break. This approach aims to assess the efficiency of the gutter system under the condition of successive precipitations. In that way, the robustness of the results obtained in the previous set of experiments are tested.

From the earlier analysis, the most extreme events were selected. The shorter and more intensity event lasting 10 minutes is followed by the 30 minutes event, which is representative of a cloudburst as defined for Copenhagen.

The sequence of events is also inverted to achieve a complete and comprehensive overview.

The interval between events is set to 1 hour to ensure that the two rainfall events are successive but not directly related.

➢ 10min-68 mm/h –- 1hour beak –- 30min-30 mm/h
➢ 30min-30 mm/h –- 1hour beak –- 10min-68 mm/h

## 4.4 Synthetic rainfall – Chicago Design Storm curve

The analysis progresses from characterizing the system and its response to a constant inflow to a more practical study involving variable intensity inflow, simulating a more realistic event.

This approach is motivated by the need to provide an initial assessment of the gutter's capacity to respond to real-world conditions. After all, in literature, numerous studies focus on the occurrence of extreme precipitation events and the resulting flooding. These studies provide storm distributions or hyetographs, which are required for the design of small storm drainage systems. Such systems are particularly sensitive to high-intensity, short-duration rainfall events, making these considerations essential for the design of hydraulic structures. (Manel Ellouze, 2009).

A storm hyetograph is a graphical representation of the variation of precipitation with time. Various methods for generating design storm hyetographs are available in the literature (Daniele Veneziano, 1999). In this context, this study assumes a triangular shape to represent and simulate the rapid rise and sharp peak of the rainfall hyetograph, since the storm floods are associated with sudden occurrence and rapid rise of precipitation events. (D. Penna, 2013)

The proposed triangular-shaped design storm, which is expected to fit rainfall time distribution, is defined through the Chicago Methods, mainly used in Denmark to represent hyetograph.
The "Chicago Design Storm" or "Chicago Method" was proposed by Keifer and Chu (1957) to calculate design rainfalls of urban storm water infrastructures. The method establishes two analytical equations for rainfall intensity over time, one valid before the peak rate and another valid after peak, both deduced from an IDF (intensity-duration-frequency) analytical expression, preserving the same volumes of all rainfall intensities. (Calculating Hyetograph from Chicago Storm Data, s.d.)

The three scenarios proposed refer to 30-minutes event, 1-hour event and 2-hours event.
The first choice was made respect the peak intensity, that was chosen for 68 mm/h for 10minutes, being the highest event tested for the gutter. Then, the CDS-Chicago Design Storm curves where designed thanks to a workbook provided by DTU university.

# 5. Analysis of data

The data are collected and processed using Excel tools.

Data were organized in a excel workbook and arranged into separate tables for each experiment. The outcomes from ThinkSpeak provided the flow rate in liter per second at each recorded time point. Therefore, the table is created accounting several columns.

The first ones regarding the time: one is to convert hours into minutes, the next one to evaluate the minutes elapsed from the beginning of the experiment, and the next one from the stopping of it. Next to them, there is the column with the corresponding flow rate in liter per second, and next one that indicate the corresponding percentage of the flow rate relative to the inflow rate. Firstly, the values are plotted in a time-series graph to analyse the flow pattern, enabling the calculation of interval times.

The fluctuations of measurements due to instrument precision are strongly evident on the graph. Two main actions are computed on it. The first addresses null flow measurements due to electronic interruptions, which are easily removed manually. The second action defines a mean behaviour during the phase where noise and outliers are more present. In particular, this phase corresponds after the filling process and before the emptying process, when the flow rate reaches an average value. This one will be calculated and indicated as the maximum flow rate of that experiment, therefore the peak.

When the maximum flow rate is more or less reached, the curve exhibits a plateau behaviour on the graph. This occurs because the gutter is completely full, the material inside is saturated, and the water simply passes through it. The maximum flow rate is reached, and fluctuations are attributed to water bouncing inside the tank before the flow meter, and turbulence at the flow meter. Therefore, the analysis calculates the average flow rate values within this interval, leading to a plateau-like behaviour.
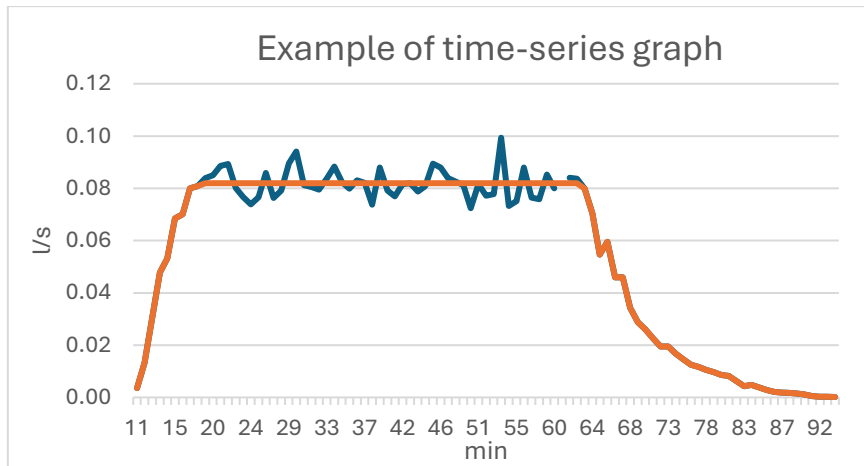
*Figure 12. Example of time-series graph with the evaluation and definition of plateau behaviour during the saturation phase*

This plateau value represents the maximum percentage of flow rate achieved during the event, and so the 'peak flow'.

This assumption is supported by analysing what happen with the filling process. Indeed, it can be observed that after the filling process, when the material is saturated, the function of the gutter effectively ceases. This remains the case until the end of the test run, when the pump is stopped, halting the flow of water, and there is no more incoming flow. Since the rockwool is saturated, it cannot retain additional water, which simply passes through.

The gutter is capable of delaying the water flow until saturation is reached and can delay the release of water after the stop. These two main goals are addressed by the following analysis.

As a result of all, the main template of the whole table is showed in the Figure 13.

| **Test** | hours as minutes | min spent since start | min spent since the stop | flow meter (l/s) | percentage | behaviour |
|----------|------------------|-----------------------|--------------------------|------------------|------------|-----------|

*Figure 13. Template of data analysis table*

## 5.1 Parameters evaluated

Regarding data from the flow meter, the primary focus lies in assessing the time taken to achieve the outflow corresponding to the maximum flow rate provided as input, and subsequently emptying the system. This aims to comprehend the system's capability to delay the arrival of peak flow and retain water during the emptying process.

The delay time is assessed in three steps:

1) When the system attains the 50% of its maximum flow rate
2) When the system reaches the 70% of its maximum flow rate
3) When the peak flow it is achieved

At first approach 80% of its maximum flow rate was evaluated, but the fluctuations of the instrument measurements at the maximum flow rate comprehend many points around 80%, so the evaluation wouldn't be clear considering it as a parameter.

Conversely, the empty process, characterized by a smoother transition, involves multiple steps, progressing through flow rates of 50%, 30%, 20%, 10%, and ultimately, null flow.

The maximum flow rate, respect which the percentage is calculated, is determined by assessing the average inflow value. It is expressed in litres per hour, so it is converted into litres per second.

Subsequently, the percentage is computed as follow: $\% = 1 - \frac{\text{max flow} - \text{instantaneous flow}}{\text{max flow}}$ .

Regarding the moisture analysis, which will be deeper performed in a dedicated paragraph, chapter number 8, the focus is primarily on evaluating the time necessary to be almost dry again, meaning that the system is again available to receive water and resume its operational functions.

The data are as well plotted on time-series graph, considering as 'time 0' the moment in which the pump is stopped. Therefore, the evaluation of intervals is based on the minute elapsed since the gutters didn't receive water anymore.

The analysis is similarly conducted by assessing the percentage of moisture recovered. The moisture value taken as the reference for calculating the percentage is determined for each sensor. Specifically, it is derived from the average value recorded during the ten minutes preceding the initiation of the test, as this period is deemed to represent the stable condition of the system.

## 5.2 General statistics

The parameters for the statistic description encompass all outcomes of the analysis.
It is assessed the average time interval, in minutes, from the beginning of the test until reaching 50% of the maximum flow rate, followed 70% of the flow rate value and the peak.
Similarly, for the emptying process, the average time interval is calculated for when the flow rates decrease through 50%, 30%, 20%, 10% and finally, to a null flow.

After determining the average values, the respective standard deviations and medians are calculated. Additionally, the maximum and minimum values are highlighted.

With this analysis is possible to obtain a general overview of the system's behaviour, understanding the expected outcome variations.
By computing key metrics such as the average, standard deviation, median, maximum, and minimum values, trends, patterns, and insights are identified.
Through the average value, it is researched a central tendency to individuate a typical datapoint within the dataset. The reliability of that point is evaluated through the standard deviation, which

will allow to gauge the variability and dispersion, providing insights into how spread out the data points are relative to the mean. With the median, it is offered an additional perspective on central tendency, by representing the middle point of the dataset that is less affected by outliers and skewed data. After the description of the central tendency, evaluate the maximum and minimum value, will help to understand the upper and lower boundary, identifying the highest and lowest point within the data range that can be assumed.

This provides a description of the data with more than one value useful to reinforce and give an idea of the consistency and straight of the statistical values.

Data were organized in a excel workbook and arranged into separate tables for each experiment, as the one provided by the data analysis. Therefore, the outcomes from ThingSpeak, providing the flow rate in litres per second at each recorded time point, are ordered in six columns: one to convert hours into minutes, the next one to evaluate the minutes elapsed from the beginning of the experiment, and the next one from the stopping of it, another column for the corresponding flow rate in liter per second, one for the percentage of the flow rate relative to the inflow rate, and a final column labelled "behaviour". This one, created throughout data analysis, accounts the pattern of the flow rate, avoiding the noise and outliers due to the instrument measurements.

With all the tables filled, the key statistic parameters are computed respectively for each outcome of analysis. For the computation it is considered the time for the first value equal to or greater than the percentage of interest: if the value is immediately greater than the subsequent reference percentage, it is not considered, if it does not reach this percentage, it is not considered.

For what concern the determination of null flow, due to its high sensitivity to instrument precision, it is not the most reliable parameter to consider. Nevertheless, the first time point where a 0% flow rate is established is chosen. In cases of oscillation, the last recorded value by the flow meter is used as the reference point.

The two variables that determine the computation, minutes and percentage, were considered with decimal error, and it is considered the unit number, accounting systematic and casual errors.

## 5.3 Constant flow rate tests

The analysis of the main set of experiments based on a constant flow input varying the duration aims to identify differences and similarities between events with the same duration but different flow rate, or same flow rate but different duration.

The study moves on the insights of IDF curves, taking into consideration the singular events.
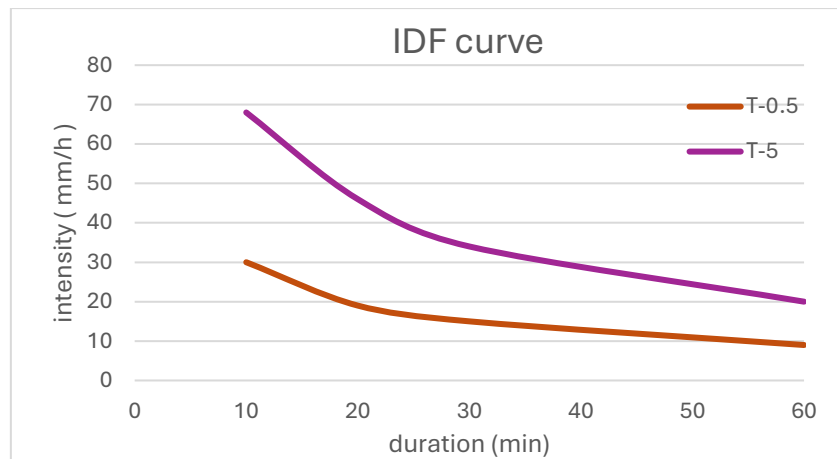


*Figure 14. IDF curves representation*

The IDF curves were derived from the book (Aflobsteknik, 2011), and the singular events considered are highlighted in Table 5.

*Table 5. Singular events chosen on IDF curves*

| T-0.5 | *duration* | mm/h | | T-5 | *duration* | mm/h |
|---|---|---|---|---|---|---|
| | 10 | 30 | | | 10 | 68 |
| | 20 | 20 | | | 20 | 46 |
| | 30 | 15 | | | 30 | 30 |
| | 60 | 9 | | | 60 | 20 |

For each event, two experiments were conducted per day, the second taking place 4 hours after the first one was interrupted. Since the first experiment was performed on a completely empty gutter, the primary analysis focuses on it. On its side, the second experiment is taken in consideration to consolidate the first result and in case evaluate any differences or similarities in the system's response to the same event occurring after a few hours.

The main parameters evaluated are the arrival delay times for 50%, 70% of the maximum flow rate and the peak, which characterize the filling process. Analogously the targets for emptying process are considered. These include the time required to retain 50% of the inflow rate, followed by 30%, 20%, and 10%, and finally, the time when all is released and null flow rate as output is obtained.

The time interval is determined by referencing the time point of the first value recorded by the flow meter and the time point corresponding to the zero-flow condition. Because of the instrument's accuracy in estimating 0%, the zero-flow point is when only 10% of the maximum flow still needs to be drained. The difference, measured in minutes, represents the duration of the

event, reflecting the gutter's response, including the delay and smoother release of water. This provides an initial indication of how the precipitation event is managed differently due to the gutter system, which mitigates the abrupt impact of the rainfall event. Through this time interval the damped intensity is thereby calculated.

Moreover, some additional control parameters are computed to gain control of the analysis: the runoff coefficient and the peak reduction.

The runoff coefficient is a dimensionless coefficient that relates the volume of stormflow to the volume of rainfall that generated it, quantifying the portion of precipitation converted into runoff (Christian Massari, 2023). In this analysis, the runoff coefficient is calculated as the ratio between the volume of water measured by the flow meter (represented by the area under the flow meter curve) and the volume of water supplied by the pump (represented by the area under the inflow curve). This parameter is critical for the design of flood control channels and delineation of potential flood hazard zones. Larger values indicate higher runoff and lower infiltration. A high runoff coefficient suggests areas susceptible to flash flooding during storms, as water moves rapidly over the surface (Board, 2011). The runoff coefficient is influenced by several factors, including land cover, topography, soil type, and basin hydrology. Typical values are provided in Table 6.

*Table 6. Guidelines for surface runoff coefficients by the Ministry of Education, Culture, Sports, Science and Technology, Japan. (Atsushi Tsutsumi, 2004)*

| Type of ground surface | Coefficient of surface runoff |
|---|---|
| Road: | |
|     Pavement | 0.70-0.90 |
|     Permeable pavement | 0.30-0.40 |
|     Gravel road | 0.30-0.70 |
| Shoulder or top of slope: | |
|     Fine soil | 0.40-0.65 |
|     Coarse soil | 0.10-0.30 |
|     Hard rock | 0.70-0.85 |
|     Soft rock | 0.50-0.75 |
| Grass plot of sand: | |
|     Slope 0-2% | 0.05-0.10 |
|     Slope 2-7% | 0.10-0.15 |
|     Slope 7% | 0.15-0.20 |
| Grass plot of clay: | |
|     Slope 0-2% | 0.13-0.17 |
|     Slope 2-7% | 0.18-0.22 |

| | |
|---|---|
| Slope 7% | 0.25-0.35 |
| Roof | 1.00 |
| Unused bare land | 0.20-0.40 |
| Athletic field | 0.40-0.80 |
| Park with vegetation | 0.10-0.25 |
| Mountain with a gentle slope | 0.30 |
| Mountain with a steep slope | 0.50 |
| A paddy field or water | 0.70-0.80 |
| Farmland | 0.10-0.30 |

Peak reduction is defined as the complement of the percentage of the peak outflow relative to the inflow, calculated as the ratio between the maximum outflow rate and the inflow rate. This could mean a reduction in the intensity of the outflow rate. However, upon further analysis, the observed variations primarily reflect differences in instrument precision rather than a real-physical reduction in peak flow, except for the 10-minute events where a real reduction is observed.

The analysis of tests begins with a fast overview of the output of preliminary tests, where a same duration test of 60minutes was tested with different amount flow rates. This can give a first easy visualization of the dependence respect the flow intensity. Then the real analysis of the set of experiments starts with an overview of the results for each single event, comparing the ones with the same duration but with different return periods (T), which correspond to varying amounts of constant flow rates. Following this initial analysis, events with the same flow rate across different years are examined to assess the dependence of the system's behaviour on the event duration.

Subsequently, experiments related to the same return period are aggregated to observe how the parameters vary on the IDF curve.

## 5.4 Successive rainfall tests

The study of successive rainfall events pay attention to evaluate the robustness of the system. Basically, the main analysis is made through the comparison of the delay time parameters between tests conducted under successive rainfall conditions and those performed without preconditioning, referred to as "single event" tests.

The objective is to determine whether the delay time remains consistent, indicating a robust system that behaves similarly regardless of prior rainfall, or if there is a significant reduction in delay time during successive rainfall events. A shorter delay time in successive events would suggest a reduced capacity of the gutter to manage runoff if it has already experienced a prior rainfall event.

A table, such as Table 7. Table for analysis of successive rainfall eventsTable 7, is utilized to summarize the results and facilitate comparisons.

*Table 7. Table for analysis of successive rainfall events*

| | Duration and input flow rate | |
|---|---|---|
| **successive rainfall** | | single event |
| Delay 50 % | | |
| Delay 70% | | |
| Delay 100% | | |
| Peak reduction % | | |
| Empty till 50% | | |
| Empty till 30% | | |
| Empty till 20% | | |
| Empty till 10% | | |
| Completely empty | | |

## 5.5 Synthetic rainfall - CDS curve

The analysis of synthetic rainfall highlighted the capacity of the gutter to deal a more realistic precipitation event, described by a triangular hyetograph.

The main parameter evaluated is the dump of intensity. This value is evaluated through the percentage of the ratio between the intensity obtained over the intensity of the event.

The intensity, obtained through the smoothing effect of the gutter system, is calculated by considering the time interval between the first value and the last value recorded by the flow meter. This interval represents the adjusted duration of the event, as influenced by the performance of the gutter system.

Moreover, the cumulated input and output volume and the respective curves are computed to visualize how the outflow is distributed over time. A flatter curve of output volume indicates slower flow.

The cumulative volume of inflow and outflow is calculated by summing the flow measured at each time interval. The flow is expressed in terms of flow rate (litres/second). The volume is obtained by multiplying the flow rate by the time interval, then summing the successive volumes over time. Following, the runoff coefficient $C_d$ is calculated since it relates the amount of water leaving the system to the amount of water entering it. If $C_d < 1$ indicates that the system has retained some of the water, while a $C_d = 1$ indicates that all the incoming water has been released.

If $C_d > 1$, indicates that the system released more water than it entered (an uncommon situation in natural scenarios) and this mean that some errors occurred in the computation.

# 6. Results and discussion section

## 6.1 Descriptive statistics

The aim of this initial evaluation is to provide a comprehensive overview of the system's behaviour, offering an indicative understanding of expected outcome variations, getting the description of the distribution of the data.

Key metrics of the general statistical analysis, such as average, standard deviation, median, maximum, and minimum values reveal trends and patterns in the data. The average indicates central tendency, which reliability is assessed through the standard deviation and the median. The former evaluates the variability and dispersion relative to the mean, while the latter offers an additional measure of central tendency that is less affected by outliers. Evaluating the maximum and minimum values helps establish the upper and lower boundaries of the data range.

The statistical parameters encompass all outcomes of the analysis. The average time intervals, measured in minutes, are calculated for reaching 50%, 70%, and peak maximum flow rates from the start of the test, as well as for the emptying process at 50%, 30%, 20%, 10%, and zero flow rates.

At first step, the analysis was concentrated on the results that comprehend all the runs of the set of experiments extrapolated by IDF curves, with different amount of constant inflow rate and the corresponding duration, presented in *Table 4. Set of constant flow tests.* The results of general statistical analysis of them are presented in Table 8.

Later the analysis moves on comparing graphically also the statistical results obtained on preliminary tests, which last all 60minutes, in order to assess the filling and emptying process starting to evaluate how them deviate from the overall results of Table 8.

*Table 8. Statistical results for set of experiments derived by IDF curves with different amount of constant inflow rate and the corresponding duration*

| Filling process | Delay 50 % | min | Delay 70 % | min | Delay peak% | min |
|---|---|---|---|---|---|---|
| | Mean value | 12 | Mean value | 13 | Mean value | 15 |
| | St. deviation | 2 | St. deviation | 3 | St. deviation | 5 |
| | Median | 12 | Median | 13 | Median | 14 |
| | Minimum | 9 | Minimum | 8 | Minimum | 8 |

| | Maximum | 18 | Maximum | 19 | Maximum | 27 |
|---|---|---|---|---|---|---|

| Emptying process | Empty till 50% | min | Empty till 30% | min | Empty till 20% | min | Empty till 10% | min | Completely empty | min |
|---|---|---|---|---|---|---|---|---|---|---|
| | Average | 7 | Average | 9 | Average | 12 | Average | 17 | Average | 39 |
| | St. dev. | 2 | St. dev. | 2 | St. dev. | 3 | St. dev. | 3 | St. dev. | 8 |
| | Median | 7 | Median | 10 | Median | 12 | Median | 17 | Median | 39 |
| | Minimum | 4 | Minimum | 5 | Minimum | 6 | Minimum | 10 | Minimum | 25 |
| | Maximum | 9 | Maximum | 13 | Maximum | 18 | Maximum | 24 | Maximum | 54 |

The first notable outcome is the delay in reaching half of the inflow rate, which consistently exceeds 10 minutes. This indicates effective control of the rain event.

The reliability of those results is supported by the low variability observed, given the acceptable low value of standard deviation, and the corroboration through the median and minimum values. Looking at the maximum it could be even higher than 10 minutes in some cases.

These insights suggest paying more attention in the extreme events characterized by short duration and high rainfall intensity, the ones lasting 10-minute.

When evaluating the delay time in reaching the peak flow rate, despite the higher mean value and increased standard deviation, the key value of interest is the minimum delay. This minimum delay, which does not fall below 8 minutes, demonstrates that even in the case of 10-minute events, the peak flow rate is generally delayed until the event has nearly or completely concluded.

The standard deviation, that indicated the variation of the values around the mean value, tends to rise in value, with the highest variation in time observed to reach peak flow. This is the parameter with the most variability among all, since it depends on both the amount of the flow rate and the duration of the event. The average delay is 15 minutes, but it varies from a minimum of 8 minutes to a maximum of 27 minutes, demonstrating substantial huge variation. The largest delay occurs in the 60-minute test with a constant flow of 0.04 l/s, that is a rain intensity of 9 mm/h, the lowest one.

This result show that the delay time depends on the duration of the event obviously, but also on the amount of input flow rate.

This assumption is properly corroborated by the statistical analysis of the preliminary test, in which for the same duration of the experiment, 60 minutes, different amount of flow rate are given as input.

With lower flow rate 200 l/h, equal to 12 mm/h of rain intensity, the peak arrival time is longer, approximately among 20 minutes. When the gutter was tested to estimate its maximum capacity with the flow rate equal to 1200 l/h, representing a rain intensity of 74 mm/h the peak is reached in just 10 minutes.

## 6.1.1 Assessing the filling and emptying process

On the graph, the preliminary tests statistic results are compared with only the statistical results of all the tests of the previous set that last 60 minutes plus themselves (denominated '60min tests'), and the one refereed to all the tests again of Table 8 (denominated 'constant flow rate'), in a way to understand the compatibility of tests that last the same interval of time and to compare again them respect a general overview of all the tests.

Computing the mean of all the test lasting 60 minutes, the average time of reaching the peak is assessed on 19 minutes, with average rain intensity of 23 mm/h. It is evident the contribution to increase the mean time of the four more tests in addition of the preliminary ones, since they have lower flow rate. This is clearly evident in Figure 15.
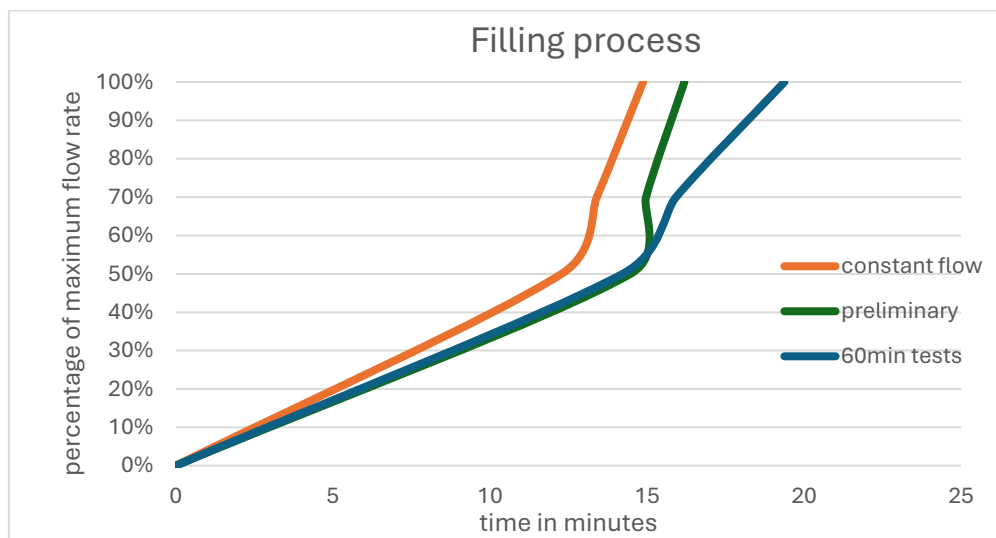


*Figure 15. Average value of filling process evolution*

Generally, it is possible to describe an initial slower filling of the gutter until 50% of the maximum flow rate, immediately 70% is approached, and then 100% is smoothly reached, but less respect the initial phase. The curves overlap for most of the initial phase, with the most significant divergence occurring at the peak. This indicates a strong dependence on the flow rate intensity in the last phase of filling, as the only variable differentiating the two set of tests represented by the

blue and green curves is the input flow rate. The blue curve also includes tests conducted with the lowest flow rate, which significantly impacts reducing the arrival time.

Regarding the emptying process, the release is gradual, decreasing monotonically and taking more than 30 minutes to reach a null flow. The initial release after the interruption of the test is rather faster: 50% of the flow rate is released within 7 minutes after stopping, but it is followed by a smoothly release. Figure 16 show the behaviour of the curves.

The large standard deviation observed at the zero-percentage value is likely attributable to the precision limitations of the instrument, rather than the inherent characteristics of the phenomenon itself.
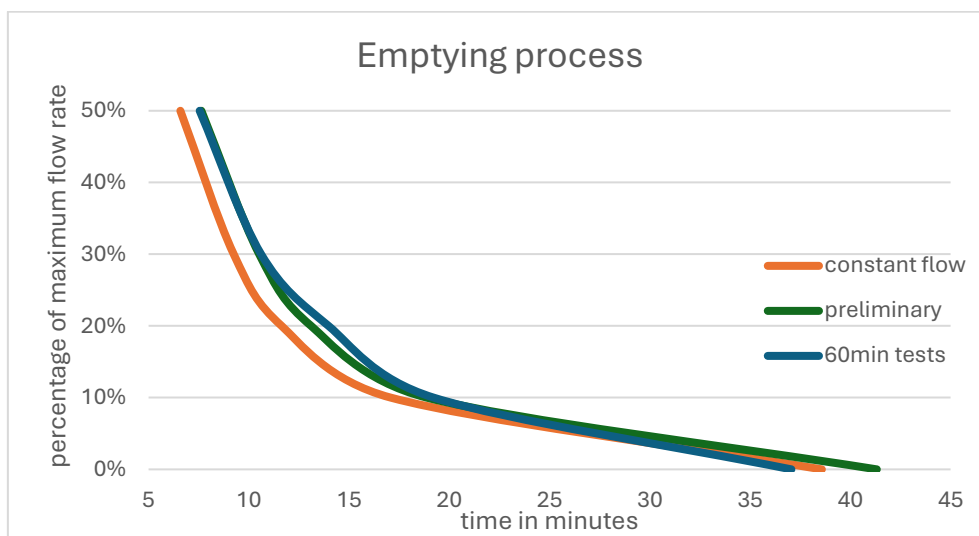


*Figure 16. Average value of emptying process evolution*

Despite the significant variation in the maximum and minimum values across all parameters, the curves exhibit a consistent overall behaviour. The single difference is observed at the onset of the curves, where the initial phase of the emptying process appears to be influenced by shorter duration of the constant flow sets. Indeed, the lower value of the constant flow may be associated with the highest intensity rainfall. Meanwhile the later stages of the process show convergence across all curves, suggesting that the emptying process is predominantly governed by the properties of the porous material.

While the first faster release might seem suboptimal at first glance, the delay time accumulated before, likely allows sufficient time to manage this flow. Additionally, the faster emptying of the gutter ensures it will be ready again and efficient for the next event. The analysis of that will be performed deeply with the moisture sensor results too.

An additional deeper analysis of the gutter's response could be conducted by focusing on the constant flow rate set of experiments, distinguishing between the first and second runs. It is

important to note that these runs were performed on the same day, with the second run conducted four hours after the completion of the first.

The graph obtained with the general statical analysis are reported in Figure 17Figure 17.
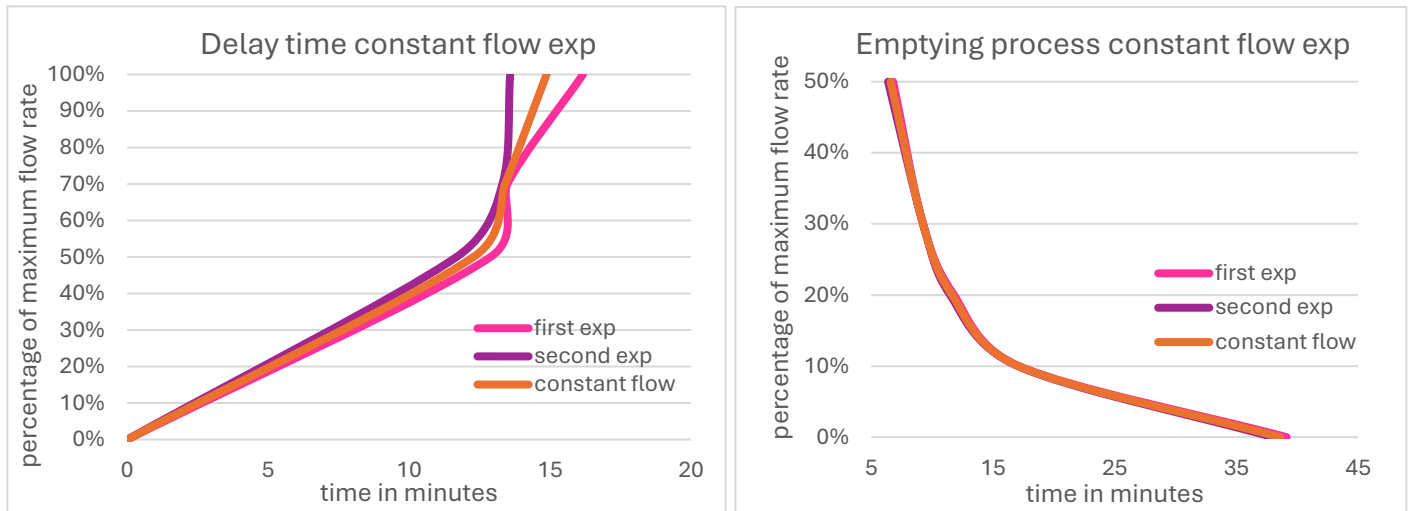


*Figure 17. Filling and empty process for constant flow rate tests*

An initial analysis of the delay time reveals what already evidenced: the curves are completely overlapping in the initial phase. Subsequently, all average values in the second run are lower than those in the first. This indicates that the filling process in the second experiment occurs more quickly, while the first experiment exhibits a slower and smoother response. Specifically, the first run maintains a consistent overall behaviour with a more gradual arrival time, whereas the second run shows a steeper increase after the 50% mark, rapidly reaching the peak. These findings suggest that, after a 4-hour interval, the gutter remains functional, although its efficiency in delaying water flow is reduced.

Regarding the emptying process, the behaviour and values are remarkably similar, with the response curves completely overlapping. This indicates that the porous material releases water in the same manner, even after just a 4-hour interval. This lays the groundwork for future studies to identify a model for the emptying equation also using moisture analysis.

## 6.2 Constant flow rate tests

The analysis of the main set of experiments, which involves a constant flow input with varying durations, begins with a preliminary overview of outputs from tests of 60-minute durations at varying flow rates, illustrating dependence on flow intensity. This is followed by detailed comparisons of results for events with the same duration but different return periods and, subsequently, events with the same flow rate over different years. Finally, experiments related to the same return period are aggregated to observe variations in parameters along the IDF curve.

The main scope is to identify differences and similarities between events with the same duration but different flow rates, and vice versa. This study draws insights from IDF curves and considers individual events, with two experiments conducted per day—one starting with an empty gutter and the second occurring four hours later. The primary focus is on the first experiment, while the second serves to validate findings and assess the system's response over time, so it is reported in the table just for completeness.

Key parameters evaluated include arrival delay times for 50%, 70%, and peak maximum flow rates, as well as the time required for the emptying process to reach 50%, 30%, 20%, 10%, and zero flow rates. The duration of each event is determined by the time from the first flow meter reading to the zero-flow condition, reflecting the gutter's response through the damped intensity. Just for this purpose, two other control parameters are calculated such as runoff coefficient and peak reduction.

From the Excel workbook already filled with general static analysis, the timeseries graph for each single experiments are created with input flow rate provided by the pump and the output flow rate, which is already analysed, and it is provided by the column 'behaviour'.

For sake of simplicity, the analysis will start with 60-minutes tests where the behaviour is clearer. It will then proceed to the 30-minutes and 20-minutes tests, where the shorter duration begins to show some variations. Finally, the 10-minute events will be examined, as they demonstrate significant results in terms of the gutter's efficiency.

## 6.2.0 Preliminary tests

Through the graph is possible to have a preliminary prompt visualization of the gutter's capacity to delay flow and manage the emptying process relative to the input flow rate. All preliminary tests were conducted over the same duration of 1 hour (60 minutes)1 hour, 60 minutes. With the duration fixed, the system's dependence on the input flow rate can be analysed.
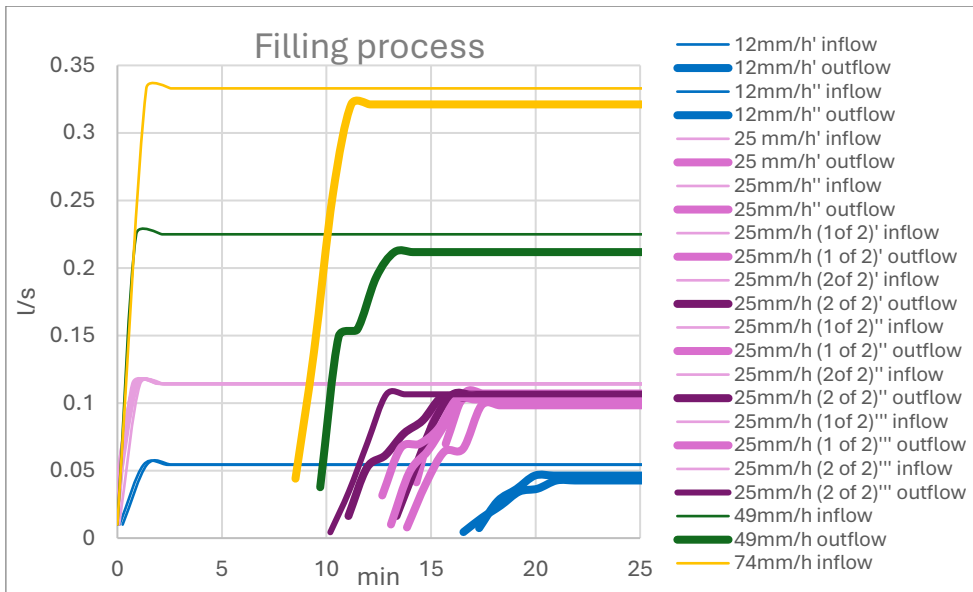
*Figure 18. Preliminary tests inflow-outflow, to assess the filling process influence dependence parameter*

The chart was zoomed on the first few minutes to focus on the inflow delay time.

Depicted are finer and in the background the inflow curves, thicker and in front the outflow curves. On shades of purple, all tests conducted with an intensity of 49 mm/h (inflow rate of 400 L/h) are displayed. The darker ones represent the second run of the day, performed just 4 hours after the first, which allowed for an evaluation of the system's response after the lag of time that the moisture sensors indicated that more than 70-80% of the drier conditions had been restored.

This analysis is highly effective, providing a clear visualization of the delay time's dependence on the inflow rate. To higher flow rates correspond shorter interval of time, since larger and the faster arriving of water produce an accountable shorter delay. Accordingly, the first curve to rise up is the yellow curve, corresponding to an inflow rate of 1200 l/h, followed by the green curve of 800 l/h, then all the purple curves, to ending with the lowest inflow of 200 l/h, the blue curves.

As previously highlighted in the general static analysis, the delay time for the second runs of the 25 mm/h tests is shorter, indicating reduced gutter efficiency.

Overall, the results are promising, as the flow is consistently delayed, even for higher inflow rates, with delay times proximal to 10 minutes.

These reasonable outcomes provide valuable insight as the constant-flow experiments analysis has to begin, offering an initial idea of what trends can be anticipated.
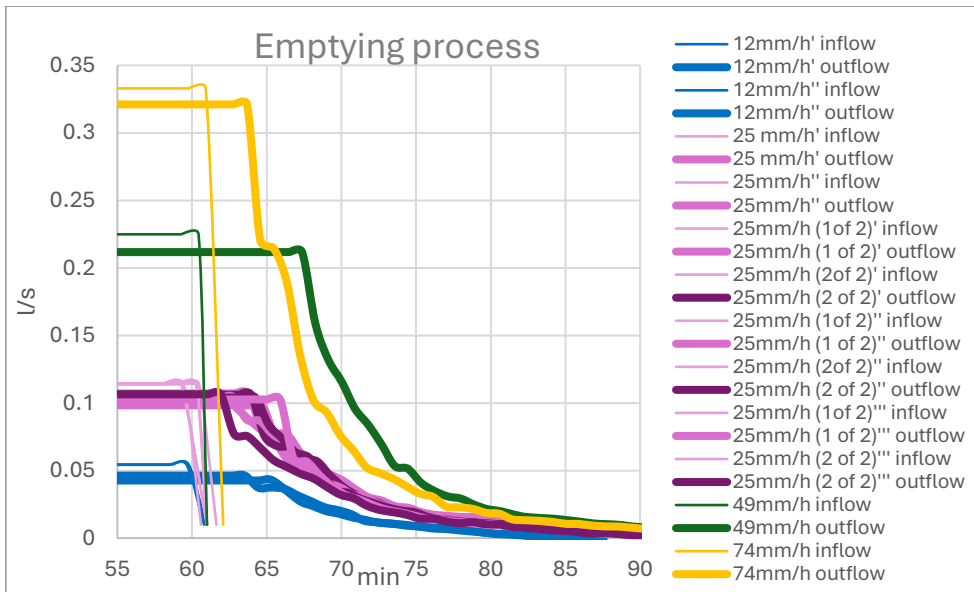
*Figure 19. Preliminary tests inflow-outflow, to assess the emptying process influence dependence parameter*

With the exception of few bumps, the curves are all very similar, with a pattern that mirrors and ends up overlapping in the final minutes. A first impression is that the lower flow rate can be maintained for longer after the test is stopped, inducing the decrease of the curve later in time.

As mentioned in the statistical analysis, the emptying process is more intuitive and easier to deal with. Depending for the most part on the properties of the material, only by some margin on the boundary is it really influenced by the test parameters.

## 6.2.1 60-minutes tests

Figure 20 presents the results of inflow and outflow for the constant flow tests with a duration of 60 min.
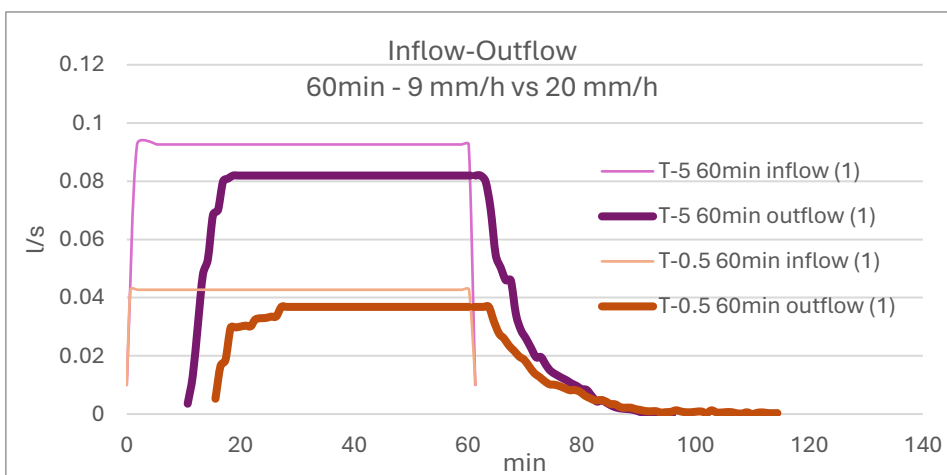


*Figure 20. Inflow-outflow of 60-minute tests*

Both experiments exhibit very similar behaviour, with the sole difference being the slower filling and releasing observed in the lower flow rate. The time interval of both events indicates that precipitation is extended by approximately 10 minutes beyond the initial 60 minutes of rainfall, suggesting that the event's intensity is attenuated of approximately 10%.

The second test in both cases demonstrates a reduction in average time, likely due to the pre-conditioned state of the gutter, but the attenuation of intensity is still consistent.

*Table 9. Parameters values for 60-minutes tests*

| | T-0.5 | | T-5 | |
|---|---|---|---|---|
| | 60min – 9mm/h | | 60min – 20mm/h | |
| | **first run** | *second run* | **first run** | *second run* |
| Delay 50% | **18** | 15 | **13** | 10 |
| Delay 70% | **19** | 18 | **15** | 12 |
| Delay peak | **27** | 21 | **19** | 14 |
| Empty till 50% | **9 after** | 7 after | **8 after** | 7 after |
| Empty till 30% | **13 after** | 10 after | **10 after** | 10 after |
| Empty till 20% | **18 after** | 14 after | **14 after** | 11 after |
| Empty till 10% | **24 after** | 17 after | **19 after** | 17 after |
| Completely empty | **54 after** | 28 after | **32 after** | 30 after |
| Interval time | **69** | 64 | **68** | 68 |
| Damp intensity | **12%** | 6% | **12%** | 12% |
| Runoff coeff. | **0.78** | 0.75 | **0.83** | 0.83 |
| Peak reduction | **14%** | 18% | **12%** | 15% |
| Max average % | **86%** | 82% | **88%** | 85% |

## 6.2.2 30-minutes tests

Figure 21Figure 21**Error! Reference source not found.** presents the results of inflow and outflow for the constant flow tests with a duration of 30 min.
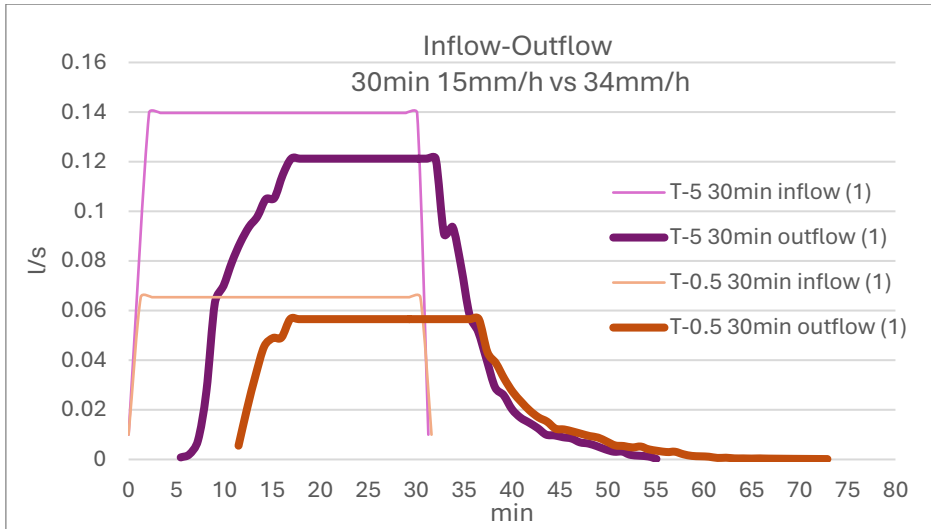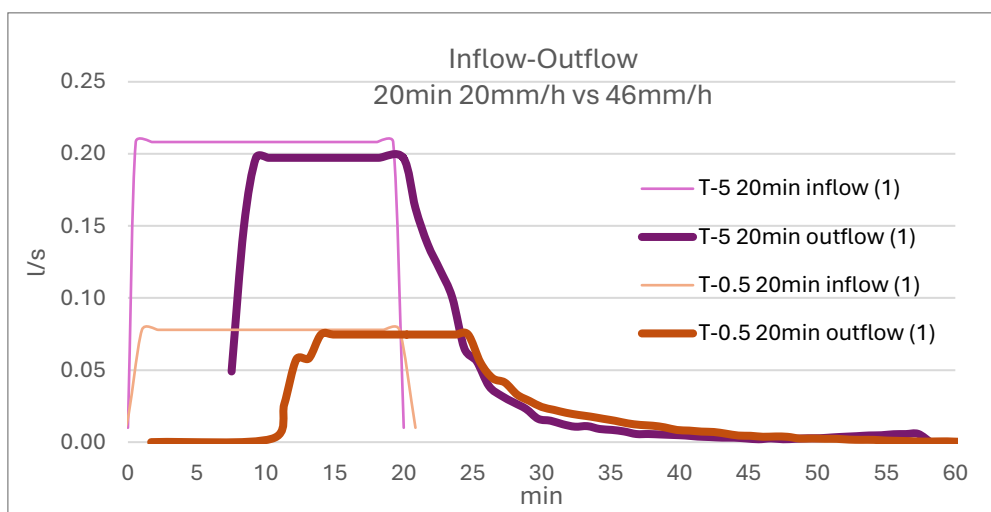
*Figure 21. Inflow-outflow of 30-minute tests*

In this case as well, the behaviour of both experiments appears to be very similar, with both reaching the peak at the same time after 17 minutes from the beginning of the tests.

The empty process is slightly slower at lower flow rates, although this is not immediately evident due to the graphical overlap of the curves.

Additionally, also in that case, the time interval suggests an extension of approximately 10 minutes, that translates in a higher attenuation of the intensity, reaching almost 20% of reduction.

Another similarity is the shorter average time of filling and emptying process observed in both second runs, confirming the previous observation.

*Table 10. Parameters values for 30-minutes tests*

|  | T-0.5 | | T-5 | |
|---|---|---|---|---|
|  | 30min - 15 mm/h | | 30min - 30mm/h | |
|  | **first run** | *second run* | **first run** | *second run* |
| Delay 50% | **13** | 13 | **10** | / |
| Delay 70% | **14** | 14 | **13** | / |
| Delay peak | **17** | 15 | **17** | 11 |
| Empty till 50% | **8 after** | 8 after | **6 after** | 5 after |
| Empty till 30% | **11 after** | 12 after | **7 after** | 8 after |
| Empty till 20% | **14 after** | 13 after | **9 after** | 11 after |
| Empty till 10% | **20 after** | 19 after | **13 after** | 16 after |
| Completely empty | **42 after** | 35 after | **25 after** | 52 after |

48

| Interval time | **39** | 37 | **37** | 37 |
|---|---|---|---|---|
| Damp intensity | **24%** | 20% | **19%** | 19% |
| Runoff coeff. | **0.84** | 0.81 | **0.77** | 0.89 |
| Peak reduction | **14%** | 13% | **13%** | 6% |
| Max average % | **86%** | 87% | **87%** | 94% |

## 6.2.3 20-minutes tests

Figure 22**Error! Reference source not found.** presents the results of inflow and outflow for the constant flow tests with a duration of 20 min.



*Figure 22. Inflow-outflow of 20-minute tests*

In this case, a similarity between the two events can be observed: both exhibit a direct rise to 70% of the maximum flow rate, characterized by steep curves. Although, the lower flow rate reaches the peak later, adhering to the customary analysis.

The behaviour of the empty process mirrors the one observed in the 30-minute test, showing a slightly slower response at lower flow rates. However, this is not immediately apparent, as the curves graphically appear to overlap.

The time interval, in this instance, seems to confirm the extension of the events for 10 minutes in the case of T-5, while an even larger attenuation for T-0.5 events whose intensity is dampened by about half.

*Table 11. Parameters values for 20-minutes tests*

| T-0.5 | | T-5 | |
|---|---|---|---|
| 20min - 20mm/h | | 20min – 46mm/h | |
| **first run** | *second run* | **first run** | *second run* |

| | | | | |
|---|---|---|---|---|
| Delay 50% | / | 12 | / | / |
| Delay 70% | **12** | 13 | **8** | / |
| Delay peak | **14** | 15 | **9** | 8 |
| Empty till 50% | **8 after** | 7 after | **4 after** | 4 after |
| Empty till 30% | **11 after** | 10 after | **5 after** | 7 after |
| Empty till 20% | **14 after** | 13 after | **6 after** | 8 after |
| Empty till 10% | **21 after** | 19 after | **10 acter** | 16 after |
| Completely empty | **46 after** | 32 after | **38 after** | 49 after |
| Interval time | **39** | 36 | **30** | 29 |
| Damp intensity | **49%** | 45% | **33%** | 32% |
| Runoff coeff. | **0.89** | 0.81 | **0.78** | 0.94 |
| Peak reduction | **4%** | 13% | **5%** | 8% |
| Max average % | **96%** | 87% | **95%** | 92% |

## 6.2.4 10-minutes tests

Figure 23 presents the results of inflow and outflow for the constant flow tests with a duration of 60 min.
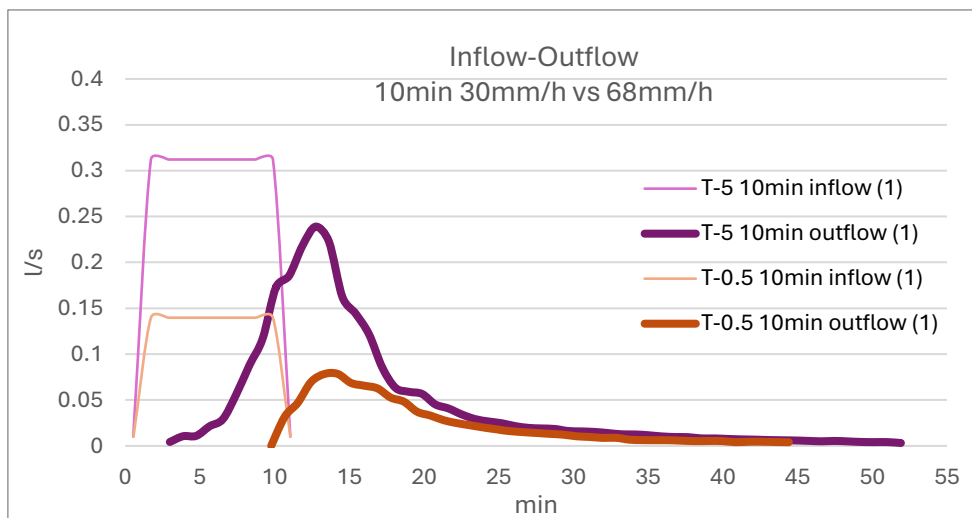


*Figure 23. Inflow-outflow of 10-minute tests*

The 10-minute events represent the highest intensity for their respective return periods. These events are characterized by the largest amount of flow rates over a short duration and are therefore predicted to be the most impactful.

In spite of that, these events produced the most favourable outcomes in terms of the gutter system's response. The peak flow is completely delayed until after the event has ended, and both graphical analysis and computation indicate a small yet significant reduction in peak flow, attributed to incomplete saturation.

This finding holds substantial practical implications for gutter systems in catchment areas, offering huge opportunities to develop water management skills. The gutter system's capacity to collect water and release it only after the most intense phase of precipitation has passed, can enhance overall water control strategies.

The two different return periods demonstrate similar filling patterns, reaching the peak at the same time, suggesting that the filling process is independent of flow rate magnitude, while higher flow rate is responsible of faster emptying process, considering the parameters of null flow not fully reliable.

Overall, this endorse the hypothesis that the filling process in some case is likewise influenced by the duration of the events rather than the flow rate. Conversely, the emptying process appears to be dependent on the flow rate, occurring more quickly at higher rates.

*Table 12. Parameters values for 10-minutes tests*

| | T-0.5 | | T-5 | |
|---|---|---|---|---|
| | 10min - 30mm/h | | 10min - 68mm/h | |
| | **first run** | *second run* | **first run** | *second run* |
| Delay 50% | **12** | 11 | **10** | 9 |
| Delay 70% | | 13 | **12** | 10 |
| Delay peak | **13** | 13 | **13** | 12 |
| Empty till 50% | **7 after** | 7 after | **5 after** | 6 after |
| Empty till 30% | **10 after** | 11 after | **7 after** | 8 after |
| Empty till 20% | **11 after** | 12 after | **8 after** | 10 after |
| Empty till 10% | **18 after** | 19 after | **13 after** | 14 after |
| Completely empty | **34 after** | 39 after | **42 after** | 39 after |
| Interval time | **18** | 21 | **20** | 17 |
| Damp intensity | **44%** | 53% | **50%** | 41% |

| | | | | |
|---|---|---|---|---|
| Runoff coeff. | **0.61** | 0.79 | **0.74** | 0.82 |
| Peak reduction | **44%** | 15% | **23%** | 7% |
| Max average % | **56%** | 85% | **77%** | 93% |

## 6.2.5 Same flow tests-different duration

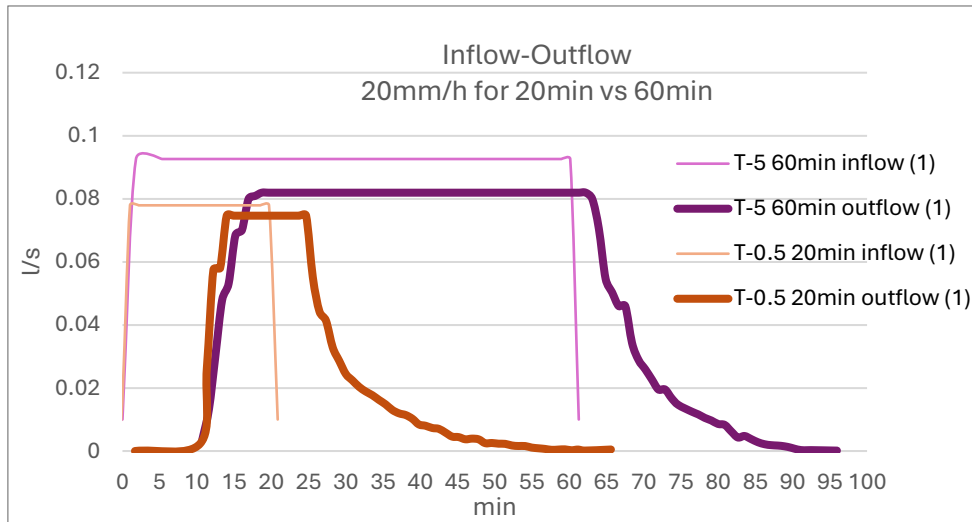*-20mm/h for 20-minute and for 60-minute*



*Figure 24. Inflow-outflow of 20mm/h tests*

In this scenario, peak flow is reached later during longer-duration events, indicating a likely dependence on the duration of the event as well as the magnitude of the flow rate. But even if, the delay of the peak is less delayed, the attenuation of the peak still remains consistently higher with shorter event, where the gutter demonstrates to be more efficient.

Similarly, the emptying process remains consistent, demonstrating that it is largely independent of the event duration.

*Table 13. Parameters values for 20mm/h tests*

| | T-0.5 | | T-5 | |
|---|---|---|---|---|
| | 20min - 20mm/h | | 60min - 20mm/h | |
| | **first run** | *second run* | **first run** | *second run* |
| Delay 50% | / | 12 | **13** | 10 |
| Delay 70% | **12** | 13 | **15** | 12 |
| Delay peak | **14** | 15 | **19** | 14 |
| Empty till 50% | **8 after** | 7 after | **8 after** | 7 after |
| Empty till 30% | **11 after** | 10 after | **10 after** | 10 after |
| Empty till 20% | **14 after** | 13 after | **14 after** | 11 after |
| Empty till 10% | **21 after** | 19 after | **19 after** | 17 after |

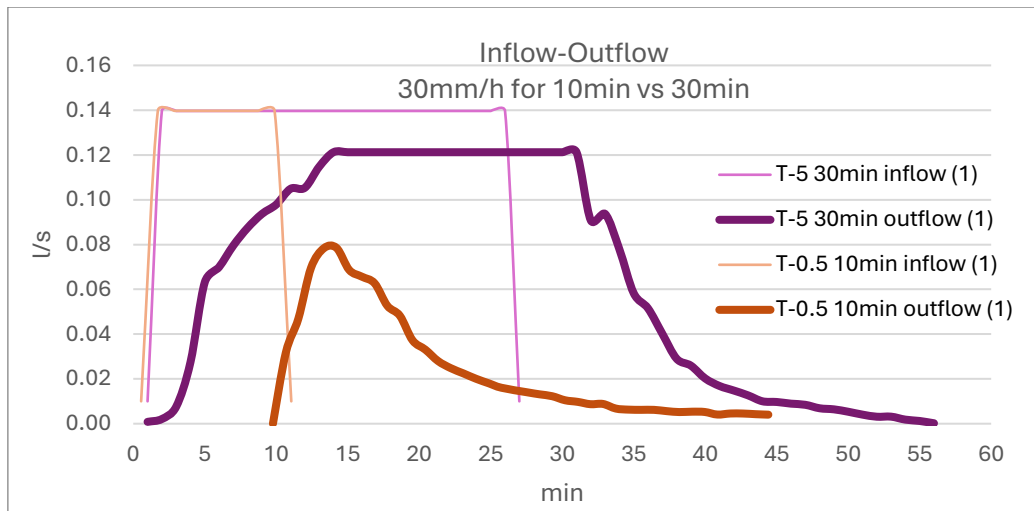| | | | | |
|---|---|---|---|---|
| Completely empty | **46 after** | 32 after | **32 after** | 30 after |
| Interval time | **39** | 36 | **68** | 68 |
| Damp intensity | **49%** | 45% | **12%** | 12% |
| Runoff coeff. | **0.82** | 0.70 | **0.84** | 0.84 |
| Peak reduction | **7%** | 13% | **12%** | 15% |
| Max average % | **93%** | 87% | **88%** | 85% |

*-30mm/h for 10-minute and for 30-minute*



*Figure 25. Inflow-outflow of 30mm/h tests*

In this case, the hypothesis regarding the filling process appears to be confirmed. However, the emptying processes differ, with a smoother release observed during 10-minute events. This variation is likely attributable to the specific characteristics of these shorter-duration events where the complete saturation is not reached.

*Table 14. Parameters values for 30mm/h tests*

| | T-0.5 | | T-5 | |
|---|---|---|---|---|
| | 10min – 30mm/h | | 30min – 30mm/h | |
| | **first run** | *second run* | **first run** | *second run* |
| Delay 50% | **12** | 11 | **10** | / |
| Delay 70% | | 13 | **13** | / |
| Delay peak | **13** | 13 | **17** | 11 |
| Empty till 50% | **7 after** | 7 after | **6 after** | 5 after |
| Empty till 30% | **10 after** | 11 after | **7 after** | 8 after |
| Empty till 20% | **11 after** | 12 after | **9 after** | 11 after |
| Empty till 10% | **18 after** | 19 after | **13 after** | 16 after |

| Completely empty | 34 after | 39 after | 25 after | 52 after |
|---|---|---|---|---|
| Interval time | 18 | 21 | 37 | 37 |
| Damp intensity | 44% | 53% | 19% | 19% |
| Runoff coeff. | 0.61 | 0.79 | 0.67 | 0.86 |
| Peak reduction | 44% | 15% | 13% | 6% |
| Max average % | 56% | 85% | 87% | 94% |

*Analysis of hydraulic parameters*

As mentioned in the data analysis section, peak reduction, complementary to the 'max average percentage,' was calculated for control purposes. Indeed, since the results indicate a peak reduction consistently ranging between 10-15%, it's more likely to be a measurement sensitivity variation between the pump and the flow meter.

Notably, the 10-minute tests demonstrated a higher peak reduction, suggesting a possible actual physical reduction in peak flow.

Due to this slight variation in instrument sensitivity, the runoff coefficient cannot be considered entirely reliable as a parameter, too. However, the observed range of results is not highly significant, as the primary function of the gutter system is to delay and smooth the water release rather than retain a portion of the water. This opens up a potential area of research about the vegetative gutter covers to enhance performance.

## 6.2.6 Variation of parameters over the IDF Curves

The analysis will now attempt to pool all the experiments respectively at the return period to understand how the parameters vary across the IDF curves as the duration of the event increases and the corresponding flow rate decreases.
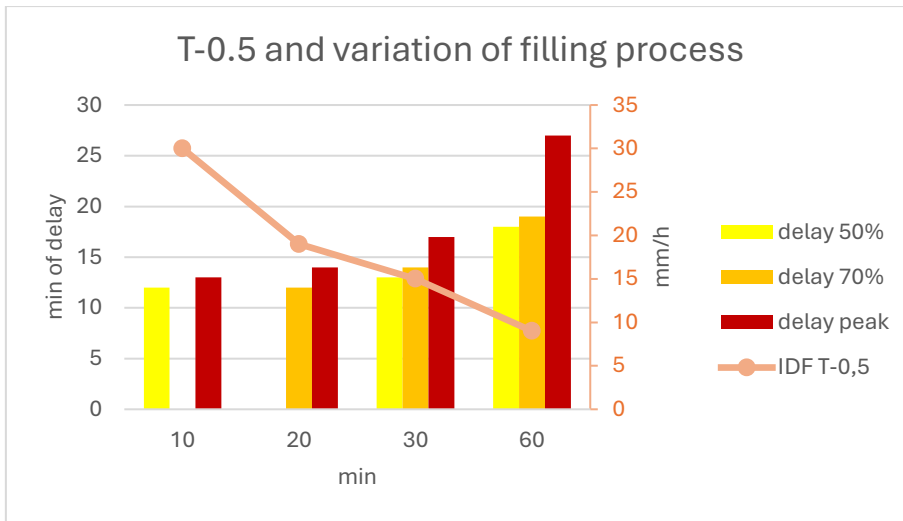
*Figure 26. Variation of parameters for filling process over the IDF curves T-0,5*

For the filling process, all the parameters vary in a similar way among the IDF curves. As it is anticipated, the average interval time will increase across all values, indicating a longer process for extended events and a much faster one for shorter events. This observation aligns with expectations, of a longer filling process with lower flow rates.

The 10-minutes event is the fastest one, but above the line of 10, remarking the complete delay of the effect after the end of the event itself.

As suggested already by the general statistics graphs, the passage between 50% and 70% is the faster one for all the experiments. The peak is reached slowly moving towards the longer event, this confirms the strong dependence on the amount of flow rate in the last phase of filling, as found in the general statistical analysis.
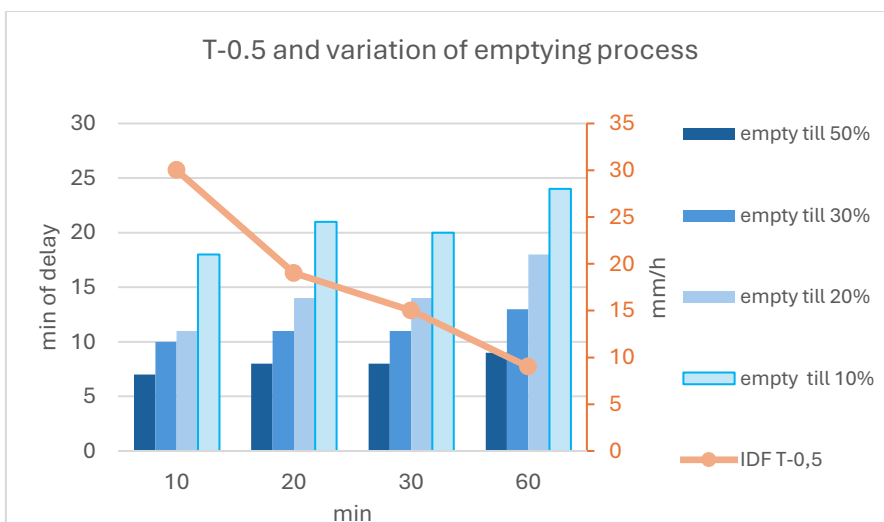


*Figure 27. Variation of parameters for empty process over the IDF curves T-0,5*

The moving of the emptying process is mostly similar with a parallel behaviour. This reveals the complete independence of the process to the parameters of the event, notably visible in the 20- and 30-minute tests, which share the same variation of values. The emptying process is characterized by a faster draining that occurs in the first 10 minutes after the event by emptying 80%, then in other 10minutes and more, the remain 20% is emptied. This slower drainage, which might seem almost like accumulation, could be coupled with the function of a plant layer that can use the remaining water.

*T-5*
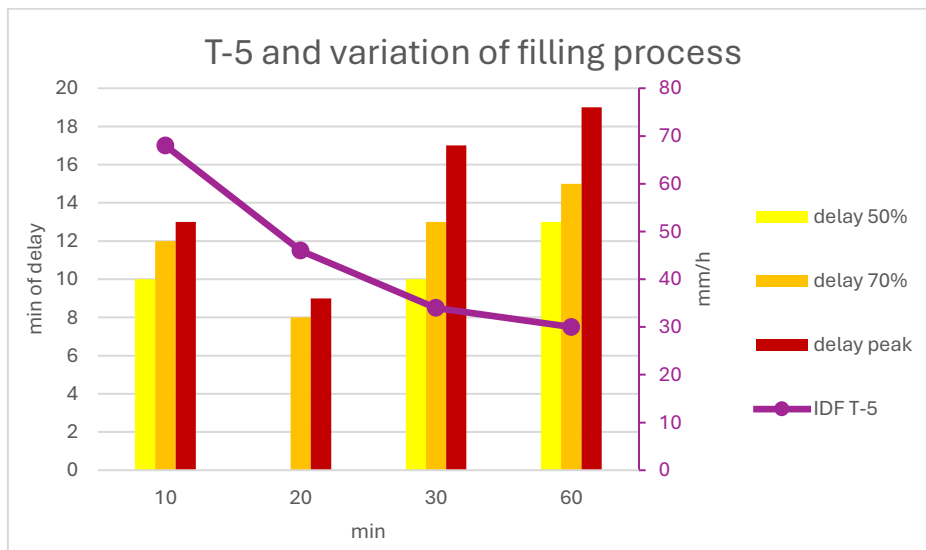


*Figure 28. Variation of parameters for filling process over the IDF curves T-5*
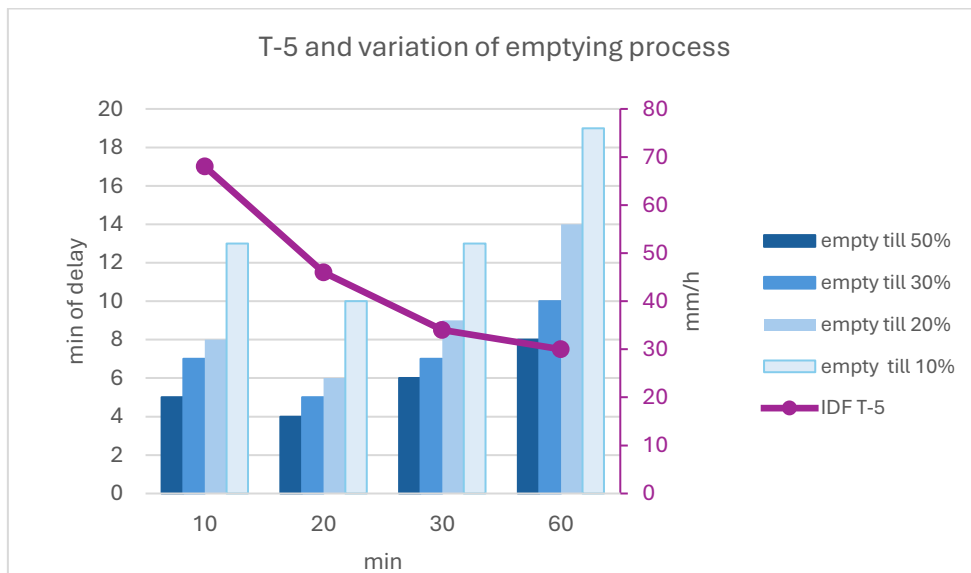


*Figure 29. Variation of parameters for empty process over the IDF curves T-5*

The analysis of the two graphs closely resembles that of T-0.5, where longer events correspond to longer interval times to reach the imposed threshold. However, a significant difference is

evident in the unusual behaviour of the curves, which display a low peak for the 20-minute event in both the filling and emptying processes.

What is also noteworthy compared to the T-0.5 events are the reduced spacing of range of values, indicating faster processes overall, especially for the filling and first emptying process. This is in line with the dependence of system operation on higher flow rates.

## Discussion

The analysis of constant flow rate experiments does the groundwork to understand the behaviour of the gutter, and how the system responds varying amount of inflow and the duration of the event.

The main findings assess that the delay time mainly depends on the duration of the event obviously, but mostly is influenced by the amount of input flow. To higher flow rates correspond shorter interval of time, since larger and the faster arriving of water produce an accountable shorter delay.

Respect the filling process, the passage between 50% and 70% is the faster one for all the experiments. While the last phase of the filling phase is strongly influenced by the rainfall intensity, with an inversely proportion dependence: high intensity rain traduces in shorter time to reach the peak with a steeper curve in the last part of the graph.

When the intensity of precipitation is the same, the dependence on the duration is expressed since the mm of precipitation changes, and this is traduced in faster peak reaching for the shorter event since it is same intensity in shorter time, but a higher capacity of the gutter to attenuate the intensity since is less water.

Regarding the emptying process the main information is that it is strongly linked to the properties of the material so independent to the parameters of the event, amount of flow and duration.

What emerge is that there is a first faster drainage and a second final lower one. The former occurs in the first 30 minutes after the vent by emptying (then in twice of the time only 10% is emptied. This slower drainage, which might seem almost like accumulation, could be coupled with the function of a plant layer that can use the remaining water.

One observation is that the lower flow rate can be maintained for longer after the test is stopped, as water accumulates more gradually, induces the decrease of the curve later in time.

With the comparison of the second runs of tests, it is found that the system's efficiency tends to decrease in repeated tests, as observed in both the filling and the emptying process, where the delay times and peak outflows attenuation are fewer due to residual moisture from the previous tests.

A good result is respect of the dependence respect the degree of saturation. Notably, the 10-minute tests displayed higher peak reductions, suggesting that during shorter, high-intensity events, the system's efficiency in managing peak flows improves because the gutter is not fully saturated.

For longer events, once the system reaches saturation, its ability to manage water diminishes, and water passes through without substantial retention, meaning that optimal performance occurs before saturation.

From a general statistical analysis, nevertheless, a sufficient lag interval of more than 10 minutes is estimated for all tests in order to delay 50% of the inflow. This peak flow delay provides urban drainage systems with the ability to handle water volumes for an extended period, allowing better preparation for peak flow arrivals. As a result, it reduces the risk of system overloading and mitigates the likelihood of urban flooding.

## 6.3 Successive rainfall tests

### 6.3.1 Successive rains scenario 1
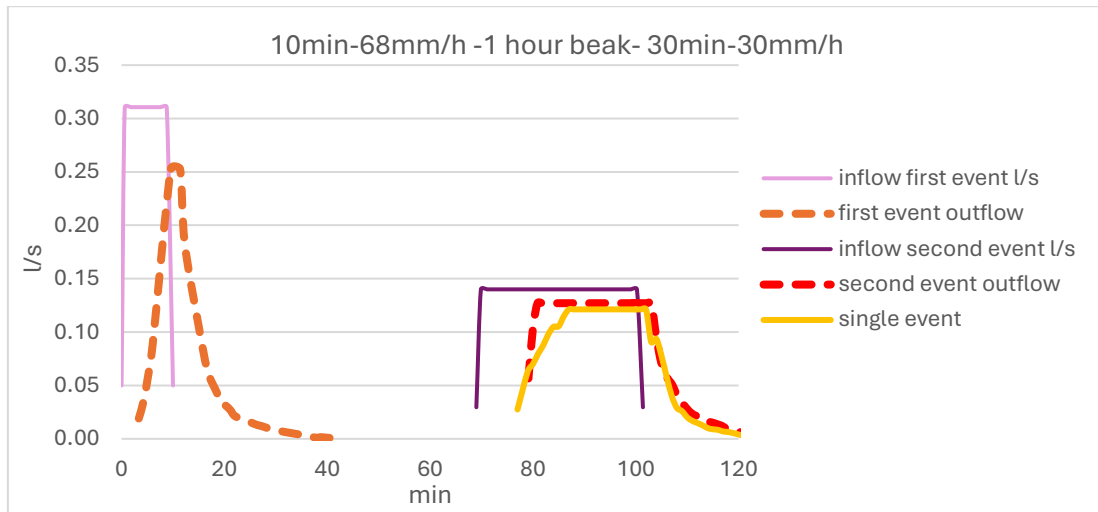


*Figure 30. Inflow-outflow of successive rains 'Scenario 1'*

The graph illustrates the sequence of two events. The analysis is focused on the response of the gutter system during the next 30-minutes event with intensity 30mm/h, a typical 'cloudburst' in Denmark, occurred after an intense rainfall characterized by high flow and short duration.

The results indicate that the system perform well also in this condition. The delay time is still significant, even if shorter, and the values remain within the expected range, consistent with the second run of the constant flow test. This suggests that the gutter retains its efficiency even after just one hour, effectively delaying the peak flow's arrival, with huge impact in the ability to manage the water load.

*Table 15. Parameters values for 'Scenario 1'*

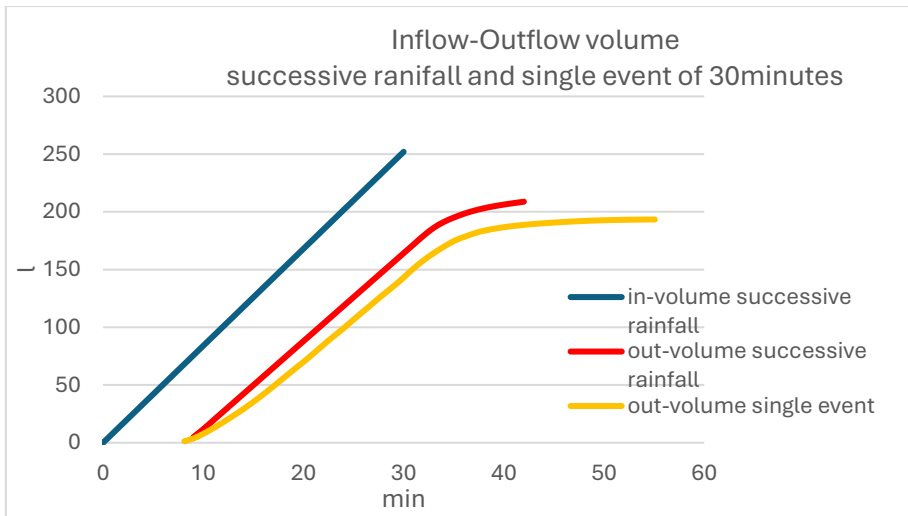| | 30min - 30mm/h | | |
|---|---|---|---|
| **successive rainfall** | | single event | |
| | | **first** | *second* |
| Delay 50 % | / | 10 | |
| Delay 70% | 10 | 13 | |
| Delay peak | 11 | 17 | 11 |
| Peak reduction | 9% | 13% | 6% |
| Empty till 50% | 5 after | 6 after | 5 after |
| Empty till 30% | 8 after | 7 after | 8 after |
| Empty till 20% | 10 after | 9 after | 11 after |
| Empty till 10% | 16 after | 13 after | 16 after |
| Completely empty | 37 after | 25 after | 52 after |
| Runoff coeff. | 0.86 | 0.77 | 0.89 |

*Figure 31. Inflow-Outflow volume comparison between successive rainfall and single event lasting 30min*

With the analysis of the cumulative out-volume the difference in efficiency is even further evident.

The two runoff curves demonstrate highly satisfactory results when compared to the inflow curve: they extend the release time and reach a lower maximum value, indicating a runoff coefficient less than one. Between the two, aside from a minor variation in the peak value, attributable to differences in peak reduction and runoff coefficient, as the gutter exhibits reduced efficiency, the curves reflect differing water release capacities. Specifically, subsequent rainfall events release water more quickly, whereas the single event has a longer release duration, with its curve extending further in time.

However, both the curves are representative of the stronger efficiency of the gutter being very different to the steep inflow-volume curve. This is a very good result in terms of water management efficiency, meaning that gutter enables more time to deal with same amount of water.

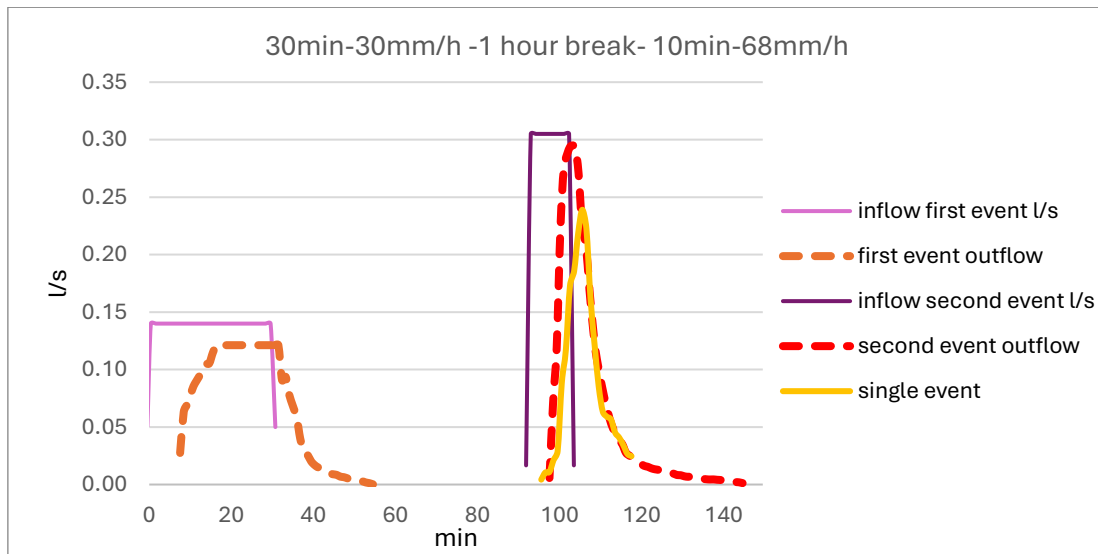## 6.3.2 Successive rains scenario 2



*Figure 32. Inflow-outflow of successive rains 'Scenario 2'*

The inverted scenario is even more interesting, as it allows for an analysis of how the most impactful 10-minute event would be managed following a cloudburst.

The primary focus in this case is on peak flow reduction. Notably, the 10-minute event was the only constant flow test that showed a reduction in the peak flow. However, after the cloudburst, this peak reduction capacity was lost, aligning with the behaviour observed during the second run of the constant flow experiments. Similar to the previous scenario, the results also in this case are more closely to those obtained in that case.

A positive outcome is that the delay time remains significant, with the peak flow occurring after the event has concluded. This represents the most favourable result in terms of the system's performance.

*Table 16. Parameters values for 'Scenario 2'*

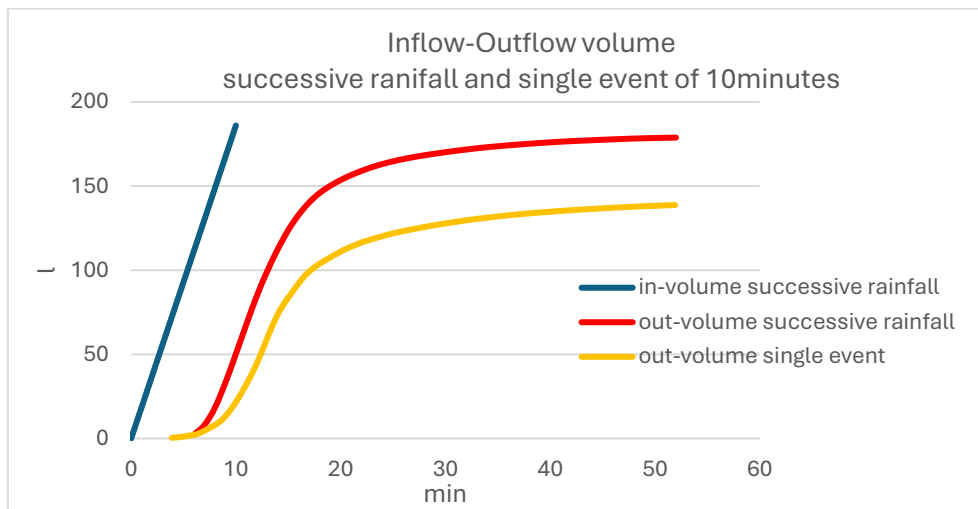| | 10min-68mm/h | | | |
| --- | --- | --- | --- | --- |
| **successive rainfall** | | single event | | |
| | | **first** | second | |
| Delay 50 % | | 10 | 9 | |
| Delay 70% | 8 | 12 | 10 | |
| Delay peak | 10 | 13 | 12 | |
| Max average % | 96% | 77% | 93% | |
| Empty till 50% | 6 after | 5 after | 6 after | |
| Empty till 30% | 8 after | 7 after | 8 after | |
| Empty till 20% | 10 after | 8 after | 10 after | |
| Empty till 10% | 14 after | 13 after | 14 after | |
| Completely empty | 42 after | 42 after | 39 after | |
| Runoff coeff. | 0.96 | 0.74 | 0.82 | |

*Figure 33. Inflow-Outflow volume comparison between successive rainfall and single event lasting 10min*

In this case, the analysis of the volume is even different and particular, due to the exceptional behaviour of the gutter with the highest event of 10minutes.

The orange curve, representative of the single event, is significantly lower due to the substantial reduction in the gutter's peak and the low runoff coefficient. While the red curve corresponding to the subsequent rainfall, reaches the same volume as the blue curve, in actual fact the runoff coefficient is 0.96. This indicates that no further water retention is occurring since the gutter is still fully saturated from the previous event. Despite this, the good work of the gutter in retarding runoff is strongly evident. The orange curve also shows a more distended trend, and the steep curve of inflow (blue curve) is completely smoothed out.

Overall, in this case the robustness of the gutter decrease more, but it has to be remembered that this event occurs after what is defined in Denmark as a cloudburst. In spite of that, the capacity of releasing slower the water, and spread it over the time, is still very high. This is confirmed as the best result, since it is more than one time highlighted that the primary function of the gutter is delaying the releasing of the water and slowdown the runoff.

## Discussion

The robustness of the respond of the gutter is tested in two different ways. Once performing the same test after the interval time indicated by the moisture sensor as necessary to recover almost 20% of dry conditions, and other testing its ability to handle successive rainfall events, which mimic real-world conditions where storms may occur in quick succession.

The results of these two practices align. All the results from the successive rainfall events resemble those of the second test run in the set of constant flow experiments than with the first.

This supports the previous observation regarding the dependency on the prior saturation experienced by the gutter, which reduced its efficiency due to residual moisture from the previous test.

Despite this, the gutter continues to demonstrate solid performance, confirming its overall robustness in managing rainfall. While it loses the most pronounced effects, its performance remains sufficient, as indicated by still good value of delay time.

Among the two scenarios, the first, where the 10-minute test precedes and does not fully saturate the gutter produces a runoff coefficient still consistent with the second run of the single event. In contrast, in scenario 2, the prior complete saturation of the gutter returns back a runoff coefficient close to 1, indicating the gutter completely fully.

However, the best result comes out is in terms of water management efficiency. The outflow volume curves consistently show a steady slowdown of water release, as they are smoothed and markedly different from the steep inflow-volume curve. This is the very good result, meaning that gutter enables more time to deal with same amount of water, which is confirmed to be the primary function of the gutter: delaying the release of water and slowing down its runoff.

The results were encouraging, showing that the green gutter retained its capacity to delay peak flows and manage water effectively even after multiple rain events, only lowering the value of its efficiency. The system could return to a near-dry condition relatively quickly, within a few hours, ensuring that it would be ready to handle additional rainfall events without losing efficiency.

This rapid recovery is critical for urban environments where unpredictable weather patterns can lead to frequent and intense rainfall.

## 6.4 Synthetic rainfall - CDS curve

### 6.4.1 CDS curve -1hour

The test was performed three times to obtain a consistent and reliable result.

The results indicate optimal performance, as evidenced by the rightward shift of the outflow curve. Specifically, the onset of precipitation is delayed by approximately 17 minutes, during which no outflow is observed. This implies that the initial stage of the CDS curve, corresponding to the first input of flow, is entirely bypassed and consolidated with the subsequent stage, whose peak is shifted of more or less 5 minutes. Notably, the delay of the peak is particularly significant, being fully displaced to the extreme right relative to the inflow, which demonstrates a highly effective delay in precipitation response. The peak arrival time is at 36minute from the beginning.

The emptying process, more bluntly, traces the filling process at the beginning, moving towards the slower and smoother final emptying reached after more or less 30 minutes since the stop of the inflow.

The total rainfall interval time, thanks to the gutter is prolonged to 81 minutes. This mean the intensity of the precipitation is damped of 26%.

*Table 17. Input values to the pump for CDS 1-h*

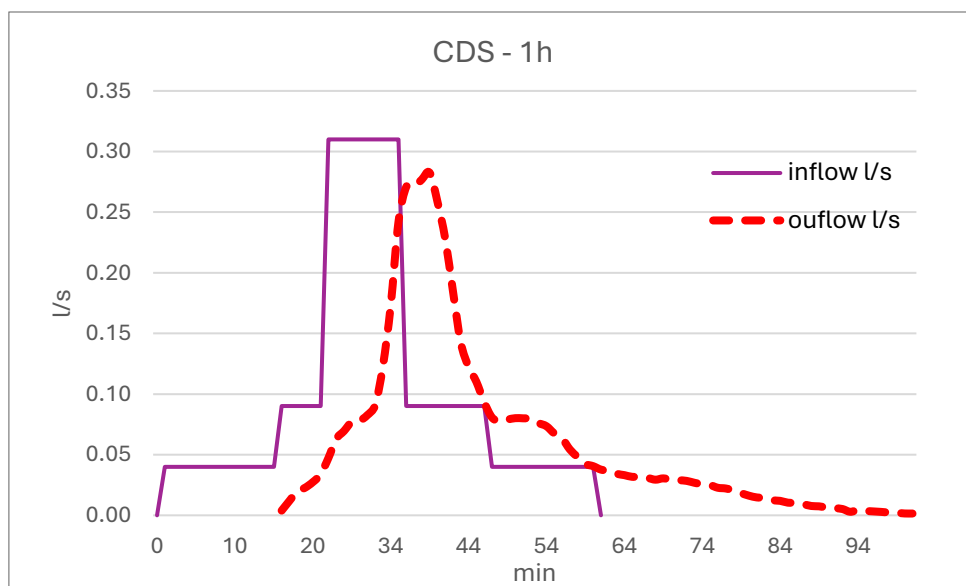| CDS curve -1h | mm/h | l/s |
|---------------|------|------|
| 15min | 9 | 0.04 |
| 25min | 20 | 0.09 |
| 35min | 68 | 0.31 |
| 45min | 20 | 0.09 |
| 60min | 9 | 0.04 |



*Figure 34. Inflow-outflow CDS-1h*

The output cumulated volume obtained is 302.8 l, while the one obtained by the inflow rate is 347.4 l. This gives a runoff coefficient equal to 0.87.

This runoff coefficient indicates that about 87% of the water that entered the system was released. This means that a good portion of the water found its way out, but a certain percentage 13% was retained in the system. The value of $C_d$ lower than one suggests a well-functioning water collection and disposal system

The difference in volume is 347.4 - 302.8 = 44.639 litres. This amount represents the water that has remained within the system, probably absorbed by the soil, evaporated or accumulated in other forms (e.g., in voids or porous materials).

If we consider the measure sample of university roof, 16 m$^2$, around 3mm of water are retained, respect a total rainfall of 22 mm. The gutter is able to retain 13% of rainwater, that with a future vegetation layer, can be absorbed by plant roots.

Moreover, the outflow water is effectively release slower as showed by Figure 35, spreading the time needed to drain the water of more than 30minutes.Figure 35. Input - output cumulated volume CDS-1h
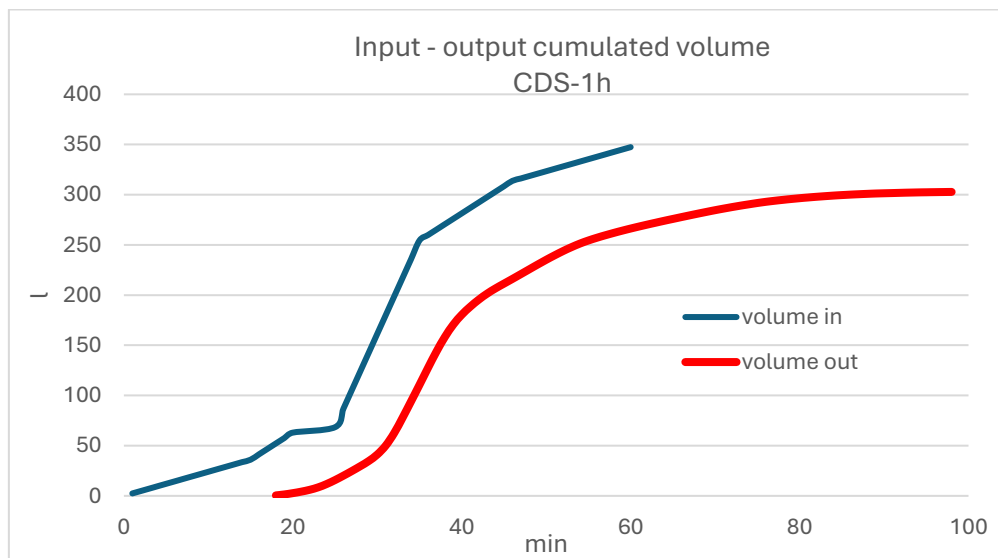


*Figure 35. Input - output cumulated volume CDS-1h*

## 6.4.2 CDS curve -2hours

In this case, the test was conducted twice, as a consistent and reliable result had already been achieved.

The overall response of the gutter exhibits a similar pattern, with the outflow curve shifted to the right, positioning the peak at the far-right end of the inflow curve. Additionally, the first inflow is entirely bypassed, with the initial outflow response occurring after 31 minutes. During the first

two minutes, a small percentage of the initial input is observed, which is subsequently accumulated with the next input, contributing more significantly to the response.

While the previous experiment demonstrated a well-aligned outflow curve with the inflow, only shifted in time, this experiment shows that the first two stages during the filling process are clearly distinguishable, while the final stage exhibits a less pronounced depth proposing a more continuous steep behaviour.

The emptying process maintains a similar behaviour, characterized by a smoother decline.

Given that the event lasts two hours, it is already less intense than the previous one, so the damping effect obtained by the gutter is reduced to only 6%.

*Table 18. Input values to the pump for CDS 2-h*

| CDS curve -2h | mm/h | l/s |
|---|---|---|
| 20min | 5 | 0.01 |
| 45min | 9 | 0.04 |
| 55min | 20 | 0.09 |
| 65min | 68 | 0.31 |
| 75min | 20 | 0.09 |
| 100min | 9 | 0.04 |
| 120min | 5 | 0.01 |
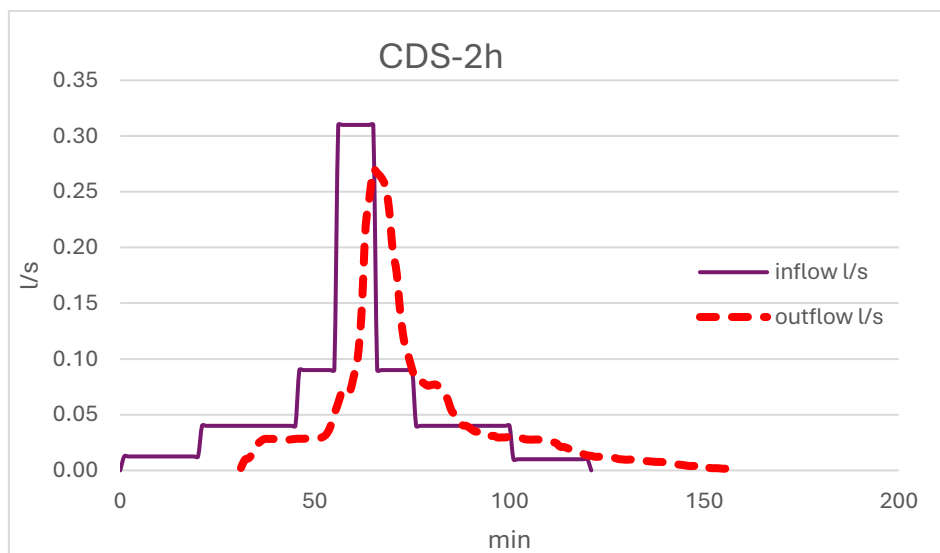


*Figure 36. Inflow-outflow CDS-2h*

The runoff coefficient obtained in this case is even low, 0.79, obtained by the respective values of input volume 441 l and output volume 349.2 l. This means an even better control of the rainwater probably due to the slower inflow rate.

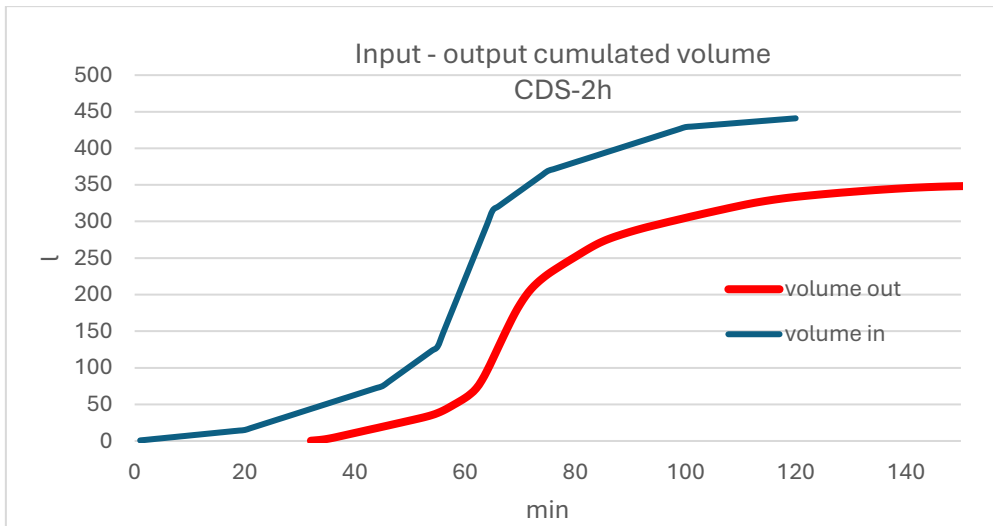The retained water is 21%, as the difference in volume is 441- 349.2= 91.8 litres, which are 6mm of precipitation.

*Figure 37. Input - output cumulated volume CDS-2h*

## 6.4.3 CDS curve -30 minutes

The final experiment, lasting approximately 30 minutes, was designed to evaluate the system under conditions of the highest intensity, using singular steps of 10 minutes. In this scenario, the stepped behaviour of the outflow curve is no longer observed, with a direct rise to the peak, which is again shifted toward the end of the highest input. This behaviour can be attributed to the complete delay of the initial inflow. Despite this, the emptying process retains a smoother, stepped decline.

A noteworthy outcome of this experiment is the substantial damping effect achieved under the highest intensity conditions, resulting in a 52% reduction in the flow rate intensity, with the event duration extending to a total of 62 minutes.

*Table 19. Input values to the pump for CDS-30min*

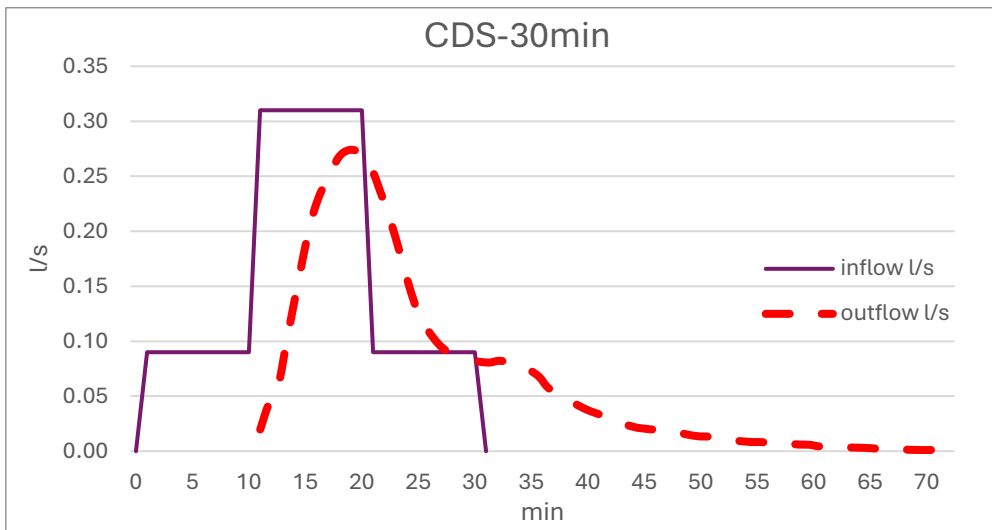| CDS curve -30min | mm/h | l/s |
|---|---|---|
| 10min | 20 | 0.09 |
| 10min | 68 | 0.31 |
| 10min | 20 | 0.09 |

*Figure 38. Inflow-outflow CDS-30min*

This represents over all the aspect the best case, probably due to a not complete saturation of the gutter.

The output volume is 250.515 l respect the input volume 294 l, with the runoff equal to 85%, retaining 3 mm of 18mm total. But from Figure 37Figure 39 is evident the spread distribution of the output flow in time, key point for a successful water management.
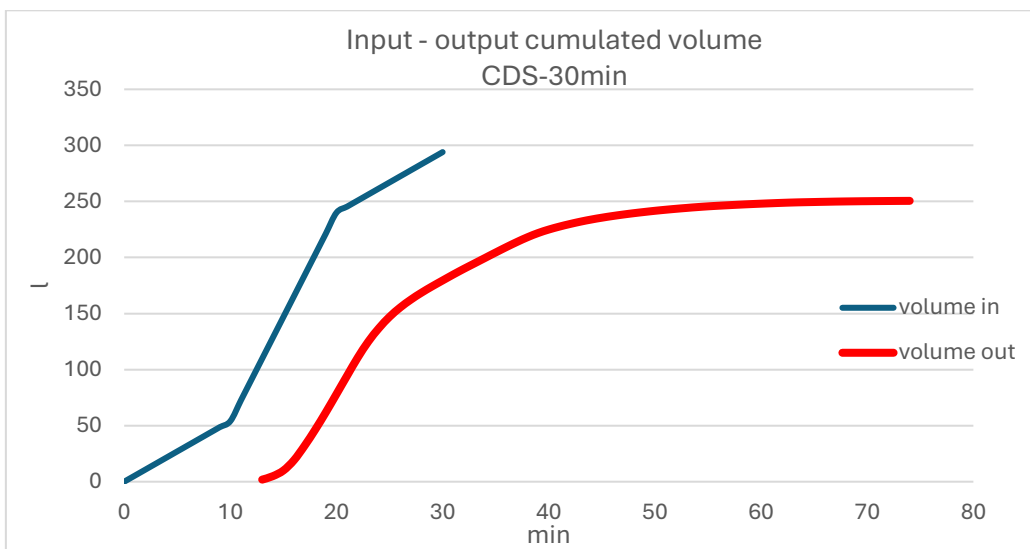


*Figure 39. Input - output cumulated volume CDS-30m*

## Discussion

This latest analysis allows for a comprehensive understanding of the gutter system by examining its performance under more realistic conditions, varying intensity over time of inflow. These tests provide a more practical assessment of the green gutter's performance under dynamic rainfall conditions, replicating how a storm's intensity rises and peaks before gradually tapering off.

Once again, the results are highly promising, demonstrating the system's exceptional ability to delay its response to precipitation.

The triangular-shaped hyetograph derived from the Chicago Design Storm method (CDS), which modelled synthetic rainfall events, effectively illustrated the green gutter's ability to smooth out sharp peaks in rainfall intensity.

By spreading the water release over an extended period, the system dampened the sudden influx of water that typically overwhelms urban drainage systems during extreme storm events.

The onset of outflow is consistently postponed, bypassing the initial input stage and shifting the peak to the end of the highest input phase. This optimal delay is crucial for preventing sudden peak flows and alleviating pressure on drainage infrastructure.

The positive impact is further confirmed by two additional analyses: the damping of intensity and the cumulative outflow volume.

The gutter system effectively moderates the intensity of rainwater outflow, reporting the best results during extreme events once again. For instance, in the final test, the shorter one which last 30min, the intensity was reduced by 52%. This damping is significant, as it slows the runoff, allowing double of the time to better manage rainwater.

This effect is also evident through the analysis of the cumulative outflow volume. The extended duration of outflow distributes the rainwater discharge more gradually, allowing it to be released into the environment or drainage system at a more manageable rate. This ensures that the same volume of water is handled over a longer period, reducing the risk of overburdening drainage systems and minimizing the likelihood of flash flooding.

The Rockflow mineral wool, with its high permeability, allows the system to absorb up to 95% of its volume in water, while its controlled release capabilities ensure a gradual and manageable flow into the drainage network. This significantly reduces the likelihood of flash floods in urban areas, where impermeable surfaces like asphalt and concrete exacerbate surface runoff. The system's capacity to mitigate short-duration, high-intensity rainfall events, which are often the cause of flash flooding, confirm the gutters as a valuable tool in mitigating the impact of heavy storms with role in alleviating the burden on existing urban drainage infrastructure as part of a comprehensive urban flood management strategy, particularly in areas prone to intense rainfall, where drainage systems could be overwhelmed, leading to flooding.

Although not the primary objective of the gutter system, all analyses have shown that it retains a small percentage of water, approximately 20% on average, with runoff coefficients around 0.8. Therefore, not only the water is released slowly, but a small part of it is retained within the system. The difference between the inflow volume and the outflow volume is the retained water, which likely evaporates or, even more beneficially, remains available for absorption by plants.

# 7. Moisture sensors analysis

The moisture sensors analysis is aimed at verifying the saturation levels and water content within the material to determine their potential influence on the gutter's functionality.

## 7.1 Analysis of data

Data were collected from the ThingSpeak platform, and the time interval required for the material to return to drier conditions was evaluated, with an analogous approach of flow meter dataset.

The data were processed using Excel and plotted as a time-series graph.
The x-axis represents the time since the pump was stopped, marking the end of the precipitation event, in order to assess the recovery of dry conditions. The y-axis indicates the percentage of moisture within the gutter. The graph illustrates the temporal evolution of moisture, showing how it gradually returns to its initial conditions, asymptotically approaching 0% over time.

The output values from the moisture sensors are analogy signals calibrated by the primary software, with dry conditions corresponding to values around 3000–3500 and values approaching 0 when the sensor is immersed in water. Since the calibration and boundary conditions are subjective and technical, yet not critical to the core analysis, the moisture assessment is conducted exclusively using percentage values, converting the raw sensor outputs accordingly.

To evaluate the moisture content and its variation as a percentage, the average baseline moisture value is calculated individually for each sensor during each run. This is necessary because each sensor exhibits its own specific "dry condition," never fully achieving the overall defined dry state.

This discrepancy is reasonable and attributed to residual moisture caused by the capillary and retention water. The water that drains and flows towards the gutter is gravitational water, which moves under the influence of gravity force. The other two types of water are bound to the solid matrix by stronger forces: capillary water, which can be removed by air drying or plant absorption and is held by cohesive forces between films of hygroscopic water, and hygroscopic water itself, a thin layer around solid particles held by molecular attraction and a strong dipole moment, which can only be released by heating the matrix sample above 100°C.

Therefore, the 0% moisture condition of each sensor, representing its own "dry condition," is determined by averaging the sensor readings over the 10-minute period preceding the test. This baseline is then used to assess and quantify moisture level changes throughout the experiment as a percentage relative to it.

During the experimental periods, it is ensured that each sensor returns to this baseline over extended time intervals, confirming the baseline's reliability for analysis.

## 7.2 Flow preferential pathway

The first type of analysis takes in consideration the preliminary tests, being useful as they have same duration and slightly different inflow rate.

By dividing the results per sensor, the focus is to assess the behaviour of each field. In addition to evaluating the time required for complete moisture recovery, the analysis also investigates whether the water follows a preferential pathway by comparing these recovery intervals.

Based on the obtained results and the observed similarity in behaviour, the sensors are grouped and presented in pairs, with each pair consisting of sensors positioned along the same horizontal line.

To reference the position of each sensor, the illustrative image **Error! Reference source not found.** displaying their numbered locations on the gutter is proposed again for clarity.



*Figure 7. Photo representing the system: the gutter, the 8-moisture sensor numerated and on the left the screen connected to the flow meter.*

## Sensors 2 and 6

Starting with the analysis of the two top sensors, Sensor 6 on the left and Sensor 2 on the right, it is possible to identify the point of water input from the left, which allows Sensor 6 to reach a higher percentage of moisture content Figure 41. Their average "dry condition" oscillate among analogic number equal to 3000.

The moisture values for these sensors remain relatively stable when the flow is lower, as the water merely passes through them without fully saturating the material.

Whit highest flow the behaviour is stronger marked, reaching higher value of saturation, but they still recover to drier conditions rapidly, as evidenced by the steep rise in the moisture recovery curves.
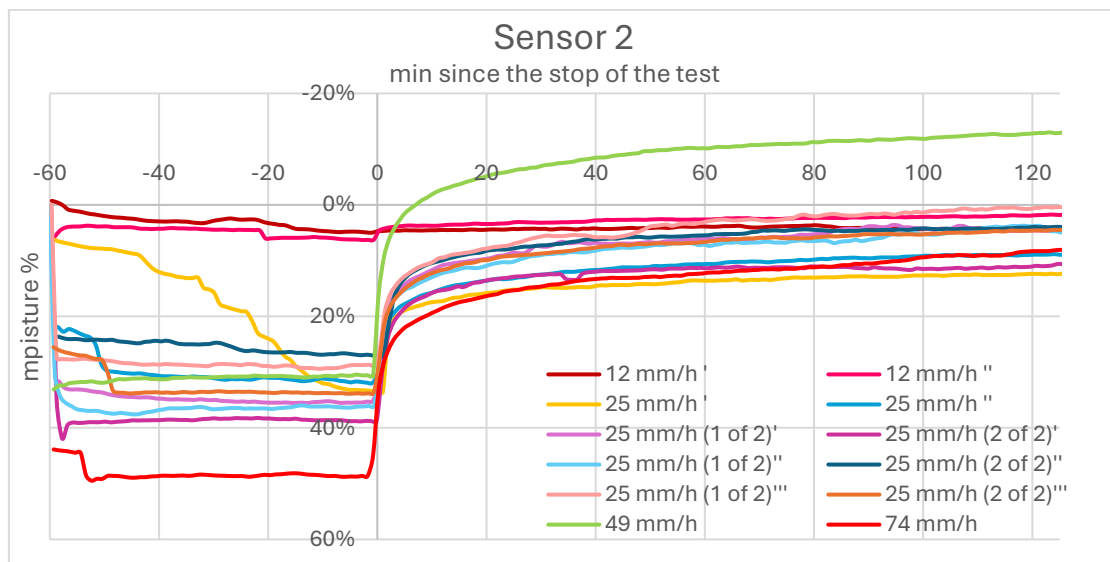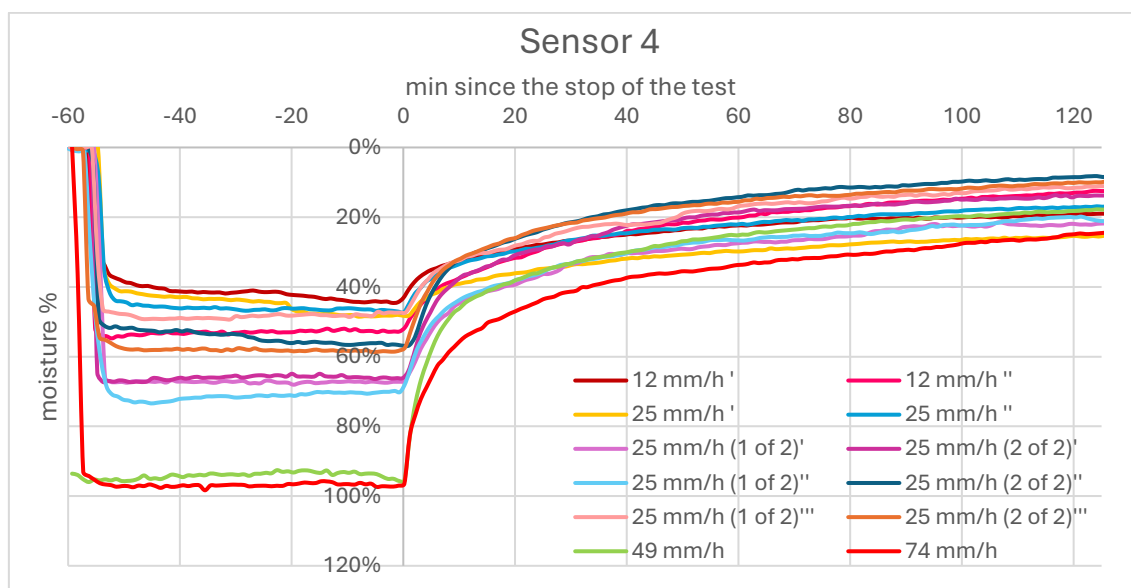


*Figure 40. Sensor 2 - Moisture variation over time*
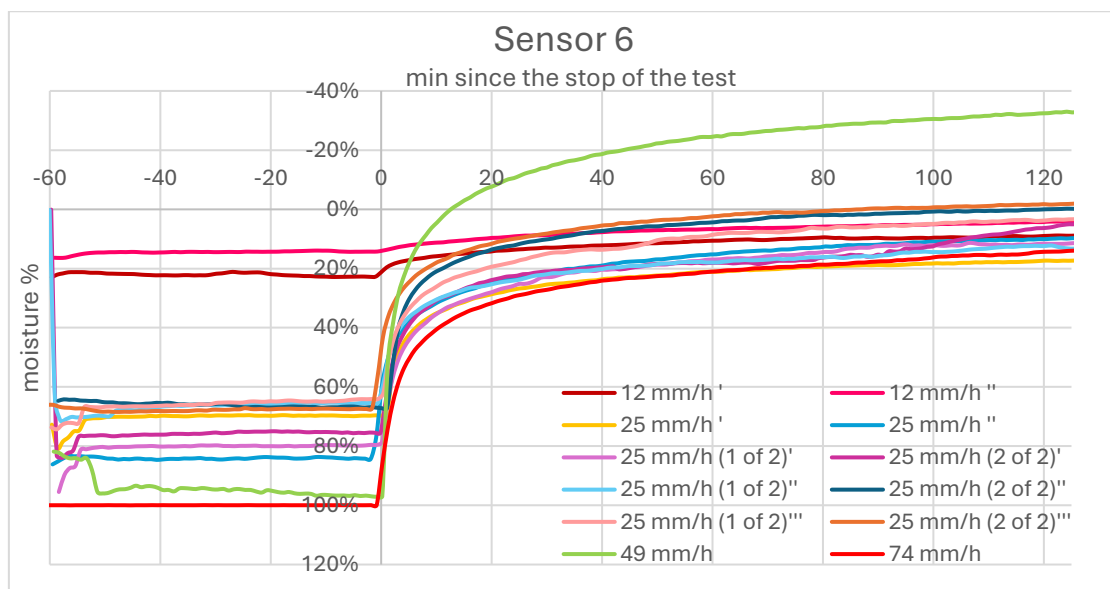


*Figure 41. Sensor 6 - Moisture variation over time*

## Sensors 4 and 8

Sensor 4 on the left and Sensor 8 on the right are the two positioned in the upper middle section. Their average "dry condition" oscillates among analogic number equal to 2700 for Field 8 and 2200 for Field 4.

Both sensors are influenced by the passage of water; however, despite the saturation of the matrix in Field 8, it appears that the left side is preferred, as the stable lower value of "dry condition" indicates. This conclusion is supported by the observation that the recovery time is longer for Field 4 compared to Field 8. Furthermore, Field 8 seems to remain dependent on the flow rate to achieve significant saturation from the passage of water.
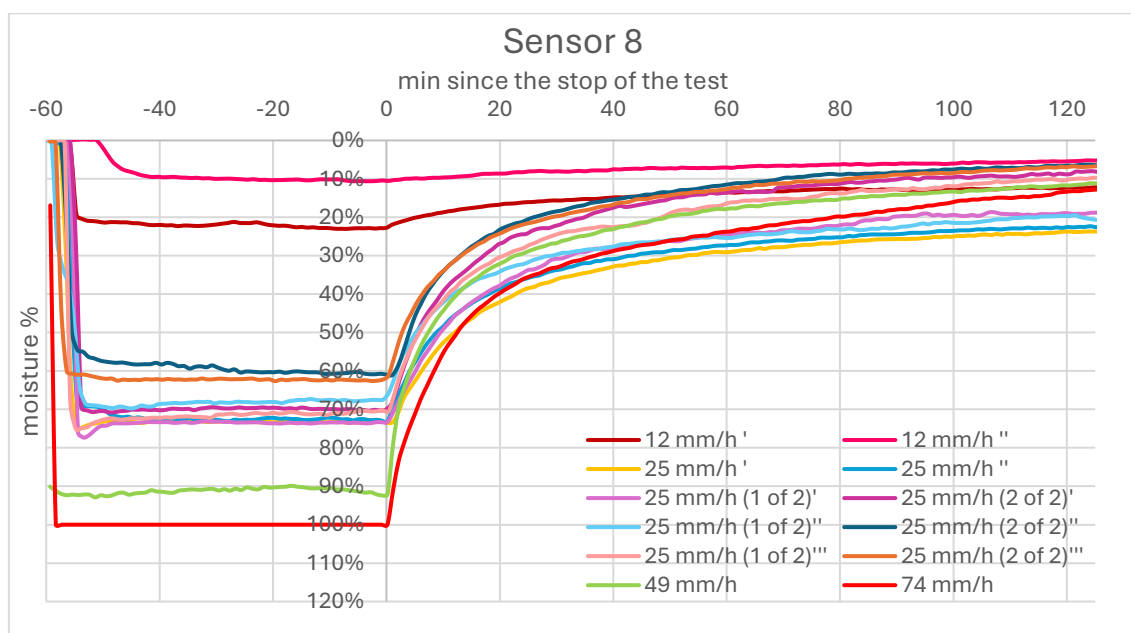


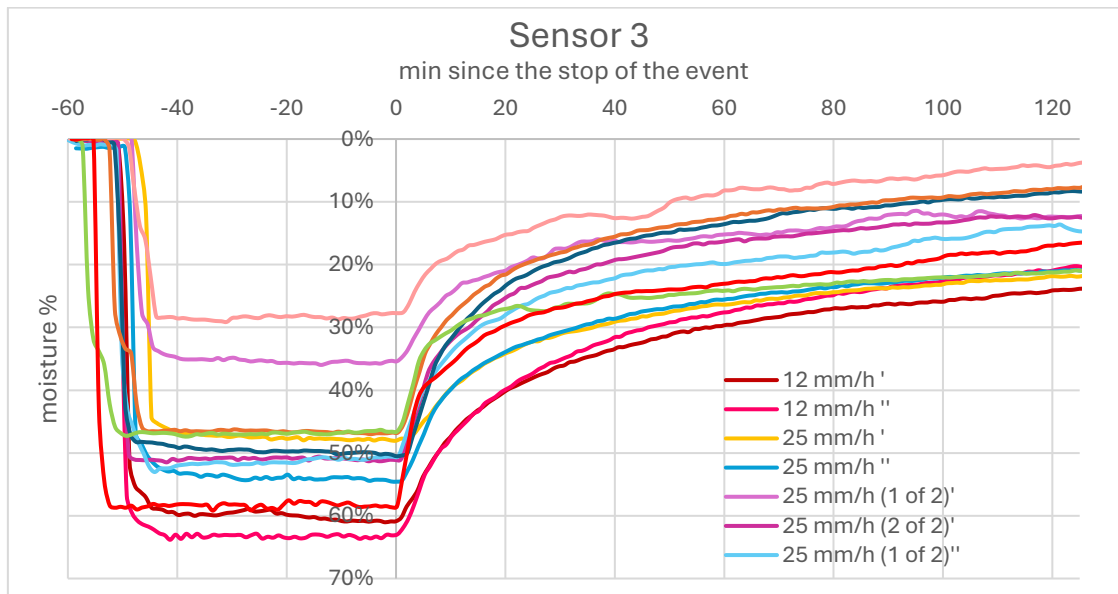*Figure 42. Sensor 4 - Moisture variation over time*



*Figure 43. Sensor 8 - Moisture variation over time*

## Sensors 3 and 7

Sensor 3 on the left and Senor 7 on the right are the two positioned in the lower middle section. Their average "dry condition" oscillates among analogic number equal to 2800 for Field 3, while 2500 for Field 7.

Based on both the moisture levels recorded and the speed of recovery to dry conditions, it appears that the water has a preferential pathway to the right side, with a greater incidence observed in Field 7, as confirmed by the difference in the mean value of "dry condition" in this case as well.


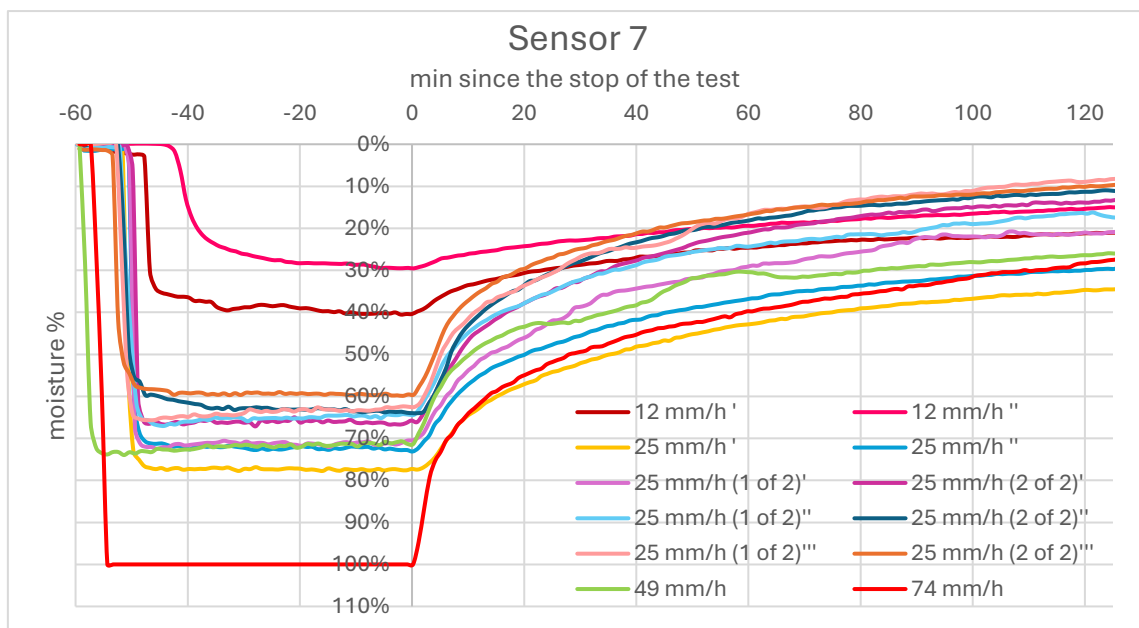
*Figure 44. Sensor 3 - Moisture variation over time*



*Figure 45. Sensor 7 - Moisture variation over time*

## Sensors 1 and 5

At the bottom, Sensor 1 on the left and Sensor 5 on the right exhibit the highest moisture values, always in average around 2100 of analogic value.

With some exceptions with the input flow very high, these sensors do not display regular behaviour; instead, they predominantly exhibit a linear trend that fluctuates around their values indicative of consistently wet conditions. The sensor in Field 5, which reaches 100% of moisture, corresponds to the maximum flow rate of 1200 L/h.

Their irregular and oscillating behaviour is consequence of their always wet conditions, never to much influenced by the new inflow, due to their position at the bottom of the gutter.
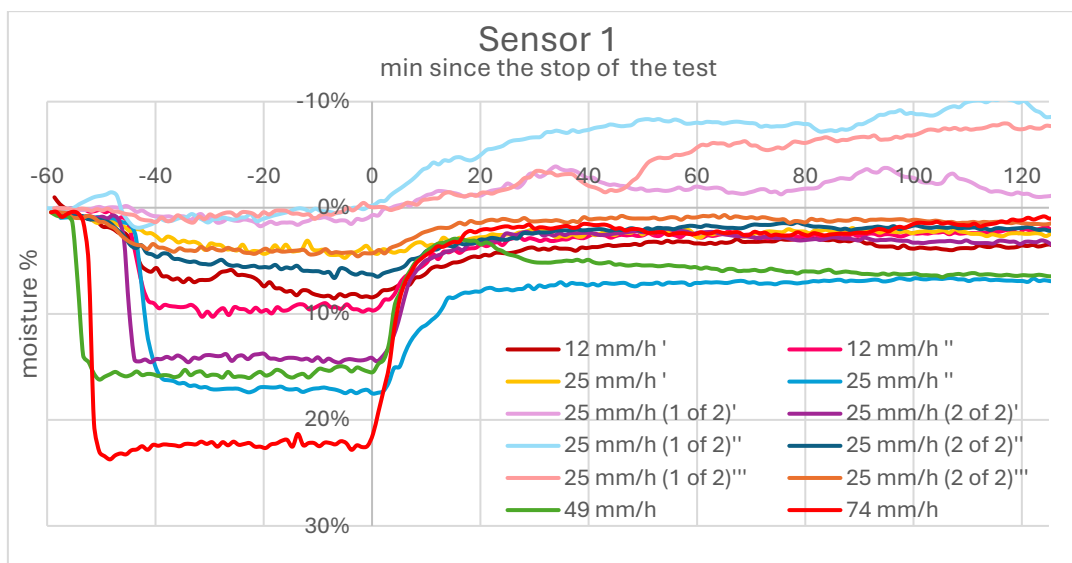


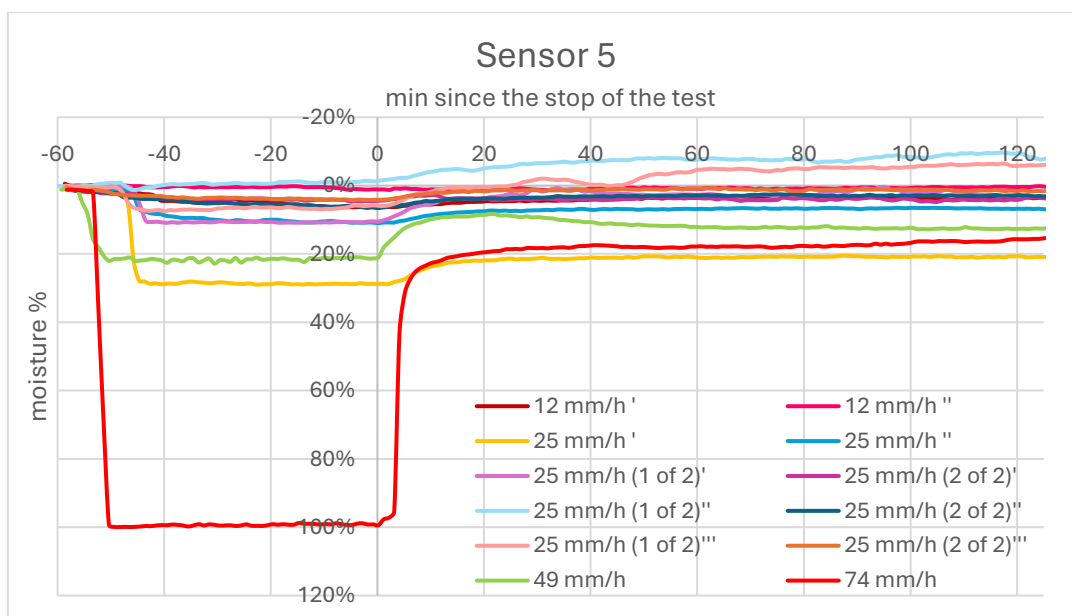*Figure 46. Sensor 1 - Moisture variation over time*



*Figure 47. Sensor 5 - Moisture variation over time*

At the end looking overall, it is possible to delineate a mainstream pathway of the water.

Beginning from Field 6 on the right, water flows toward the left side, passing through Field 4, and then returns to the right side in Field 7. From Field 7, the water flows vertically downward, ultimately terminating in Field 5.

## 7.3 Time to recover dry condition

As it is already said and visualised, the sensors more involved in the passage of the water being saturated by that, are the two lines in the middle, Sensor 4, Sensor 8, Sensor 3 and Sensor 7.

The most sensible sensor in recovering moisture conditions is Field 7, which in two hours has still 40% of moisture content Figure 48. But Field 4, the other one highly involved, recover 70% in two hours Figure 49, while field 3 and field 8 have already recover those value just after 1 hour (60min) Figure 50 and Figure 51.

Therefore, with exception of Field 7, after two hours (120min) all the sensors have recovered 70% of dried condition, leaving only 30% of moisture content. This is a positive outcome regarding the system's capacity to recover its functionality, as it is able to efficiently return to a state where it can collect new water after recovering from saturation conditions.
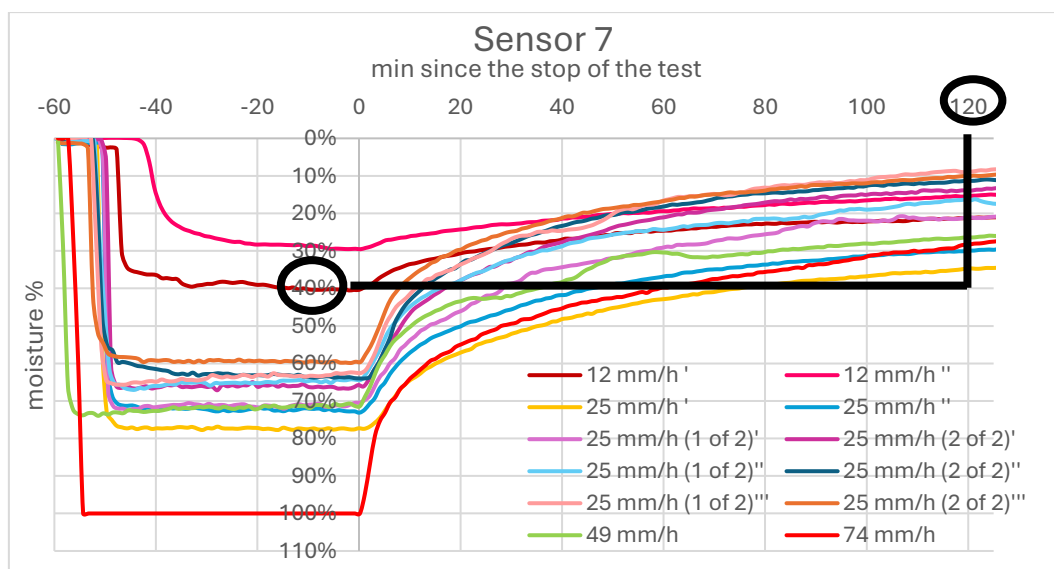


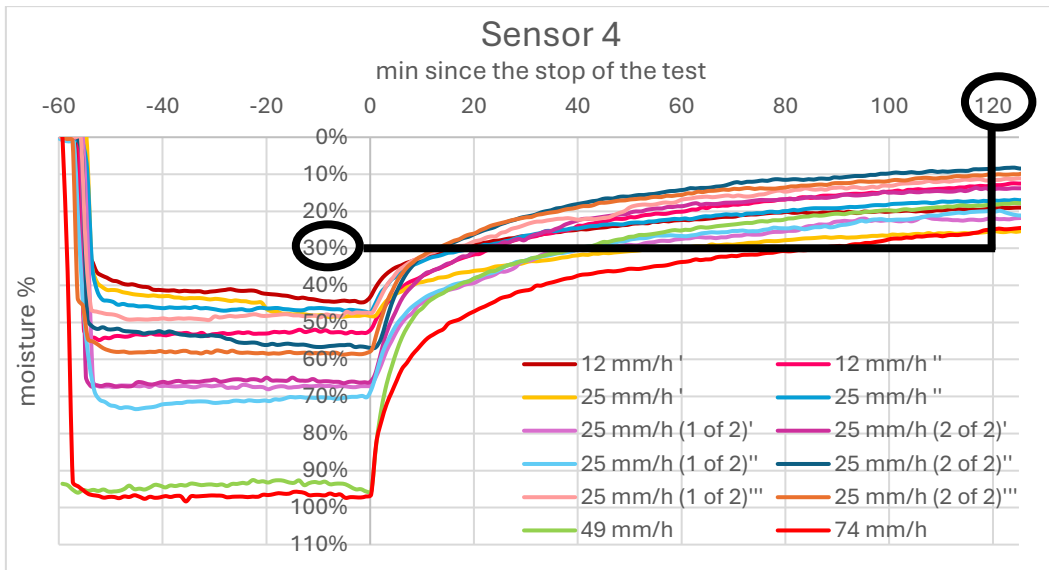*Figure 48. Recovering time of Field 7*
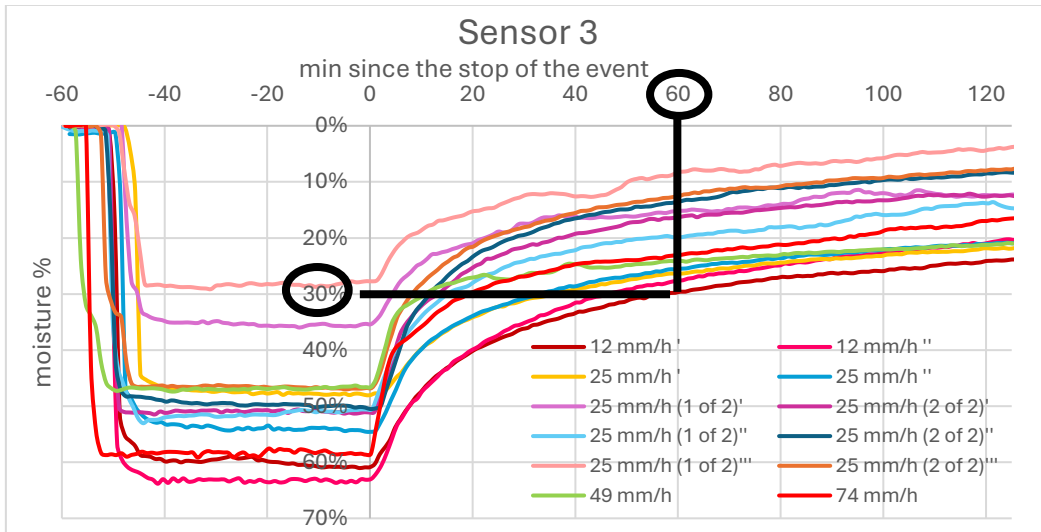
*Figure 49. Recovering time of Field 4*



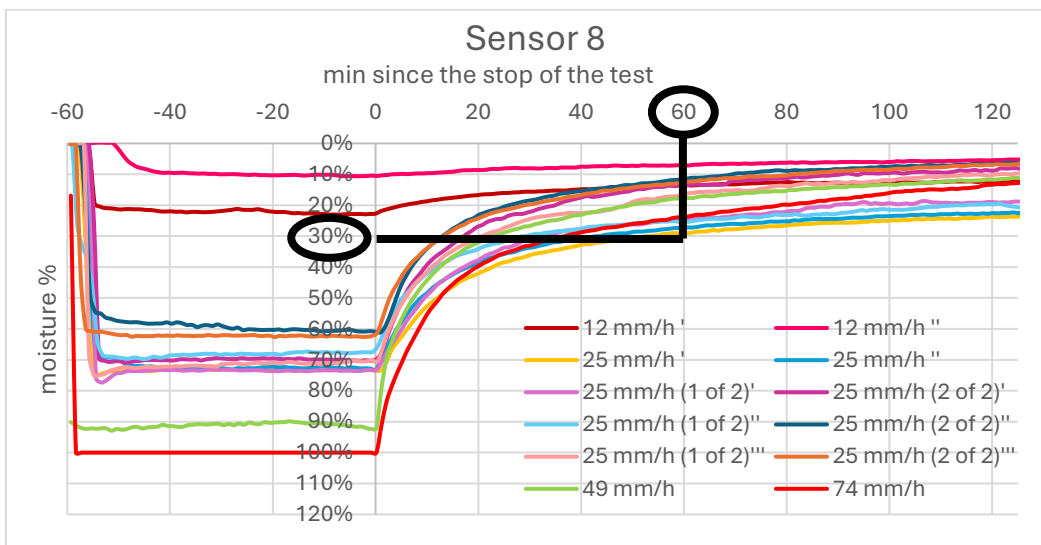*Figure 50. Recovering time of Field 3*



*Figure 51. Recovering time of Field 8*

## 7.4 Flow meter and Moisture sensor correlation

The emptying process is mainly influenced by the material properties and shows a curve behaviour mostly constant over all the tests.

The main scope of this part, as anticipated in the general statical analysis, is to understand if there is a relation among the outflow value of flow meter and the value recorded by the moisture sensor during the emptying phase.

This could have practical repercussions, since the cost of flow meter is markable higher respect the one of the moisture sensors. If this relation exists, the emptying process could be controlled by the moisture sensor, avoiding the use of the flow meter sensor, having economic benefit.

The relation is searched plotting on y-axis the value of flow meter and on x-axis the value of moisture obtained over time during the emptying phase, since the flow starts going down. From the graph obtained, the trendline that fits at best the results is searched among polynomial, exponential or power relations. The $R^2$ value and the equation of the trendline is showed on the graph.

$R^2$ is the coefficient of determination and is a statistical measure of how well the regression line approximates the actual data. Being between 0 and 1, it indicates a range of goodness of fit of a model, which is better the closer the coefficient approaches the value 1 (Coefficient of Determination, R-squared, s.d.).

The field with best interpolation is chosen, and its equation is taken as model to predict the flow rate value of another event, with the respective value of moisture sensor.

In the equation model, the flow rate values represent the dependent variable estimated using the moisture values from the same event as the independent variable.

The estimation is evaluated through RMSE. Root Mean Square Error quantifies how dispersed the residuals are. The residuals are the difference between the predicted and the actual value. They represent the distance between the regression line and the data points. Mathematically, RMSE is the standard deviation of the residuals. Being the average difference between the statistical model's predicted values and the actual values, it reveals how tightly the observed data clusters around the predicted values. Closer are the points to the model line, smaller are the residuals, so RMSE is smaller, indicating a good model prediction  (Root Mean Square Error (RMSE), s.d.).

*T-5 68mm/h-10minutes event*

The analysis obtained good result for the event of 10minutes with return period of 5 years and intensity of 68mm/h.

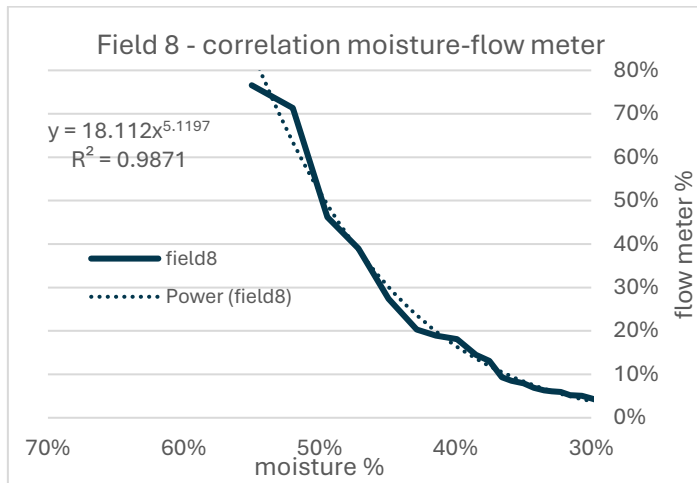The two sensors that perform a better interpolation are Field 4 and Field 8.



*Figure 52. Correlation between flow meter values and moisture values of Field 8 for T-5 10min event*



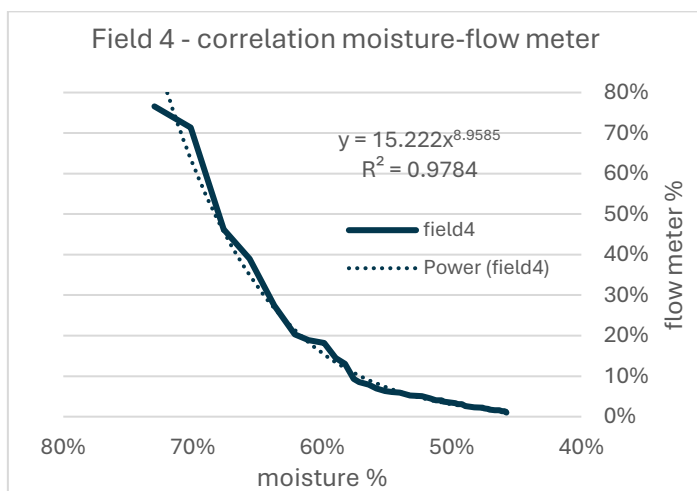*Figure 53. Correlation between flow meter values and moisture values of Field 4 for T-5 10min event*

The value of $R^2$ obtained are quite close, with Field 8 slightly better.

The two equations, obtained by the corresponding values of moisture sensors and flow meters of the first run of 10min, are used to estimate the flow meter values of the second run of T-5 10min experiment, using its moisture values.
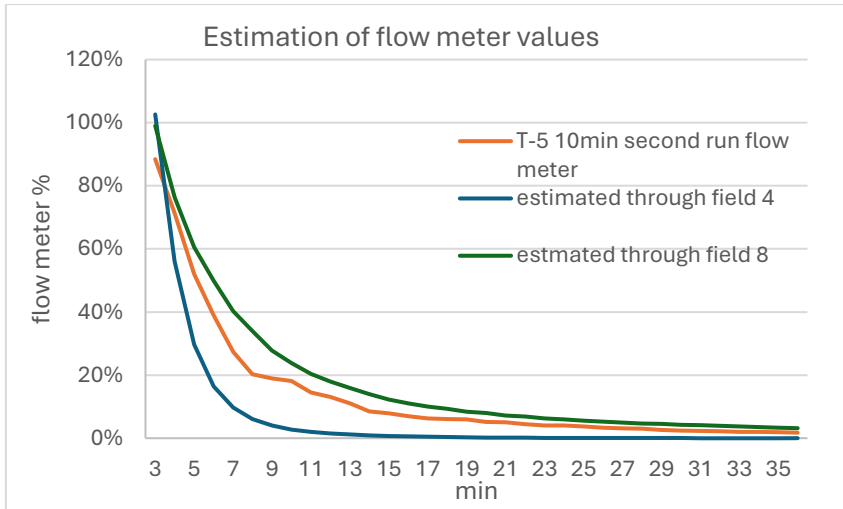
*Figure 54. Estimation of flow meter values of 10min-second run through moisture values of Field 4 and Field 8*

*Table 20. RMSE of estimation through Field 4 and Field 8*

|  | Field 4 | Field 8 |
|---|---|---|
| RMSE | 0.0990 | 0.0560 |

Supported by the RMSE (Root Mean Square Error) values, Field 8 emerges as the sensor that most accurately estimates the outflow values, as clearly illustrated in the graph.

### T-5 30mm/h -30minutes event

The same analysis is conducted on the event representative of a cloudburst in Denmark, 30mmm/h, that correspond to the event of 30min with a return period of 5 years.

Starting from the interpolation of the flow meter and humidity values from the first event, the equation model is used to predict the same variables for the second event.
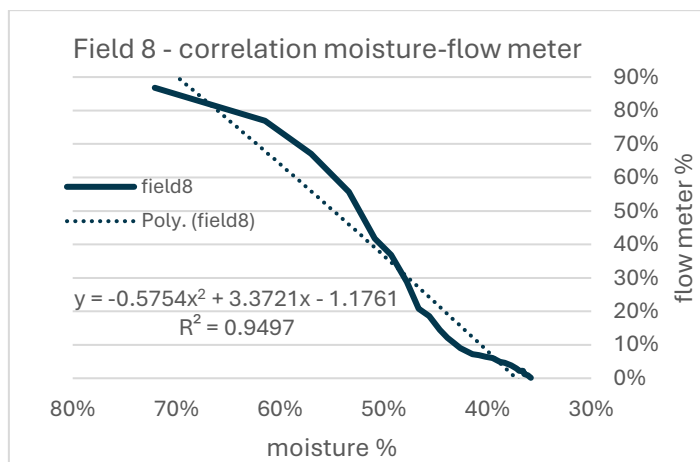


$$y = -0.5754x^2 + 3.3721x - 1.1761$$
$$R^2 = 0.9497$$

*Figure 55. Correlation between flow meter values and moisture values of Field 8 for T-5 30min event*
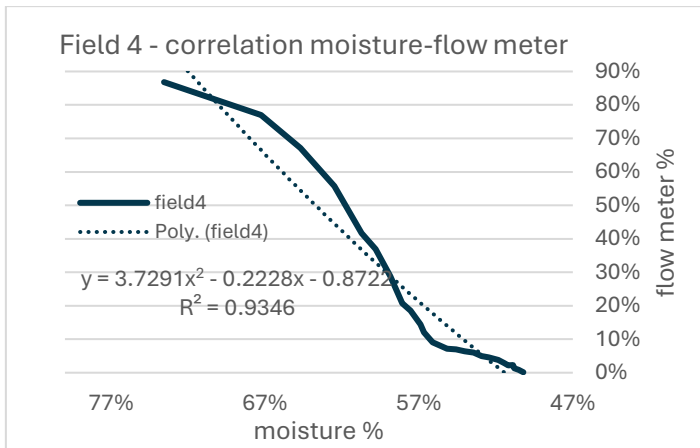
*Figure 56. Correlation between flow meter values and moisture values of Field 4 for T-5 30min event*

Again, fields 4 and 8 seem to work best, but it is already noticeable the lowest $R^2$ values, which means worse interpolation.

The interpolation in this case is through polynomial equation, where for the x value will be used the values of the moisture sensor of the second run of 30min. Once with the values corresponding to Field 4, the other with those from Field 8, and the respective predicted values of flow meter will be obtained. Analogous to the previous case, the goodness of the estimate is validated by the RMSE value.
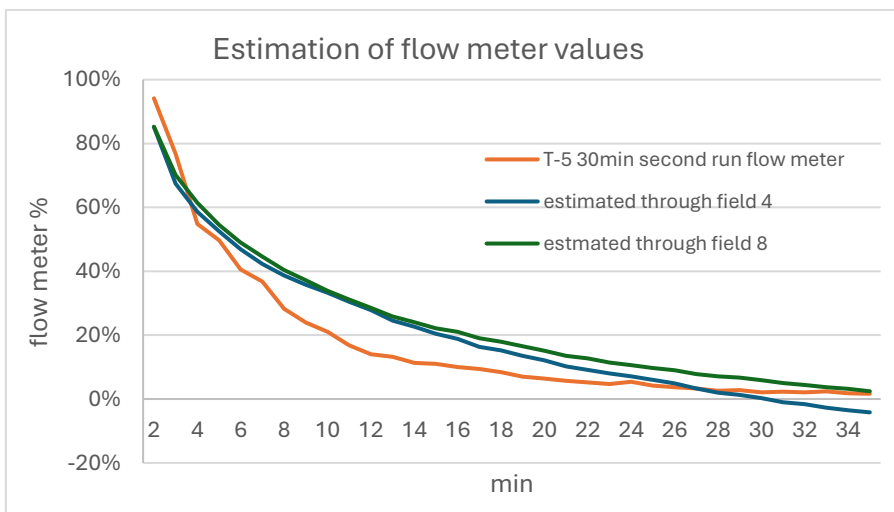


*Figure 57. Estimation of flow meter values of 30min-second run through moisture values of Field 4 and Field 8*

*Table 21. RMSE of estimation through Field 4 and Field 8*

|  | Field 4 | Field 8 |
|---|---|---|
| RMSE | 0.0734 | 0.0861 |

Again Field 8 performs a better prediction.

# Discussion

Despite the promising results of this analysis, the study conducted to achieve this outcome highlighted the sensitivity of the analysis to different events. The sensors' ability to predict flow values varies from event to event, with no single sensor consistently performing as the best among the eight.

Specifically, the model equation used appears to be event-specific, depending on the duration and input flow, and also to the starting point of "dry condition".

For example, the model of sensor 8 for 68mm/h-10min event, used to evaluate the same intensity-duration event but as a successive rainfall, doesn't work well anymore. The RMSE in this case increases to 1.7478.

This is mainly due to the difference range of value in which operates. With the preconditioned state of the successive rainfall, moisture is already higher within the gutter and does not recover in the same way as the single event, whose the moisture variation is lower. The larger difference is observed in the first phase where, larger moisture values of the successive rainfall predict highly wrong flow values.
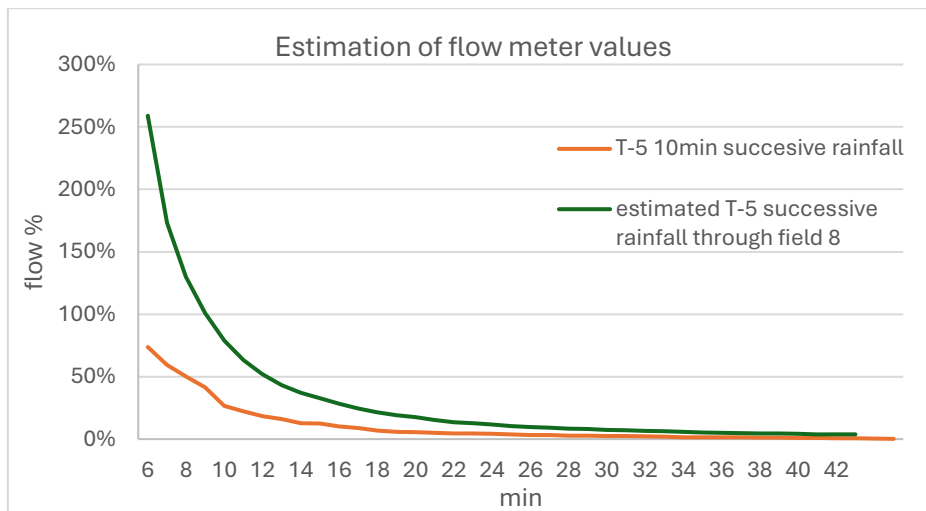


*Figure 58. Estimation of flow meter value of successive rainfall, with the model of the single event with same intensity-duration 68mm/h-10min*

Analogously happens trying to evaluate with a model created for one event, an event of the same duration but different intensity, and secondly, an event of the same intensity but different duration. In both case the RMSE increases, and the model lost the capacity in well predict the outflow of the new events.

Summarizing the model obtained by 30mm/h-30min event is used to evaluate 30mm/h-10min event and 15mm/h-30min.

This first graph, Figure 59, show in orange the actual outflow of 15mm/h-30min event, while in green the estimation of that through the model of 30mm/h-30min event, where there is a change in intensity.



*Figure 59. Estimation of 15mm/h-30min event through the model of 30mm/h-30min*

The RMSE approach 0.3267 value. This increase in error of prediction is attributable to the change in intensity. Within the gutter, lower in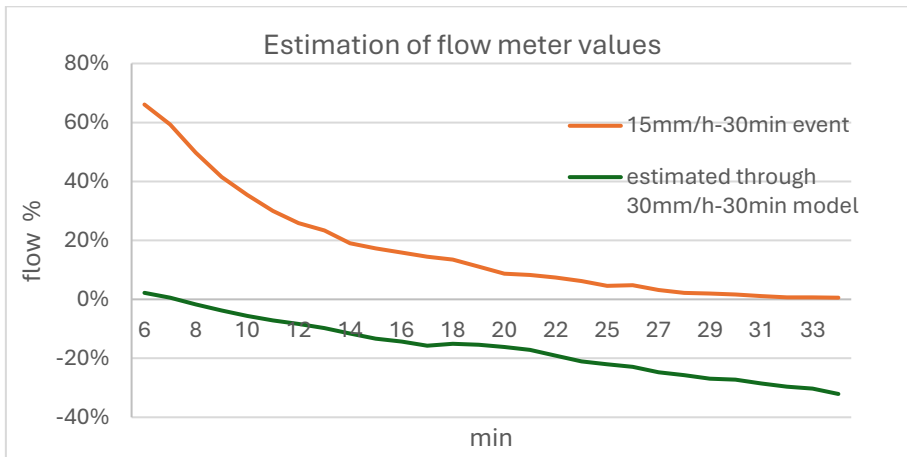tensity involves a different level of accumulation, which, at the time of the emptying process, will have moisture levels that vary differently.
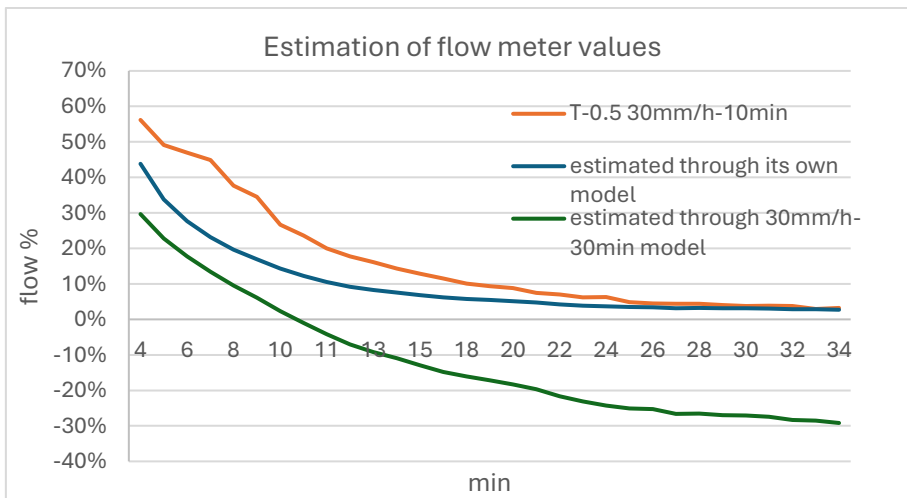


*Figure 60. Estimation of 30mm/h-10min event through the model of 30mm/h-30min*

In the Figure 60, in orange, it is represented the actual value of the flow meter corresponding to the emptying phase of 30mm/h-10min event. In blue, the value predicted of a second run of same event through its own model (with RMSE equal to 0.0935). In green, the new result: the value of 30mm/h-10min predicted through the model of 30mm/h-30min event, where to the same intensity corresponds different duration. In this case the error increases to 0.2098.

In this case the time spent within the gutter demonstrated to be relevant, making the model no longer optimal to predict its values of flow rate. This is readily deducible in this case since in the

event lasting 10min full saturation is not even reached, with strictly linked consequences in terms of moisture value, which will be lower respect the 30min event.

However, it could be estimated that between a change in duration or intensity, the largest increase in error is attributable to a change in flow rate.

These findings validate the potential for moisture sensors to predict outflow values but emphasize the need for further, more detailed analysis. The results obtained may point a way forward for future model implementation, where initial conditions must be strictly imposed, but the duration of the event is the least influential parameter while the intensity and starting moisture conditions are largely more relevant.

# Conclusion

The experimental study on the green gutter highlights its significant potential as an effective water management system, offering substantial benefits in reducing the stress on urban drainage infrastructure. Tested under various rainfall scenarios, the system demonstrated its ability to delay and reduce peak flows, mitigate rainfall intensity, and enhance short-term water retention, making it a promising addition to sustainable urban water management.

The system's performance shows a consistent capacity to delay peak flows, especially during shorter, high-intensity rainfall events, such as those lasting 10 minutes, where it reduced peak flow by approximately 50%, and postpone it completely at the end of the precipitation.

The robustness of the respond of the gutter is tested by successive rainfall events mimic real-world conditions where storms may occur in quick succession. It is proven that a good level of efficiency is preserved.

The green gutter's ability to smooth out sharp peak rainfall intensity is also performed even under dynamic rainfall conditions providing a simulation of realistic storm behaviour. The shorter experiments of 30min once again report the best result with a damp effect of 50% of the initial intensity, demonstrated that the green gutter could consistently manage the inflow and reduce peak flow output.

The system's key advantages, thanks to Rockflow mineral wool hydraulic properties, lie in its ability to delay, partially absorb and gradually release the water, ensured a manageable flow into the drainage network. The green gutter showcases itself as a sustainable solution in real-world application minimizing flash flood risks in urban areas vulnerable to extreme weather events with impermeable surfaces.

Beyond its hydraulic advantages, the green gutter system provides broader environmental and ecological benefits as a Nature Based Solution. The proposed enhancement with a vegetative layer, transforming the gutter into a prospective green wall, will improve air quality, mitigate the urban heat island effect, reduce building energy requirement and foster biodiversity in otherwise concrete-heavy environments. Additionally, the system's materials, Rockflow, is non-toxic, highly durable, and fully recyclable, making this an environmentally friendly solution that aligns with circular economy principles.

Despite its efficacy, the study identifies areas for future research and further development.

First of all, to achieve simpler and more cost-effective system control, the moisture sensor analysis and their correlation with the flow meter pattern should be fine-tuned.

After that, one possible optimization is a design improvement, to challenge rainfall events that exceed its maximum capacity of 75 mm and produce overflow. Future research could investigate the synergistic effects of a more comprehensive stormwater management network combining the green gutter with other urban green infrastructures, such as green roofs or permeable pavements. One important aspect of this project is its scalability. While this study focused on a single green gutter, scaling up this approach could involve deploying multiple systems across urban environments. By placing these systems at strategic locations in areas prone to flooding, it can create a network that significantly reduces the risk of inundation during extreme rainfall events.

Additionally, further exploration of the system's long-term performance is necessary, focusing on the durability of Rockflow under continuous exposure to urban pollutants and varying weather condition, with the possibility of obstructing the functionality, and the incorporation of vegetation. Ongoing studies at DTU university will focus on plant selection to choose the one with the characteristics that best fit to all the purpose and the well integrate the irrigation requirements.

Overall, the green gutter system presents itself as a Nature-Based Solution (NBS) that addresses urban water management challenges posed by climate change and urbanization.

The system presents a novel approach to enhance the resilience of cities, which up to now depict themselves completely vulnerable to hazards of flash floods. The integration of the green gutter into urban landscapes should become an essential tool for urban planners and policymakers, as it supports long-term sustainability by promoting ecological balance via addressing human challenges through natural solutions. This approach enhances urban living conditions while benefiting both people and the environment.

# References

*11-Sustainable Cities And Communities*. (2015). Retrieved from The Global Goals: https://www.globalgoals.org/goals/11-sustainable-cities-and-communities/

A. M. Lacasta, A. P. (2018). Green Streets for Noise Reduction. *Nature Based Strategies for Urban and Building Sustainability*.

A.M. Lacasta, A. P. (2016). Acoustic evaluation of modular greenery noise barriers. *Urban Forestry & Urban Greening*.

Addo-Bankas, O., Zhao, Y., Vymazal, J., Yuan, Y., & Fu, J. (2021). Green walls: A form of constructed wetland in green buildings.

Affairs, T. D. (2012). *World Urbanization Prospects -The 2011 Revision*. United Nations Secretariat.

Ahmad M., P. J. (2021). Modelling the dynamic linkages between eco-innovation, urbanization, economic growth and ecological footprints for G7 countries: Does financial globalization matter? *Sustainable Cities and Society*.

Alexandra Price, E. C. (2015). Vertical Greenery Systems as a Strategy in Urban Heat Island Mitigation. *Water, Air, & Soil Pollution*.

Almaaitah T., J. D. (2022). Hydrologic and thermal performance of a full-scale farmed blue-green roof.

Amit Kumar, P. E. (2023). Urban Green Spaces for Environmental Sustainability and Climate Resilience. *The Palgrave Handbook of Socio-ecological Resilience in the Face of Climate Change*.

Anita Gidlof-Gunnarsson, E. O. (2007). Noise and well-being in urban residential environments: the potential role of perceived availability to nearby green areas. *Landscape Urban Planning*.

*Aquatrans AT600 clamp-on flowmeter*. (n.d.). Retrieved from InstruMetrics-Engineering : https://instrumetrics.com/product/aquatrans-at600-clamp-on-flowmeter/

Atsushi Tsutsumi, K. J. (2004). Guidelines for surface runoff coefficients by the Ministry of Education, Culture, Sports, Science and Technology, Japan. *Hydrological Sciences-Journal*.

Ayako Nagase, N. D. (2012). Amount of water runoff from different vegetation types on extensive green roofs: Effects of plant species, diversity and plant structure. *Landscape and Urban Planning*.

Besir, A. B., & Cuce, E. (2018). Green roofs and facades: A comprehensive review. *Renewable and Sustainable Energy Reviews*.

Bevilacqua, P., Mazzeo, D., Bruno, R., & Arcuri, N. (2016). Experimental investigation of the thermal performances of an extensive green roof in the Mediterranean area.

Bibri S. E., J. K. (2017). Smart sustainable cities of the future: An extensive interdisciplinary literature review.

Board, C. S. (2011). *Runoff Coefficient (C) Fact Sheet*. Retrieved from The Clean Water Team Guidance Compendium for Watershed Monitoring and Assessment: https://www.waterboards.ca.gov/water_issues/programs/swamp/docs/cwt/guidance/513.pdf

Brenda B. Lin, S. M. (2017). Urban Agriculture as a Productive Green Infrastructure for Environmental and Social Well-Being. *Greening Cities*.

*Calculating Hyetograph from Chicago Storm Data*. (n.d.). Retrieved from Bentley StormCAD CONNECT Edition Help: https://docs.bentley.com/LiveContent/web/Bentley%20StormCAD%20SS5-v1/en/GUID-A0096667-D870-426C-A77A-233BE0A41A32.html

*Capacitive Soil Moisture Sensor*. (n.d.). Retrieved from Biomaker: https://www.biomaker.org/block-catalogue/2021/12/17/soil-moisture-sensor-aideepen-v12#:~:text=Most%20capacitors%20contain%20at%20least,separated%20by%20a%20dielectric%20medium.&text=A%20capacitive%20moisture%20sensor%20works,the%20changes%20in%20the%20die

Cascone, S. (2019). Green Roof Design: State of the Art on Technology and Materials. *Sustainability*.

Castleton, H., Stovin, V., Beck, S., & Davison, J. (2010). Green roofs; building energy savings and the potential for retrofit.

Centre, W. R. (n.d.). *Urban floods intensifying, countryside drying up*.

Charoenkit, S., & Yiemwattana, S. (2016). Living walls and their contribution to improved thermal comfort and carbon emission reduction: A review.

Chatti W., M. T. (2022). Information communication technology (ICT), smart urbanization, and environmental quality: Evidence from a panel of developing and developed economies.

Christian Massari, V. P. (2023). On the relation between antecedent basin conditions and runoff coefficient for European floods. *Journal of Hydrology*.

Christopher J. Walsh, A. H. (2005). The urban stream syndrome: current knowledge and the search for a cure. *J. of the North American Benthological Society*.

*Coefficient of Determination, R-squared*. (n.d.). Retrieved from Newcastle University: https://www.ncl.ac.uk/webtemplate/ask-assets/external/maths-resources/statistics/regression-and-correlation/coefficient-of-determination-r-squared.html

Conrad Wasko, A. S. (2015). Steeper temporal distribution of rain intensity at higher temperatures within Australian storms. *Nature Geoscience*.

*Current clamp*. (n.d.). Retrieved from Wikipedia: https://en.wikipedia.org/wiki/Current_clamp#Clamp_meter

D. Penna, M. B. (2013). 6.07 - Analysis of Flash-Flood Runoff Response, With Examples From Major European Events. In John (Jack) F. Shroder, *Treatise on Geomorphology (Second Edition)* (pp. 100-109).

Daniele Veneziano, P. V. (1999). Best linear unbiased design hyetograph. *WATER RESOURCES RESEARCH*.

Ding, G. K. (2024). Managing Water Scarcity – The Role of Sustainable Water Management. *Encyclopedia of Sustainable Technologies (Second Edition)*.

Dunnett, N., & Kingsbury, N. (2008). Planting green roofs and living walls.

Egorov A, M. P. (2016). Green spaces and health. *Copenhagen: world health organization regional office for europe*.

Elizabeth J. Kendon, S. B. (2018). When Will We Detect Changes in Short-Duration Precipitation Extremes? *Journal of Climate*.

Flavie Mayrand, P. C. (2018). Green Roofs and Green Walls for Biodiversity Conservation: A Contribution to Urban Connectivity? *Sustainability* .

Gabriel Pérez, J. C. (2016). Acoustic insulation capacity of Vertical Greenery Systems for buildings. *Applied Acoustics*.

Getter K.L., D. R. (2009). Carbon sequestration potential of extensive green roofs.

Gourdji, S. (2018). Review of plants to mitigate particulate matter, ozone as well as nitrogen dioxide air pollutants and applicable recommendations for green roofs in Montreal, Quebec. *Environmental Pollution*.

*Gravity: Analog Waterproof Capacitive Soil Moisture Sensor*. (n.d.). Retrieved from DFRobot-Drive the future: https://wiki.dfrobot.com/Waterproof_Capacitive_Soil_Moisture_Sensor_SKU_SEN0308

H. J. Fowler, G. L. (2021). Anthropogenic intensification of short-duration rainfall extremes. *Nat. Rev. Earth Environ*.

H. J. Fowler, H. A. (2021). Towards advancing scientific knowledge of climate change impacts on short-duration rainfall extremes. . *Philos. Trans. R. Soc. London Ser*.

Hedblom M, G. B. (2019). Reduction of physiological stress by urban green space in a multisensory virtual experiment. *Sceince reports*.

Hoeben A.D., A. P. (2021). Green roof ecosystem services in various urban development types: a case study in Graz, Austria.

Hooman Ayat, J. P. (2022). Intensification of subhourly heavy rainfall. *Science*.

Hosein, A. ,. (2013). Sustainable energy performances of green buildings: A review of current theories, implementations and challenges.

Ichihara K, C. J. (2011). New York City property values: what is the impact of green roofs on rental pricing.

Imane Hachoumi, B. P.-F. (2021). Impact of Green Roofs and Vertical Greenery Systems on Surface Runoff Quality. *Water*.

International Energy Agency. (2007). Key world energy statistics (p. 6). In *Paris: International Energy Agency.*

J. Jacobs, N. B. (2023). Green roofs and pollinators, useful green spots for some wild bee species (Hymenoptera: Anthophila), but not so much for hoverflies (Diptera: Syrphidae). *Scientific Reports*.

Jian-feng Li, O. W.-m. (2010). Effect of green roof on ambient CO2 concentration. *Building and Environment*.

*Kamstrup Heat meter multical®403 1.5m3/h, 110 mm with battery, return.* (n.d.). Retrieved from Proshop: https://www.proshop.dk/Maaleinstrumenter/Kamstrup-Varmemaaler-multical403-15m3h-110-mm-med-batteri-retur/2897769?utm_source=google&%E2%80%A6

Kandel S., N. F. (2024). Nature-based solutions and buildings: A review of the literature and an agenda for renaturing our cities one building at a time .

Katia Perini, P. R. (2013). Cost–benefit analysis for green façades and living wall systems. *Building and Environment* .

Kingsbury, N., & Kingsbury, N. (2004). Planting green roofs and living walls. *Timber Press*.

Knut Veisten, Y. S. (2012). Valuation of Green Walls and Green Roofs as Soundscape Measures: Including Monetised Amenity Values Together with Noise-attenuation Values in a Cost-benefit Analysis of a Green Wall Affecting Courtyards. *Int. J. Environ. Res. Public Health*.

Leif Winther, J. J. (2011). *Aflobsteknik.*

Locatelli, L., Mark, O., Mikkelsen, P., Arnbjerg-Nielsen, K., Deletic, A., Roldin, M., & Binning, P. (2017). Hydrologic Impact of Urbanization with Extensive Stormwater Infiltration. *J. Hydrol.* .

Loh, S. (2008). Living walls–a way to green the built environment.

M. Uhl, L. (2008). Green Roof Storm Water Retention –Monitoring Results. *International Conference on Urban Drainage.* Edinburgh.

Mamatha Tomson, P. K. (2021). Green infrastructure for air quality improvement in street canyons. *Environment International*.

Manel Ellouze, H. A. (2009). A triangular model for the generation of synthetic. *Hydrological Sciences Journal*.

Manso, M., & Castro-Gomes, J. (2015). Green wall systems: A review of their characteristics.

Maria Manso, I. T. (2021). Green roof and green wall benefits and costs: A review of the quantitative evidence. *Renewable and Sustainable Energy Reviews*.

Masson V., A. L. (2020). *Urban Climates and Climate Change.*

Matthew J. Burns, T. D. (2012). Hydrologic shortcomings of conventional urban stormwater management and opportunities for reform. *Landscape and Urban Planning*.

Medl, A., Stangl, R., & Florineth, F. (2017). Vertical greening systems e A review on recent technologies and.

Mohammed, A. B. (2022). Employing systems of green walls to improve performance and rationalize energy in buildings. *Journal of Engineering and Applied Science*.

Nadia Saifi, D. B. (2023). Effects of green roofs and vertical greenery systems on building thermal comfort in dry climates: an experimental study. *Journal of Building Pathology and Rehabilitation*.

Nations, U. (2012). *World urbanization prospects: The 2011 revision. new york: United nations department of economic and social affairs/population division.* UN Proceedings.

Nations, U. (2020). Goal 11: Make cities inclusive, safe, resilient and sustainable.

*Nature-based solutions research policy*. (n.d.). Retrieved from An official website of the European Union: https://research-and-innovation.ec.europa.eu/research-area/environment/nature-based-solutions/research-policy_en

Omri A., S. B. (2024). When do climate change legislation and clean energy policies matter for net-zero emissions?

Paithankar D. N., S. G. (2020). Investigating the hydrological performance of green roofs using storm water management model.

Paolo Rosasco, K. P. (2018). Evaluating the economic sustainability of a vertical greening system: A Cost-Benefit Analysis of a pilot project in mediterranean area. *Building and Environment*.

Pérez, G., Coma, J., Martorell, I., & Cabeza, L. F. (2014). Vertical Greenery Systems (VGS) for energy saving in buildings: A review.

Perini, K., Ottelé, M., Fraaij, A., Haas, E., & Raiteri, R. (2011). Vertical greening systems and the effect on air flow and temperature on the building envelope.

Perini, K., Ottelé, M., Haas, E. M., & Raiteri, R. (2011). Greening the building envelope, façade greening and.

Pugh T., M. A. (2012). Effectiveness of Green Infrastructure for Improvement of Air Quality in Urban Street Canyons.

R.S. Ulrich, R. S. (1991). Stress recovery during exposure to natural and urban environments.

Radić, M., Dodig, M. B., & Auer, T. (2019). Green Facades and Living Walls—A Review Establishing the Classification of Construction Types and Mapping the Benefits.

*Rethink urban water*. (n.d.). Retrieved from Rockwool: https://rain.rockwool.com/uk/

*Rockwool - Our heritage*. (n.d.). Retrieved from Rockwool: https://www.rockwool.com/asia/about-us/history/

Rockwool. (n.d.). *Rockflow attenuation and infiltration systems- Durable and easy to maintain*. Rockwool .

Rockwool. (n.d.). *Rockflow attenuation and infiltration systems- High absorption capacity*. Rockwool.

Roggero M., R. (2020). Social dilemmas, policy instruments, and climate adaptation measures: the case of green roofs.

*Root Mean Square Error (RMSE)*. (n.d.). Retrieved from Statistics By Jim- Making statistics intuitive: https://statisticsbyjim.com/regression/root-mean-square-error-rmse/

Ross W.F. Cameron, J. E. (2014). What's 'cool' in the world of green façades? How plant choice influences the cooling properties of green walls. *Building and Environment*.

S.S.G. Hashemi, H. B. (2015). Performance of green roofs with respect to water quality and reduction of energy consumption in tropics: A review. *Renewable and Sustainable Energy Reviews*.

Safikhani, T., Abdullah, A. M., Ossen, D. R., & Baharvand, M. (2014). A review of energy characteristic of vertical greenery systems.

Santamouris M. (2007). Heat Island Research in Europe: The State of the Art.

Santamouris M. (2014). Cooling the cities - A review of reflective and green roof mitigation technologies to fight heat island and improve comfort in urban environments.

*SCALA2*. (n.d.). Retrieved from GRUNDFOS: https://product-selection.grundfos.com/uk/products/scala/scala2?tab=documentation

Scharf, B., Pitha, U., & Oberarzbache, S. (2012). Living walls – More than scenic beauties.

Sebestyén V., G. D. (2023). Identifying the links among urban climate hazards, mitigation and adaptation actions and sustainability for future resilient cities.

Serena Vitaliano, S. C. (2024). Mitigating Built Environment Air Pollution by Green Systems: An In-Depth Review. *Applied Sciences* .

Shafique, M., Kim, R., & Rafiq, M. (2018). Green roof benefits, opportunities and challenges – A review.

Shafique, M., Xue, X., & Luo, X. (2020). An overview of carbon sequestration of green roofs in urban areas.

Snigdhendubala Pradhan, S. G.-G. (2019). Greywater recycling in buildings using living walls and green roofs: A review of the applicability and challenges. *Science of The Total Environment*.

Sohn, W., Kim, J.-H., Li, M.-H., Brown, R., & Jaber, F. (2020). How Does Increasing Impervious Surfaces Affect Urban Flooding in Response to Climate Variability? *Ecol. Indic.*

Suzanne Kandel, N. F. (2024). Nature-based solutions and buildings: A review of the literature and an agenda for renaturing our cities one building at a time. *Nature-Based Solutions*.

T. Kjellstrom, A. M. (2013). Climate change threats to population health and well-being: the imperative of protective solutions that will last. *Global Health Action*.

*The EU and nature-based solutions*. (n.d.). Retrieved from An official website of the European Union: https://research-and-innovation.ec.europa.eu/research-area/environment/nature-based-solutions_en

Timur, Ö., & & Karaca, E. (2013). Vertical Gardens, Advances in Landscape Architecture.

Tomson, M., Kumar, P., Barwise, Y., Perez, P., Forehead, H., French, K., . . . Watts, J. F. (2021). Green infrastructure for air quality improvement in street canyons.

Trenberth, K. E. (2003). The changing character of precipitation. . *Bull. Am. Meteorol. Soc.* .

Twohig-Bennett C., A. J. (2018). The health benefits of the great outdoors: A systematic review and meta-analysis of greenspace exposure and health outcomes.

*Ultrasonic flow meter*. (n.d.). Retrieved from Wikipedia: https://en.wikipedia.org/wiki/Ultrasonic_flow_meter

Ulysse Pasquier, P. V. (2022). Quantifying the City-Scale Impacts of Impervious Surfaces on Groundwater Recharge Potential: An Urban Application of WRF–Hydro. *Water*.

V. Benedito Dur`a, E. M. (2023). Contribution of green roofs to urban arthropod biodiversity in a Mediterranean climate: a case study in Valencia, Spain. *Building and Environment*.

Veljko Prodanovic, B. H. (2017). Green walls for greywater reuse: Understanding the role of media on pollutant removal. *Ecological Engineering*.

Vijayaraghavan, K. (2016). Green roofs: A critical review on the role of components, benefits, limitations and trends. *Renewable and Sustainable Energy Reviews*.

Yao Li, P. W. (2024). Assessing urban drainage pressure and impacts of future climate. *Journal of Hydrology: Regional Studies*.